COMPUTER MODELLING OF DIGITAL DISTANCE AND DIRECTIONAL RELAYS

A Thesis

Submitted to the Faculty of Graduate Studies and Research

in Partial Fulfilment of the Requirements

for the Degree of

Master of Science

in the

Department of Electrical Engineering

University of Saskatchewan

by

THOMPSON ADU

Saskatoon, Saskatchewan

February 1989

UNIVERSITY OF SASKATCHEWAN

DEPARTMENT OF ELECTRICAL ENGINEERING

CERTIFICATION OF THESIS WORK

We, the undersigned, certify that Mr. Thompson Adu, candidate for the Degree of Master of Science in Electrical Engineering, has presented his thesis on the subject "Computer Modelling of Digital Distance and Directional Relays"

that this thesis is acceptable in form and content, and that this student demonstrated a satisfactory knowledge of the field covered by his thesis in an oral examination held on February 23, 1989.

External Examiner: S. S. [illegible]

of Agricultural Engineering

Internal Examiners:

[illegible]

[illegible]

[illegible]

[illegible]

Date: February 23, 1989

COPYRIGHT

ACKNOWLEDGEMENTS

The author is glad of the opportunity to thank Dr. M.S. Sachdev, his supervisor. It was through his good guidance and encouragement which has made this project a success. His advice and assistance in the preparation of this thesis is thankfully acknowledged.

The author also wishes to express his deepest gratitude to his parents and other family members for their encouragement and moral support. Thanks are due all his friends who helped in making this project a reality.

Special thanks are due the University of Saskatchewan and the Natural Sciences and Engineering Research Council of Canada for providing financial assistance in the form of a graduate scholarship and research assistantship.

UNIVERSITY OF SASKATCHEWAN

Electrical Engineering Abstract 89A303

COMPUTER MODELLING OF DIGITAL DISTANCE AND DIRECTIONAL RELAYS

Student: Thompson Adu Supervisor: Dr. M.S. Sachdev

M. Sc. Thesis Presented to the

College of Graduate Studies and Research

February 1989

ABSTRACT

With recent advances in microelectronics, the use of micro-processor based relays for power system protection has received much attention from power system researchers. To develop micro-processor relays suitable for use in power systems, their performance must be evaluated during the design stage. For achieving this, two approaches can be used. One approach is to design a prototype of the relay and test it. This procedure will be expensive if it becomes necessary to change the design several times. The second approach is to develop models of the relay and its expected performance on a digital computer. This procedure will allow an engineer to check the performance of several designs without building prototypes. Moreover, the design process will take less time than the time required to optimize the designs using the first option.

This thesis is concerned with the development of an interactive software which implements the models of digital distance and directional relays on a digital computer. The software uses four techniques for implementing the models. These are amplitude comparison, phase comparison, impedance estimation and memory mapped targeting techniques. The software facilitates

the execution of the programs in two modes of operation. In the first mode, the computations are performed using the floating point format of numbers. In the second mode, the effects of analog to digital converters, truncations or roundings and bit shift multiplications are incorporated.

The capabilities of the software are demonstrated by including cases of transmission line shunt faults. The movement of the trajectory of the calculated line impedances from the pre-fault to the post-fault states shows the speed with which a relay detects faults that are in its operating zone.

Table of Contents

List of Figures

List of Tables

1. INTRODUCTION

1.1. Background

An electric power system generates, transmits and distributes electrical energy. The essential components of a power system are:

1. generators, which convert the mechanical energy in steam or water to electrical energy,
2. power transformers, which step up the generated voltage to higher levels for transmission,
3. transmission lines, which transmit electrical energy from one location to another,
4. power transformers, which step down transmission voltage to lower levels for distribution,
5. distribution lines, which transport electrical energy to industrial and domestic customers and
6. circuit breakers, which isolate the faulty equipment from the power system.

A power system has either a radial or a network configuration. Figure 1.1 shows a sample power system with network configuration. The electrical components such as generators, transformers, transmission lines and distribution lines forming this network are susceptible to faults which do occur in the power system. These faults can cause considerable damage to the equipment. The equipment is therefore, protected with devices known to the engineer as protective relays.

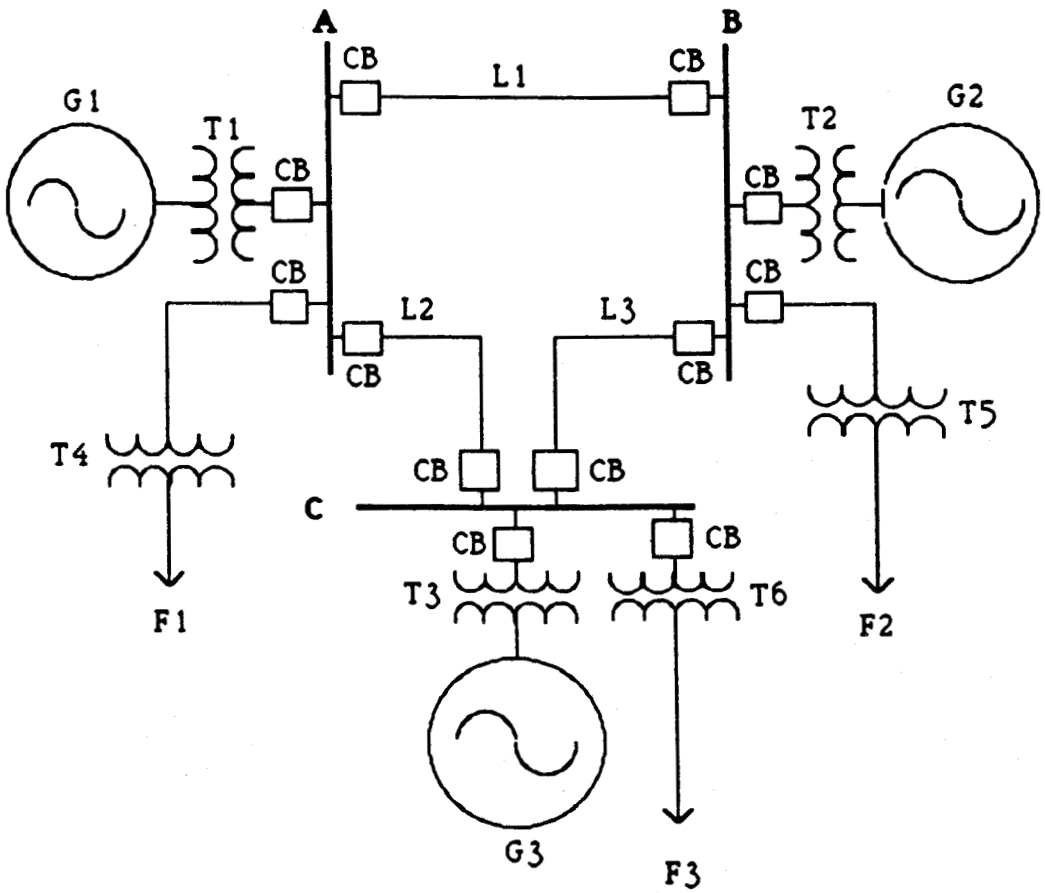

G1, G2 and G3 are generators.
L1, L2 and L3 are transmission lines.
T1, T2 and T3 are step up transformers.
T4, T5 and T6 are step down transformers.
A, B and C are bus bars.
F1, F2 and F3 are distribution feeders.
CB's are circuit breakers.

Figure 1.1: A single line diagram of a typical power system.

1.2. Power System Protection

Many types of relays are used in a power system for protecting the electrical equipment. These relays are generally described by their connections, the actuating quantities and the disturbances to which they respond. Some of these are distance, directional, differential and overcurrent relays. Distance and directional relays are used for transmission line protection. Differential relays protect equipment such as transformers and generators. Small transformers, distribution feeders, motors, etc. are protected with overcurrent relays. Overcurrent relays are also used as backups to most distance relays.

1.3. Changing Trends in Power System Protection

Fuses were the first automatic devices to be employed to isolate the faulted equipment as quickly as possible. They are effective but suffer from the disadvantage of requiring replacement immediately after the fault current is interrupted. This inconvenience was alleviated by the use of automatic circuit breakers and later electro-mechanical relays whose contacts controlled the trip coils of the circuit breakers. Protective devices with greater sensitivity, better selectivity and faster speed of operation were developed later to meet the requirements of the increasingly complex power system.

Research into the development of solid state electronic relays started in the 1950's. These relays were not generally accepted in the early stages due to the high failure rates of the electronic components and inappropriate designs. In later developments newer semiconductor technology and improved designs were used. Several kinds of solid state relays are presently being used in power systems. The continuing growth of generating capacities and formation of regional pools have resulted in the development of improved protection and control techniques.

With the advent of digital technology, the development of micro-

processor based relays has received considerable attention [1, 2]. The accuracy and speed with which a processor can perform computations have aroused the interest of relay engineers. F.H. Last and A. Stalewsky [3] were the first to propose the use of real time computations for power system protection in 1966. This was followed in 1969 by Rockefeller [4] who studied the feasibility of using a digital computer for the protection of a substation and the transmission lines emanating from it.

Research, development and economics of digital relays have reached a proportion where commercial production of digital relays is possible. Speed and accuracy of these relays depend mainly on the software and hardware used. Accuracy of the results computed by a digital relay is influenced by the word size of the analog to digital converter, the digital processor, the relay software or algorithm, the relay characteristic and the operating environment.

The performance of a digital relay during the design stage should be evaluated. To achieve this, two approaches can be used. One is to build a prototype of the relay and then test it. If a design has to be changed several times, it would be expensive. An alternative approach, which is considered in this thesis, is to model the digital relay on a digital computer.

1.4. Objective and Outline of Thesis

The major object of the work reported in this thesis is the development of an interactive software which implements models of digital distance and directional relays on a digital computer.

The thesis is organized in eight chapters. The first chapter introduces the subject of this thesis and the changing trends in power system protection. It also outlines the organization of the thesis. Chapter 2 introduces the subject of distance and directional relays.

Polarization and memory action are important in the distance protection of transmission lines. The concepts involved with polarization and memory action are introduced in Chapter 3. The types of polarization and the choice of polarizing signals used in this project are discussed. Directional relays do not use the type of polarization and memory action used in distance relays. The directional relays use some special forms of connections and these are also discussed in Chapter 3.

Chapter 4 describes the major functional blocks of a typical digital relay and outlines the advantages of using digital relays for power system protection. This chapter also discusses digital relaying algorithms presently in use and identifies the sources of errors associated with them.

Chapter 5 illustrates the techniques used in this project for formulating the tripping logic of digital distance and directional relays. The development of an interactive software that implements the formulated techniques on a digital computer is discussed in Chapter 6. The specifications of the software and its structure are outlined. The overall organizational block-diagrams and brief descriptions of the major software programs are also included.

In order to determine the accuracy of the software package, it should be tested using fault data derived from a power system. Chapter 7 describes the power system used in this project and also the tests conducted. The summary of the thesis is given in Chapter 8. Also discussed in this chapter are the conclusions drawn from the work reported in this thesis.

2. TECHNIQUES OF TRANSMISSION LINE PROTECTION

2.1. Introduction

Distance relays are used for the protection of medium and high voltage transmission lines. A distance relay measures the impedance of the line from its location to the fault. It makes decisions considering the measured values of the magnitude and phase angle of the impedance. A distance relay uses inputs which are proportional to the line voltages and line currents.

Another family of relays used in line protection schemes are directional relays. These relays sense the direction in which the power flows. This permits a directional relay to trip for the flow of current in a specified direction only. Directional relays are used together with distance relays which are not inherently directional. A directional relay develops maximum torque when the relay current lags the voltage applied to the relay by an angle determined by the design parameters and connections of the relay.

This chapter briefly describes a distance protection scheme. It also describes the characteristics of comparators used in distance and directional relays.

2.2. Distance Protection Schemes

Figure 2.1 shows, in the single line diagram form, a generator, transformer, station bus and a section of a transmission line. Also shown in the figure is a distance relay and its connections to the power system via a coupling-capacitor voltage transformer (ccvt) and a current transformer (ct). These transformers reduce the high levels of voltages and currents to low levels that are suitable for use in relays. The heart of a distance relay, is

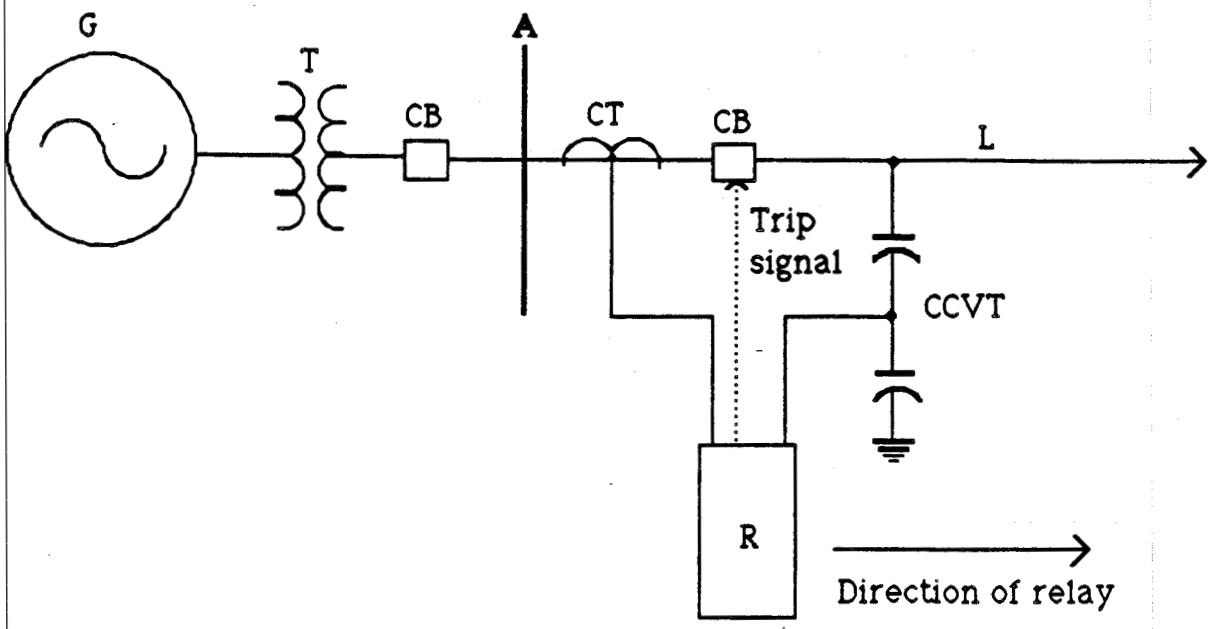

G - generator.
T - transformer.
CB - circuit breaker.
CT - current transformer.
CCVT - coupling capacitor voltage transformer.
R - distance relay.
A - station bus.
L - section of transmission line.

Figure 2.1: A typical schematic arrangement showing connections between a distance relay and a power system.

the measuring unit that uses voltages and currents to perform the relaying function. These voltages and currents are carefully chosen such that the relays operate satisfactorily for shunt faults. In the following section the procedure for obtaining the voltage and current combinations will be discussed.

2.2.1. Power System Shunt Faults

A power system experiences five types of shunt faults. They are: three-phase, phase-to-phase, phase-to-ground, two-phase-to-ground and three-phase-to-ground faults. Six measuring units are incorporated in most distance relays. Three units supervise interphase conditions and the remaining three supervise phase-to-ground conditions. The inputs to the measuring units are chosen such that at least one unit measures the positive sequence impedance of the line from the relay to the fault. This is achieved by providing the measuring units for phase fault protection with delta voltages and currents. For example, a measuring unit uses the difference between the phase B and phase C voltages (V_{BC}) and the currents (I_B - I_C). The single phase units use phase-to-ground voltages and compensated phase currents. The compensating current, is derived from the zero sequence current which is present during a ground fault condition. For example, a measuring unit uses phase A to ground voltage (V_A) and compensated A-phase current ($I_A + 3K_0I_0$). I_0 is the zero sequence current and K_0 the zero sequence compensating factor. Table 2.1 lists the voltage and current inputs to the six measuring units. Most distance protection schemes use six measuring units to supervise all shunt faults. In some cases these measuring units exhibit abnormal behavior when a three phase fault occurs near to the relay location. A seventh unit is, therefore, provided to supervise three-phase faults. The impedance and time settings of the measuring units can be selected such that a distance protection scheme is divided into zones of protection.

Table 2.1: The voltage and current inputs to distance relay measuring units.

NO.	MEASURING UNIT FOR PHASE	VOLTAGE (V_L)	CURRENT (I_L)
1	AB	V_{AB}	I_A-I_B
2	BC	V_{BC}	I_B-I_C
3	CA	V_{CA}	I_C-I_A
4	AG	V_A	$I_A+3K_0I_0$
5	BG	V_B	$I_B+3K_0I_0$
6	CG	V_C	$I_C+3K_0I_0$

G represent ground.

2.2.2. Zones of Distance Protection

Figure 2.2 shows a radial arrangement of three transmission lines, 12, 23 and 34. Loads L_1, L_2, L_3 and L_4 are connected to the buses, 1, 2, 3 and 4. The figure also shows distance relays R_{11}, R_{12}, R_{21}, R_{22}, R_{31}, R_{32}, R_{41} and R_{42}. Relays R_{12} and R_{21} protect line 12. Similarly relays R_{22} and R_{31} protect line 23 and relays R_{32} and R_{41} protect line 34. The settings and time delays of these relays are generally selected to accomplish three zone distance protection at each relay location. For some schemes, six distance measuring units are used at each relay location to implement each zone of protection. In this manner, eighteen measuring units are used at each relay location. Figure 2.2 also shows the distance and time delay settings of the relays provided to protect line 23. Times t_1, t_2 and t_3 are respectively the time settings for zones one, two and three relays. The zone one relay at bus 2 provides primary protection of line 23. Time t_1 is so small that this relay is assumed to trip instantaneously when the distance of

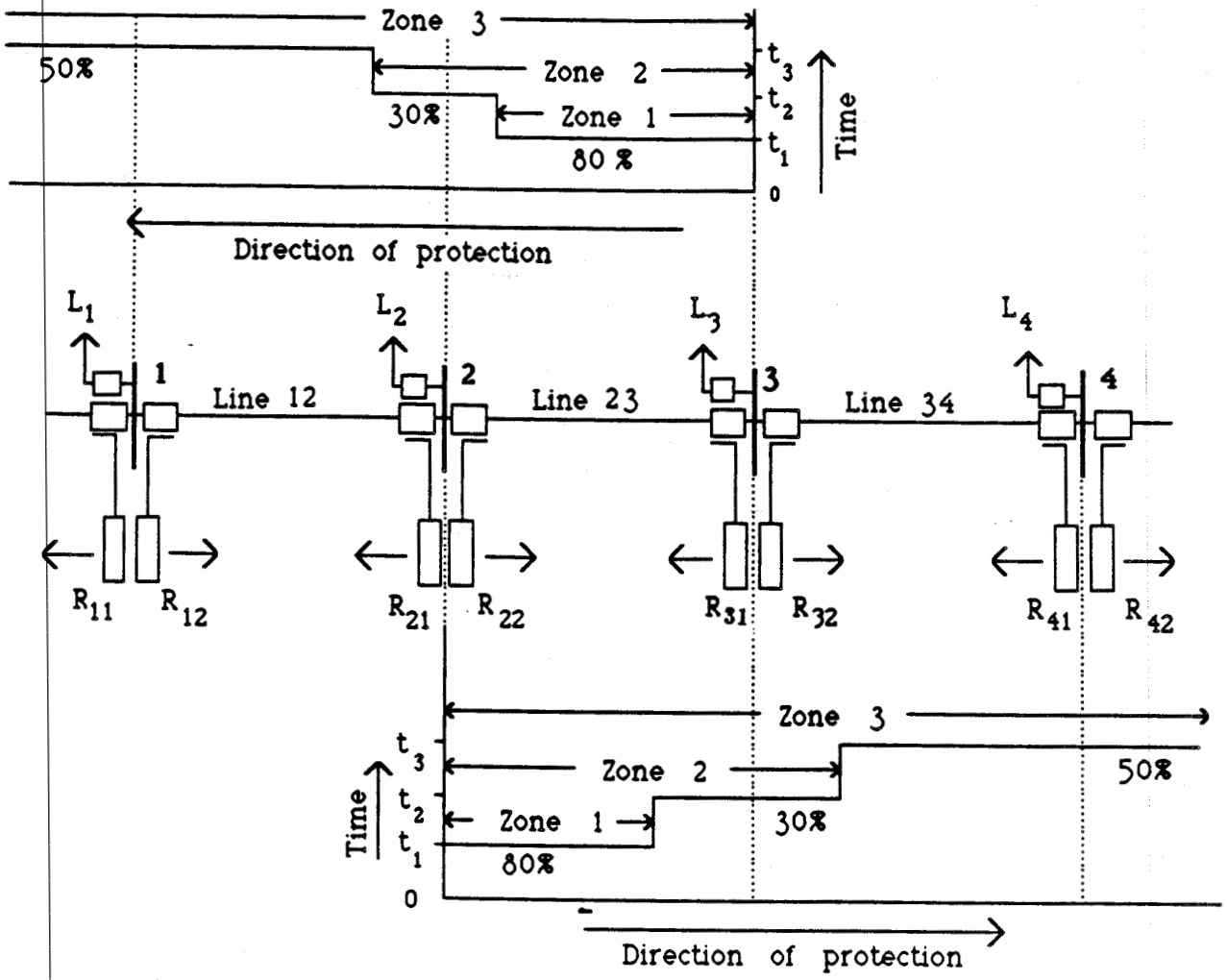

Figure 2.2: The time-distance characteristics of a three-zone distance protection scheme.

the fault on line 23 is less than 80% of line length from the relay location. The zone two relay at bus 2 provides backup protection for the first 80% of the line 23, primary protection for the last 20% of the line 23 and backup protection for the first 20%-30% of the line 34. The relay opens the circuit breaker after a time delay of 0.25s to 0.40s. Zone three relay at bus 2 provides backup protection for the lines 23 and 34, and 50% of the line beyond bus 4. This relay operates after a time delay of about 0.80s. The relays at bus 3, that protect line 23, perform similar functions except that they measure distance in the direction of bus 3 to bus 2 and beyond. Similar arrangements are implemented at the other relay locations for the protection of the other lines.

The measuring units of distance relays either compare the magnitudes of the input signals or respond to the phase angles between the input signals. In this manner they measure the impedance of the transmission line as seen from a relay's location. These units are called comparators.

2.3. Distance and Directional Relay Comparators

The measuring units of distance and directional relays are either amplitude or phase comparators. The operation of an amplitude comparator depends on the magnitudes of its inputs or combinations of these inputs. The operation of a phase comparator, however, depends on the phase angle between the input signals or combinations of the signals. An amplitude comparator is provided with two inputs, an operating signal and a restraining signal. The comparator operates when the magnitude of the operating signal is larger than the magnitude of the restraining signal. This is mathematically expressed as

$$|S_0| > |S_R| \tag{2.1}$$

where:

S_0 is the operating signal and

S_R is the restraining signal.

The two inputs to a phase comparator are the measuring signal and the polarizing signal. This comparator operates when the phase angle between the measuring and polarizing signals is within a specified range. The operation of a phase comparator is mathematically expressed as

$$-90^\circ \leq \beta \leq +90^\circ \qquad (2.2)$$

where:

β is the angle between the input signals S_1 and S_2.

Usually, S_0, S_R, S_1 and S_2 are phasors representing signals derived by mixing voltages and currents proportional to the system voltages and currents. This section presents the theory behind distance and directional relay comparators, the input signals to these comparators and their representation on an impedance plane.

2.3.1. Block Diagrams of Typical Comparators

Figure 2.3 [5] shows the block diagram of a comparator that compares the amplitudes of two currents. Bridge connected rectifiers convert ac inputs I_0 and I_R to equivalent unidirectional currents, i_0 and i_r. The difference between the operating and restraining currents feeds an averaging circuit. The output of the averaging circuit is applied to a polarity detecting circuit. The comparator provides an output when the average of the difference current is positive and exceeds a threshold value.

Figure 2.4 [5] shows the block diagram of a typical phase comparator. A coincidence circuit accepts inputs S_1 and S_2 and provides a positive output when the signals S_1 and S_2 are of the same polarity. It provides a negative output when the signals are of opposite polarity. The output of the coincidence circuit is applied to an integrating circuit. The output of the integrating circuit increases linearly when the input to the circuit is positive and falls at the same rate when the input is negative. The level detector

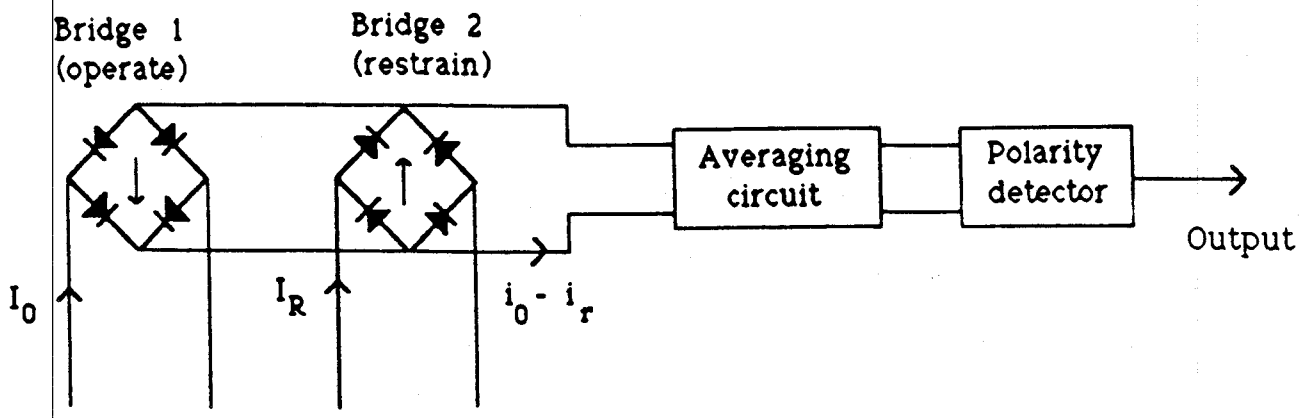

Figure 2.3: A block diagram of a typical amplitude comparator.

Figure 2.4: A block diagram of a typical phase comparator.

switches on when the integrator output exceeds a preset value. It resets when the output falls below another preset value.

Figure 2.5(a) [6] shows signals presented to a phase comparator when the system is under normal operating conditions and when there is a fault. When applied to the coincidence circuit, it provides the outputs displayed in Figure 2.5(b). The outputs are positive when both signals are of the same polarity and are negative when polarities of the inputs are not similar. Figure 2.5(c) shows the output from the integrator. The level detector output is displayed in Figure 2.5(d). When the power system is operating under normal conditions, the integrator output does not reach the level detector setting and therefore, the relay does not operate. During the fault, the relay operates at t_1 seconds when the integrator output exceeds the level detector setting. The characteristics of the measuring units are normally represented on an impedance plane and this is presented in the next section.

2.4. Typical Distance and Directional Relay Characteristics

The input signals for comparators are selected such that their characteristics are either circles or straight lines. They are usually plotted on an impedance plane with axes R and jX. R is resistance and X is reactance. The directional relay characteristic is also represented on an impedance plane as any distance relay. There are many types of distance relay characteristics. Some of these relays are,

1. impedance,
2. offset impedance,
3. mho,
4. offset mho,
5. reactance and

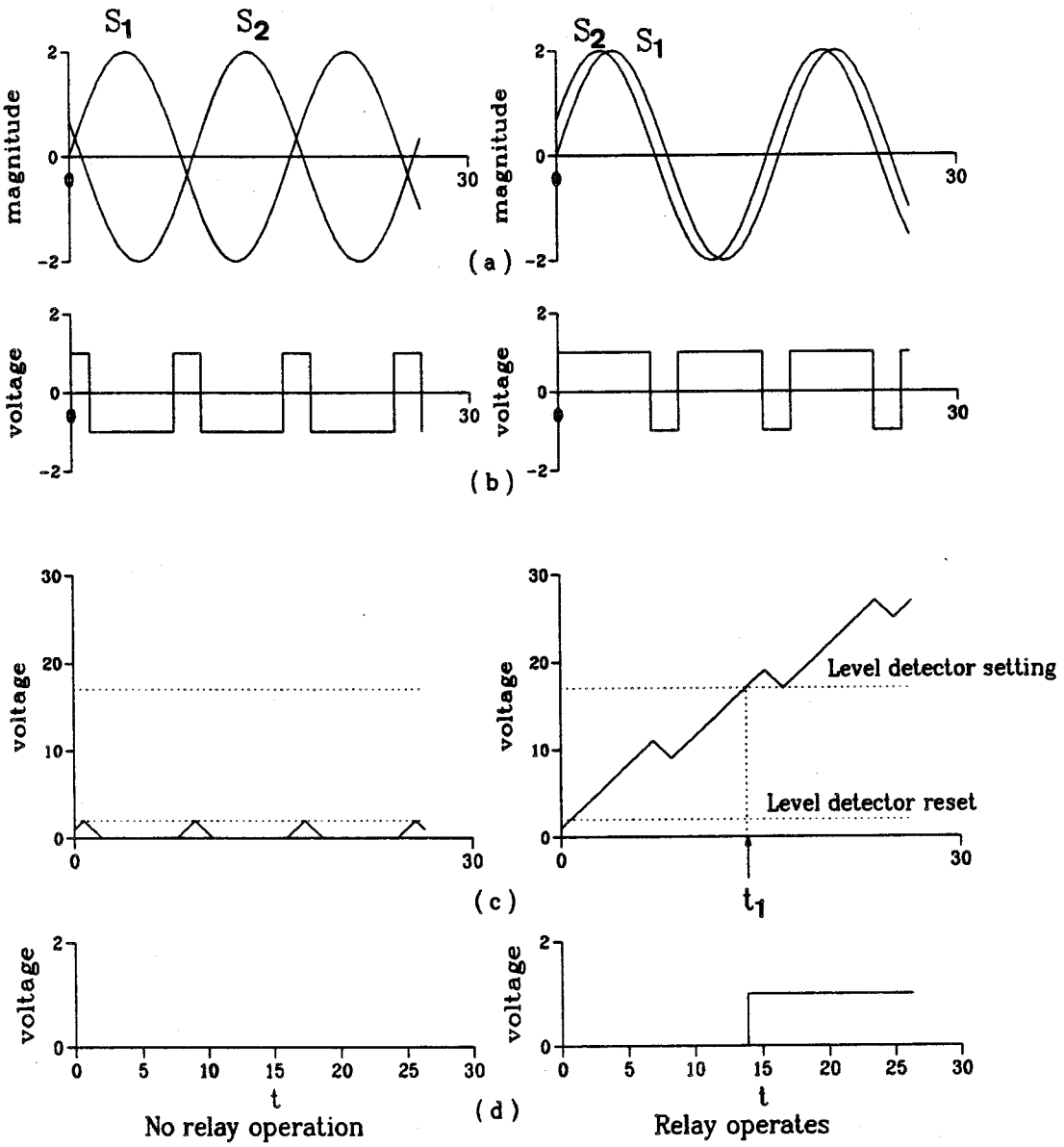

Figure 2.5: The waveforms depicting the action of a phase comparator.

6. quadrilateral characteristics.

Figure 2.6(a) shows the characteristic of an impedance relay plotted on the impedance plane. This relay is non-directional and operates during reverse faults within the reach of the relay. For effective transmission line protection, a directional relay is used in conjunction with the impedance relay. The composite distance relay has the features of both an impedance relay and a directional relay.

Figure 2.6(b) shows a mho relay characteristic plotted on the impedance plane. This relay is inherently directional and is suitable for protecting long transmission lines. Figures 2.6(c) and 2.6(d) show the offset mho characteristics drawn on an impedance plane. The characteristics are obtained by biasing a mho relay with additional impedance, Z_{R1}. The biasing can either be positive or negative.

The characteristic of a reactance relay is parallel to the resistance axis. Figure 2.6(e) depicts this on the impedance plane. This relay is not affected by the resistance of the arc during a fault. It is, therefore, suitable for protecting short lines where the fault resistance is comparable to line reactance.

Figure 2.6(f) shows the quadrilateral characteristic of a distance relay plotted on the impedance plane. This relay is inherently directional and performs well under power swing and heavy load conditions.

Figure 2.6(g) shows the characteristic of a directional relay drawn on the impedance plane. Its characteristic is a straight line passing through the origin of the impedance plane.

The behavior of each characteristic discussed earlier in the section depends on the type of the input signals to the relay. The next section discusses the derivation of these signals.

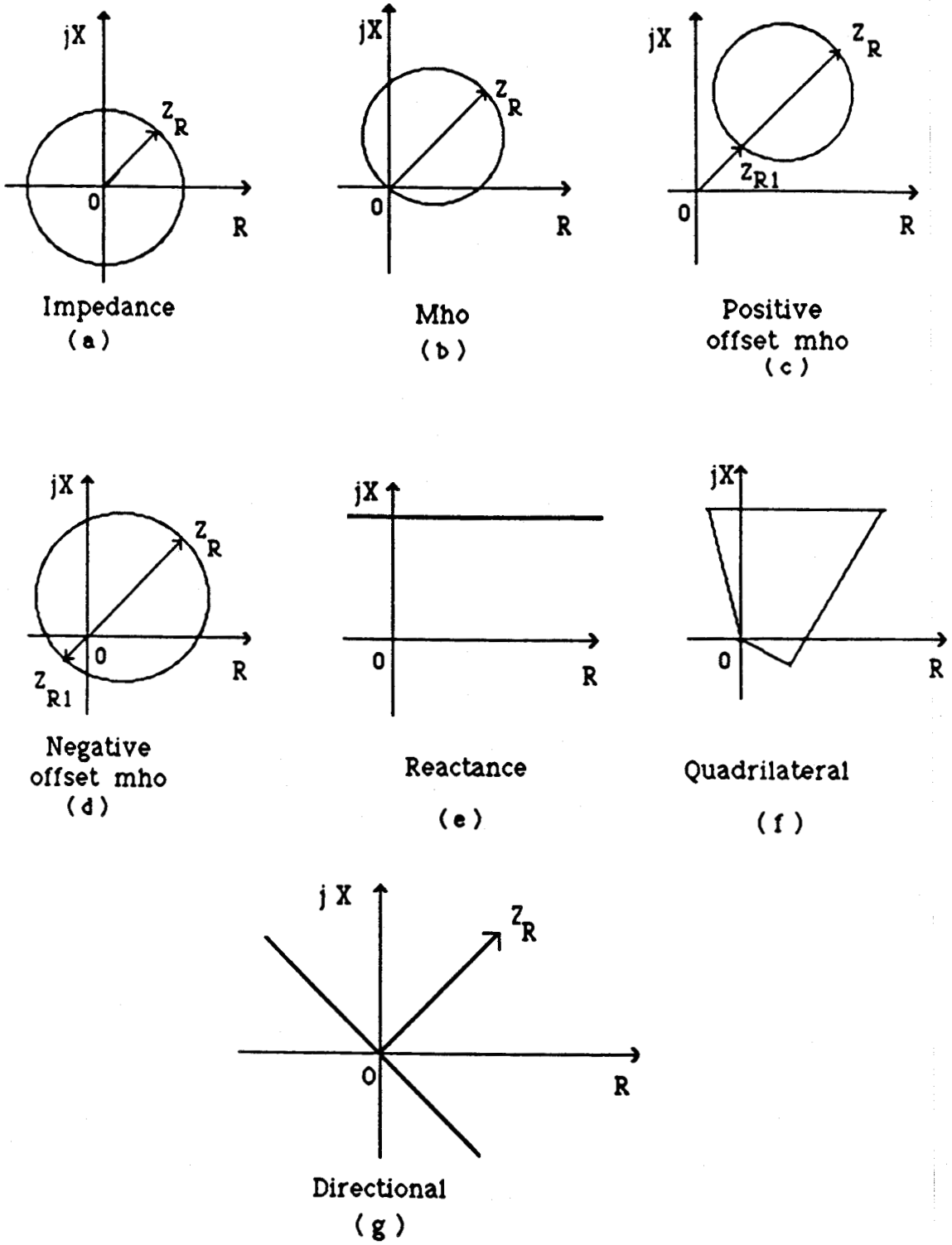

Figure 2.6: Typical distance relay characteristics drawn on the impedance plane.

2.5. Input Signals for Distance and Directional Relay Comparators

The comparators used in distance and directional relays define the characteristics exhibited by the relays on an impedance plane. The comparators receive signals proportional to the power system voltages and currents as described earlier. In general, the inputs signals are [7, 8]

$$S_0 \text{ or } S_1 = K_1 \angle \alpha_1 V_L + Z_{R1} I_L \tag{2.3}$$

$$S_R \text{ or } S_2 = K_2 \angle \alpha_2 V_L + Z_{R2} I_L \tag{2.4}$$

Figure 2.7 [7] shows a circuit diagram of a 2-input comparator. It illustrates a method of deriving the signals from a three phase power system. Suitable values are chosen for the constants K_1, K_2, Z_{R1} and Z_{R2} to achieve a wide range of comparator characteristics.

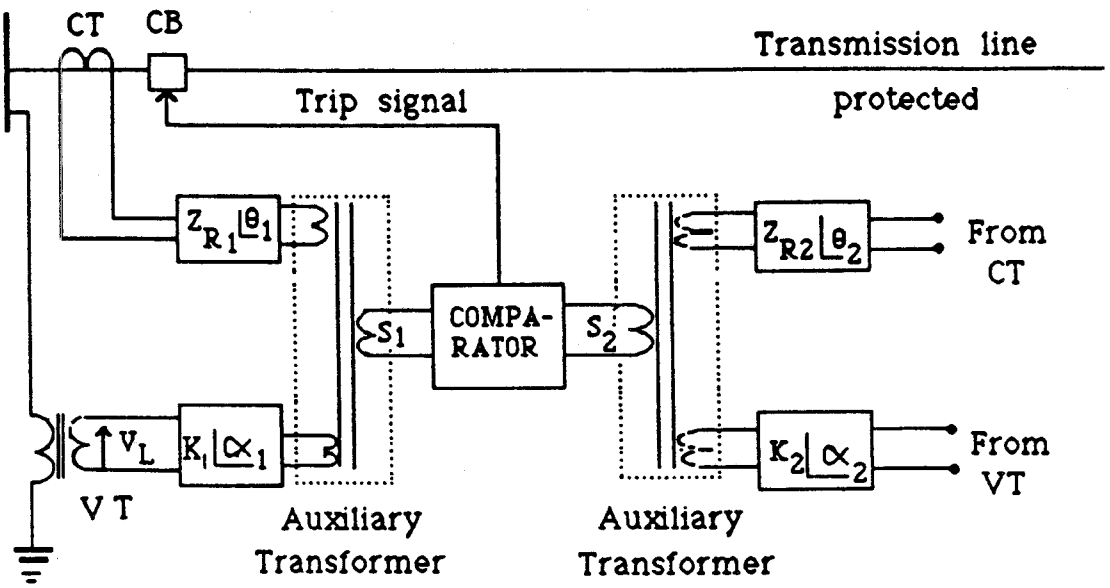

Figure 2.7: A circuit diagram of a 2-input comparator.

Tables 2.2 and 2.3 list the inputs for some of the comparators. More complex characteristics like the one exhibited by the quadrilateral relay can be derived by combining some of the inputs listed in the tables. Referring to the tables, V_L and I_L are the appropriate power system voltage and current at the relay location; Z_R is the replica impedance of the protected transmission line; and Z_{R1} is the impedance offset for an offset mho relay characteristic. The next subsection describes the input signals to a quadrilateral relay.

Table 2.2: The input signals for an amplitude comparator.

RELAY TYPE	OPERATING SIGNAL	RESTRAINING SIGNAL
Impedance	$I_L Z_R$	V_L
Mho	$I_L Z_R/2$	$V_L - I_L Z_R/2$
Offset Mho	$I_L(Z_R - Z_{R1})$	$2V_L - I_L(Z_R - Z_{R1})$
Reactance	$I_L X_R - V_L$	V_L
Directional	$0.5(V_L + I_L Z_R)$	$0.5(V_L - I_L Z_R)$

2.5.1. Inputs to a Quadrilateral Relay Comparator

The quadrilateral relay is realized with either a combination of four comparators or a combination of three comparators. The relay with three comparator arrangement is easy to implement and its input signals are discussed in this section. The signals to these comparators were first proposed by Johns [6] and they were derived from the signals of Tables 2.2 and 2.3. The amplitude comparator signals are derived as,

Table 2.3: The input signals for a phase comparator.

RELAY TYPE	MEASURING SIGNAL	POLARIZING SIGNAL
Impedance	$I_L Z_R$ - V_L	$I_L Z_R$ + V_L
Mho	$I_L Z_R$ - V_L	V_L
Offset Mho	$I_L Z_R$ - V_L	V_L - $I_L Z_{R1}$
Reactance	$I_L Z_R$ - V_L sin θ	$I_L Z_R$
Directional	$I_L Z_R$	V_L

$$S_{01} = -\ 0.5\ V_L + I_L\ Z_L \tag{2.5}$$

$$S_{R1} = -\ 0.5\ V_L \tag{2.6}$$

$$S_{02} = 0.5\ (V_L + I_L\ Z_R) \tag{2.7}$$

$$S_{R2} = 0.5\ (V_L - I_L\ Z_R) \tag{2.8}$$

$$S_{03} = 0.5\ I_L\ Z_R \tag{2.9}$$

$$S_{R3} = -\ V_L + 0.5\ I_L\ Z_R \tag{2.10}$$

For phase comparison the signals are as follows:

$$S_1 = -\ V_L + I_L\ Z_R \tag{2.11}$$

$$S_2 = V_L \tag{2.12}$$

$$S_3 = I_L\ Z_R \tag{2.13}$$

Figure 2.8 shows the quadrilateral distance relay characteristic drawn on the impedance plane. Boundary ABC results from a comparison of signals S_1

and S_3. The complete characteristic is obtained when signals S_2 and S_3 are compared to produce boundary COA. Reference [6] discusses the procedure for obtaining the limits of comparison for the quadrilateral relay phase comparators. From Figure 2.8, these limits are $-\theta$ and $+(\psi - \theta)$ and $-(\theta + \phi_2)$ and $+(\psi + \phi_1 - \theta)$.

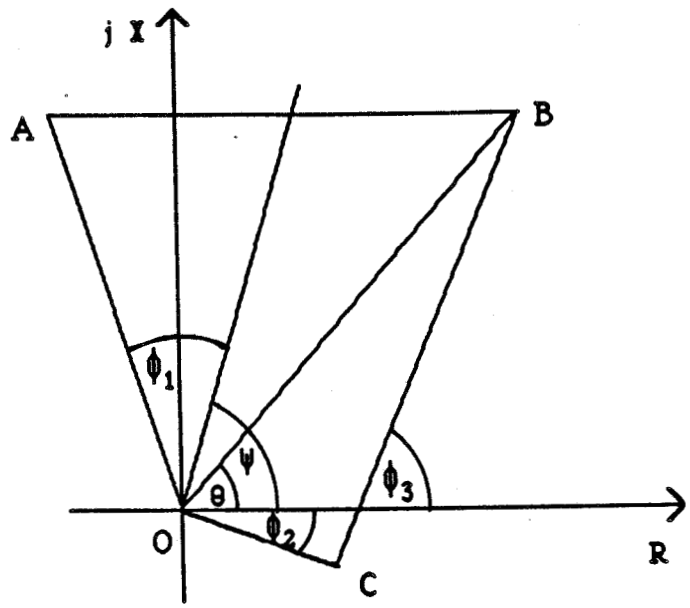

Figure 2.8: The operating characteristic of a quadrilateral relay.

2.6. Summary

The fundamental concepts of distance and directional relays and distance protection schemes have been presented in this chapter. The protection scheme for a transmission line is usually in the form of zones. A protection zone defines the length of a transmission line which a distance relay can protect. Comparators which measure the distance and direction of the fault have also been presented in this chapter. The behavior of a comparator depends on its input signals, therefore, when any of these signals collapses to zero, incorrect results are obtained from the comparator. The next chapter describes how this situation is corrected.

3. POLARIZATION AND MEMORY ACTION IN DISTANCE AND DIRECTIONAL RELAYS

3.1. Introduction

Comparators for distance relays use two or more inputs to perform amplitude or phase comparison. Close in faults cause one or more voltages to collapse. In these circumstances, the operation of the relay becomes uncertain. This situation is alleviated by using one of two approaches. One approach is to supplement the input voltages with the voltage of the healthy phase(s) or a combination of part healthy-phase voltage and part faulted-phase voltage. The use of the healthy phase voltage or combination of part healthy-phase voltage and part faulted-phase voltage is called polarization. The second approach uses the pre-fault voltages of the phases whose voltages are found to have collapsed. The use of a pre-fault voltage to compensate for the collapsed signal is referred to as memory action.

Wedepohl [9] investigated and reported the polarization applied to distance relays. Subsequent publications [10, 11] studied polarization of mho relays only. This chapter describes different forms of polarization and polarizing signals for mho relays. The technique is extended and applied to other distance relays.

3.2. Simplified Theory of the Polarized Distance Relay

Figure 3.1(a) [9] shows the single line diagram of a distance relay applied at a power system bus. The power system is represented as an equivalent source comprising of an *emf* behind a lumped impedance. Figure 3.1(b) [9] shows the block diagram for a phase comparator of the mho type distance relay. As discussed in Chapter 2, the two inputs are,

$$S_1 = - V_L + I_L Z_R \tag{3.1}$$

$$S_2 = V_L \tag{3.2}$$

where:

V_L is the voltage at the relay location,

I_L is the current at the relay location and

Z_R is the impedance setting of the relay.

Circuit analysis applied to Figure 3.1(a) shows that

$$V_L = \frac{E\ Z_L}{Z_S + Z_L} \tag{3.3}$$

and

$$I_L = \frac{E}{Z_S + Z_L} \tag{3.4}$$

where:

E is the induced *emf* of the equivalent source and

Z_S is the equivalent impedance of the source.

Substituting these equations in Equations 3.1 and 3.2 provides the input signals represented by the following equations.

$$S_1 = \frac{E(Z_R - Z_L)}{Z_S + Z_L} \tag{3.5}$$

$$S_2 = \frac{E\ Z_L}{Z_S + Z_L} \tag{3.6}$$

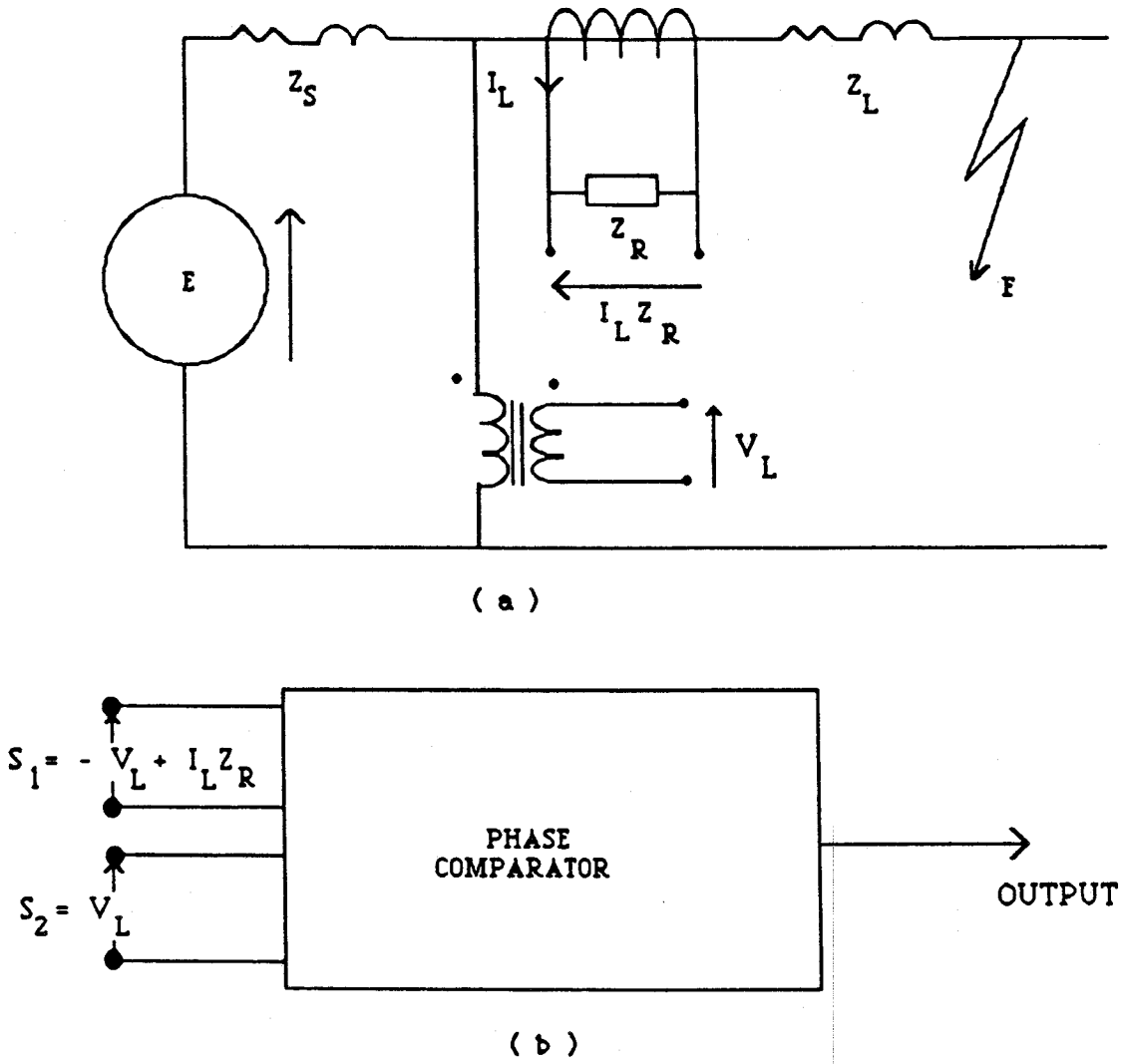

Figure 3.1: The schematic diagram of a mho relay; (a) system and relay connection arrangements and (b) phase comparator inputs.

Dividing both sides of the above equations with E and multiplying with $(Z_S + Z_L)$ provides the following equations:

$$S_1' = - Z_L + Z_R \tag{3.7}$$

$$S_2' = Z_L \tag{3.8}$$

The phase angle between S_1 and S_2 is the same as the phase angle between S_1' and S_2'. Applying the operating criterion $-90° \leq arg(S_1) - arg(S_2) \leq 90°$ provides the operating characteristic of the relay plotted on an impedance plane. The characteristic is the mho circle with Z_R as diameter. The relay requires a finite value of S_2 to operate. When a fault is close to the relay, S_2 is zero and the relay does not operate. This problem is solved by compensating S_2 with an additional voltage. Equations 3.5 and 3.6 are modified as follows:

$$S_1'' = \frac{E(Z_R - Z_L)}{Z_S + Z_L} \tag{3.9}$$

$$S_2'' = \frac{EZ_L}{Z_S + Z_L} + E_P \tag{3.10}$$

where:

E_p is the compensating voltage.

If the phase angle of E_P is the same as the phase angle of $EZ_L/(Z_L + Z_S)$, the phase angle between S_1'' and S_2'' would be the same as the phase angle between S_1 and S_2. Dividing with E and multiplying with $Z_S + Z_L$, Equations 3.9 and 3.10 transform to the following:

$$S_3'' = - Z_L + Z_R \tag{3.11}$$

$$S_4'' = Z_L + Z_P \tag{3.12}$$

where:

Z_p is $E_P(Z_S + Z_L)/E$ and is the impedance due to polarization.

Figures 3.2(a) and 3.2(b) [9] show the vector diagrams for the above analysis. The diagrams are for the mho relay and the polarized mho relay respectively. In practice, E_p, the polarizing voltage and V_L, the faulted phase voltage are not in phase for terminal faults. This is because of the characteristics of the system, principally unequal source-impedance / line-impedance angles. The effect of phase shifts between these two voltages modifies the relay input equations to the equations below.

$$S_3^{''} = - Z_L + Z_R \tag{3.13}$$

$$S_4^{''} = Z_L + Z_P \angle \alpha \tag{3.14}$$

Z_P and Z_L have the same phase, and the angle between E_P and V_L is accounted for by the additional rotation α.

The analysis assumes that the fault is near the location of the relay and that the additional voltage does not cause the relay to under-reach. If the fault is at the boundary of the protective zone, the increase in relay voltage due to polarization causes the apparent impedance of the line to be greater than the setting of the relay. In this situation the relay under-reaches. To alleviate this negative effect, different levels of the faulted phase voltage and the polarizing voltage are used. As a result Equation 3.14 is transformed to the equation below.

$$S_4^{''} = K_1 Z_L + K_2 Z_P \angle \alpha \tag{3.15}$$

where:

K_1 and K_2 are the polarization constants.

The constants K_1 and K_2 are chosen such that the impedance seen by the relay for an end of zone fault is the same as the setting of the relay. In some instances K_1 is made unity and the only way to avoid relay under-

reaching is to make K_2 as small as possible. These constants together with other power system parameters cause the position of the characteristic of a polarized relay to vary on an impedance plane. The next section describes the behavior of a polarized mho relay on the impedance plane for terminal faults.

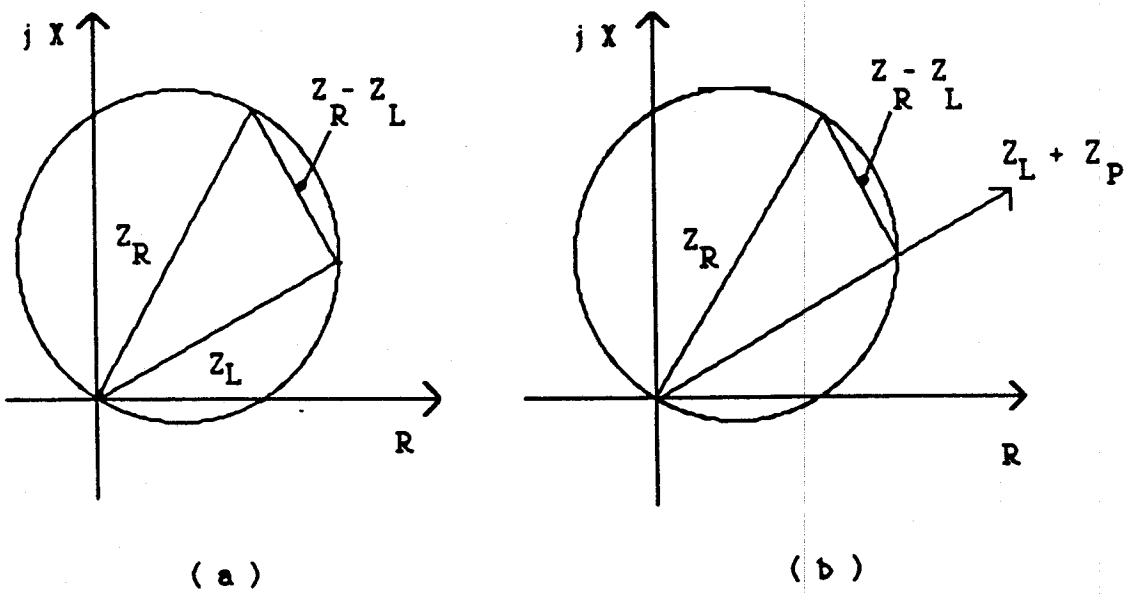

Figure 3.2: A simplified polarized mho behavior; (a) polarize and restraint voltages are the same and (b) polarize from different voltages.

3.3. Relay Characteristics During Close in Faults

Figure 3.3(a) shows a power system comprising of two generating stations. Two transmission lines transmit power between the buses A, B and C. Interphase or single phase to ground faults are assumed at locations F_1 and F_2. A mho type distance relay R, protects line BC. The characteristics of Figures 3.3(b) and 3.3(c)/3.3(d) [11] represent the behavior of the mho relay and the polarized mho relay for the two fault locations. The diagram of Figure 3.3(b) is the characteristic of the mho relay. This relay assumes

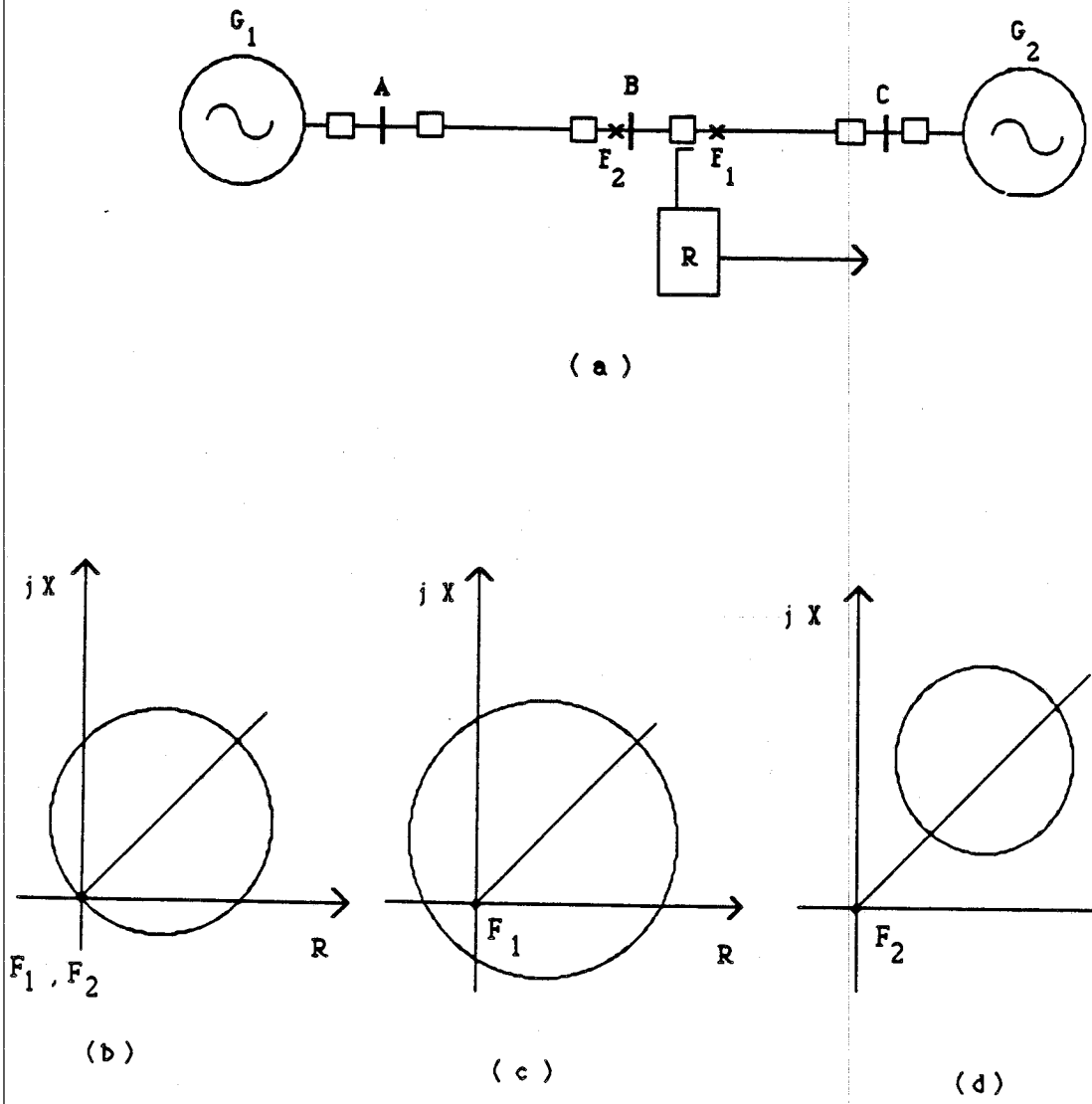

Figure 3.3: The operating characteristics of a mho relay and a polarized mho relay.

that the faults at F_1 and F_2 occur at the same location in the power system. In this situation the relay no longer becomes directional and operates falsely. When the fault is on the line side, F_1 in Figure 3.3(a), the characteristic of the polarized relay moves to include the origin, if the fault is on the bus side, F_2 in Figure 3.3(a), the characteristic moves to exclude the origin. Figures 3.3(c) and 3.3(d) show these two conditions.

It can be realized from these figures that the operating characteristic of a polarized distance relay is more complex than the conventional relay. The position and size of the characteristic depends on the various power system parameters including the polarization constants. The two main effects of polarization, therefore, are to offset the characteristic of a distance relay

1. in the negative direction for most forward faults and
2. in the positive direction for most reverse faults.

This increases the margin of operation for forward faults and non operation for reverse faults.

3.4. Forms of Polarization

There are two types of polarization. These are dual polarization and single polarization. A dual polarization controls the degree of offset of a distance relay characteristic by using different levels of faulted phase voltage and healthy phase voltage or the faulted phase voltage and a combination of part faulted-phase voltage and part healthy-phase voltage. The offset in the circular characteristic of the polarized mho relay is evident only during unbalanced short circuit conditions. For a cosine comparator, the mathematical expression for the polarizing signal S_2, of a mho relay is

$$S_2 = K_1 V_L + K_2 V_p \tag{3.16}$$

where:

V_P is the polarizing voltage.

The polarization constants K_1 and K_2 can be calculated if the fault levels of the power system are known. Appendix E describes a method for assigning values to these constants.

Single polarization uses only a healthy phase voltage or a combination of part healthy-phase voltage and part faulted-phase voltage with a suitable phase shift angle to produce the circular characteristic on the impedance plane. The equation for the polarizing signal is given as

$$S_2 = V_p. \tag{3.17}$$

When there is a three phase close in fault, all relay voltages collapse to zero. Polarization, therefore, becomes ineffective. A different technique of deriving the voltage combinations is used in this situation.

3.5. Memory Action

For an unbalanced close in fault, the voltage at the relay location collapses to near zero. Elements with no polarization have difficulty in determining the direction of the fault. Those with polarization however, have voltage from either the healthy phases or a combination of part healthy-phase voltage and part faulted-phase voltage. This ensures sufficient signal to make a measurement. Whether directional discrimination is satisfactory depends on the type of polarization. On a balanced three phase to ground fault, all phase-phase and phase-neutral voltages collapse to zero or near zero. Dual or single polarization becomes ineffective and the relay loses its ability to discriminate. In this situation memory action is required to make a meaningful measurement about the direction of the fault. In memory action, the polarizing signal is the pre-fault voltage of the faulted phase. A tuned (LC) circuit maintains this pre-fault voltage for a sufficient period of time after the occurrence of the fault.

3.6. Range of Polarizing Signals Considered

The polarization schemes presently in use have signals with various phase shift angles. This project uses polarizing signals that were proposed by Cook [10, 11]. Table 3.1 contains signals for four polarization schemes suggested in References [10] and [11].

From the table, the phase-phase unit of scheme one uses a phase-ground voltage at a phase shift of -90° for polarization. The phase-ground unit for this scheme uses a phase-phase voltage at a phase shift of +90°. The phase-phase unit of scheme two uses a phase-phase voltage and a phase shift of +60° for polarization. In the case of the phase-ground unit, a phase-ground voltage with a phase angle shift of +60° is used. Scheme three is an example of a single polarization technique where the phase-phase unit uses a phase-phase voltage with a phase angle shift of -60°. The phase-ground unit also uses a phase-phase voltage but with an angle shift of +90°. In scheme four, the phase-phase unit uses a phase-phase voltage and a phase shift of -90°. The phase-ground unit uses a phase-ground voltage with a shift of -60° for polarization. Scheme five is an example of memory action.

Directional relays encounter problems similar to those encountered by distance relays when there is a close in fault. When a directional relay is used in conjunction with a distance relay, the schemes described above can be applied to the composite relay. With other protective relays such as an over-current relay, a different method of deriving the input signals is used [12]. The next section discusses the inputs to directional relays.

Table 3.1: A list of recommended polarizing signals.

SCHEME	MEASURING UNIT FOR PHASE	POLARIZING SIGNAL
1	AB	$K_1V_{AB} + K_2V_C\angle -90^\circ$
	BC	$K_1V_{BC} + K_2V_A\angle -90^\circ$
	CA	$K_1V_{CA} + K_2V_B\angle -90^\circ$
	AG	$K_1V_A + K_2V_{BC}\angle +90^\circ$
	BG	$K_1V_B + K_2V_{CA}\angle +90^\circ$
	CG	$K_1V_C + K_2V_{AB}\angle +90^\circ$
2	AB	$K_1V_{AB} + K_2V_{AC}\angle +60^\circ$
	BC	$K_1V_{BC} + K_2V_{BA}\angle +60^\circ$
	CA	$K_1V_{CA} + K_2V_{CB}\angle +60^\circ$
	AG	$K_1V_A - K_2V_C\angle +60^\circ$
	BG	$K_1V_B - K_2V_A\angle +60^\circ$
	CG	$K_1V_C - K_2V_B\angle +60^\circ$
3	AB	$V_{CB}\angle -60^\circ$
	BC	$V_{AC}\angle -60^\circ$
	CA	$V_{BA}\angle -60^\circ$
	AG	$V_{BC}\angle +90^\circ$
	BG	$V_{CA}\angle +90^\circ$
	CG	$V_{AB}\angle +90^\circ$
4	AB	$K_1V_{AB} + K_2V_{CB}\angle -90^\circ$
	BC	$K_1V_{BC} + K_2V_{CA}\angle -90^\circ$
	CA	$K_1V_{CA} + K_2V_{BA}\angle -90^\circ$
	AG	$K_1V_A + K_2V_B\angle -60^\circ$
	BG	$K_1V_B + K_2V_C\angle -60^\circ$
	CG	$K_1V_C + K_2V_A\angle -60^\circ$
5	AB	V_{AB}
	BC	V_{BC}
	CA	V_{CA}
	AG	V_A
	BG	V_B
	CG	V_C

G represents ground.

3.7. Directional Relay Connections

If directional relays are made to respond to the actual fault voltages and currents, their operation would not always be satisfactory. The fault power-factor is usually low giving rise to a low operating signal. The relays in this case are much slower than expected. This is, however, not the only issue.

The other problem associated with directional relays is to preserve their discriminative feature at very low voltages which occur during faults close to the bus. To correct the problems discussed, voltages which will not reduce excessively during a fault except during a three-phase fault and which will retain a satisfactory phase relation to the current under all probable conditions are chosen to polarize each relay element. The voltage selection depends on the manner of relay connection to the instrument transformers. The type of connection gives the type of directional relay.

A directional relay commonly employs four main types of connections. These are, 90-degree, two forms of 60-degree and 30-degree connections. Table 3.2 [5, 13] contains the voltages and currents derived for the four main connections. Figure 3.4 depicts the phasor diagrams for the connections of the phase A elements. The phases B and C elements have similar phasor diagrams. The directional elements listed in the table are single-phase elements and their purpose is to achieve directional discrimination for phase-phase faults. Polyphase and ground directional units have been excluded since they require some special considerations.

3.8. Recommended Input Signals

Due to extensive research in distance relay polarization schemes, Cook [11] recommended that the input signals to a measuring element should be selected such that:

Table 3.2: The voltage and current inputs to a directional relay.

CONNECTIONS	RELAY A		RELAY B		RELAY C	
	V	I	V	I	V	I
90°	V_{BC}	I_A	V_{CA}	I_B	V_{AB}	I_C
60° No.1	V_{AC}	I_A-I_B	V_{BA}	I_B-I_C	V_{CB}	I_C-I_A
60° No.2	-V_{CN}	I_A	-V_{AN}	I_B	-V_{BN}	I_C
30°	V_{AC}	I_A	V_{BA}	I_B	V_{CB}	I_C

1. high speed protection is achieved for faults within the protected circuit,
2. the unit does not operate for reverse faults,
3. the operating characteristic accommodates sufficient fault resistance,
4. the relay should neither over-reach nor under-reach and
5. the healthy phase relays should not operate during forward faults.

These call for, carefully selecting the type of phase voltage, the polarization constants and the phase shifting angle.

3.9. Summary

In this chapter the theory of polarization as applied in distance protection schemes has been presented. The behavior of a distance relay or a directional relay depends on its comparator and the input signals. Greater care should therefore, be exercised when selecting relay input signals. Chapter 2 and this chapter have described distance relay comparators and their input signals. These comparators consist of digital hardware, such as sample and hold hardware, multiplexing hardware, analog to digital converters and

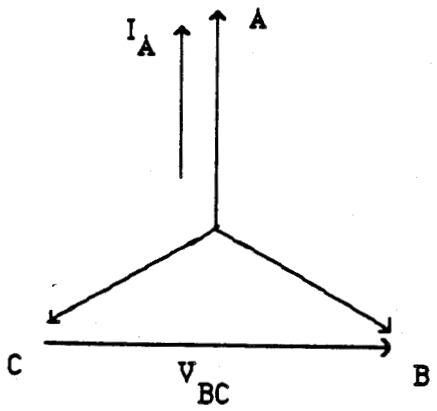

90° QUADRATURE CONNECTION

(a)

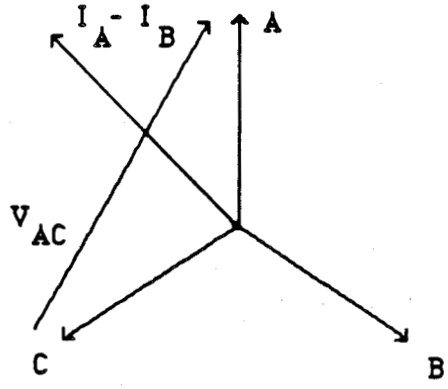

60° NO. 1 CONNECTION

(b)

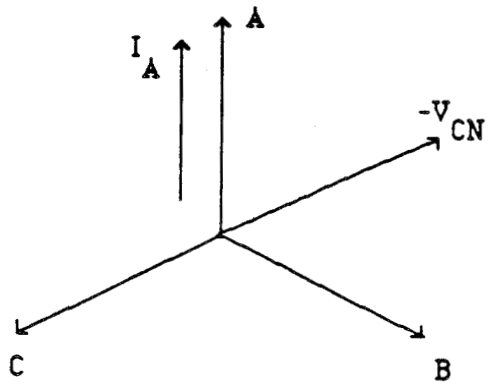

60° NO. 2 CONNECTION

(c)

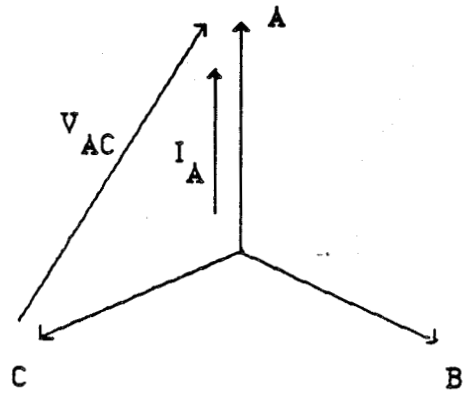

30° CONNECTION

(d)

Figure 3.4: The vector diagrams of voltages and currents for the phase A element of a directional relay.

micro-processors. The outputs from the comparators are affected by the characteristics of these devices. Chapter 4 describes these characteristics and their effects on the results computed by a digital relay.

4. DIGITAL RELAYS FOR TRANSMISSION LINE PROTECTION

4.1. Introduction

Transmission lines are protected by using combinations of different relays and circuit breakers. The relays detect the incidence of faults and if necessary, initiate the closing of contacts which open circuit breakers to isolate the faulted line. With increasing demand for electrical energy, power systems have become complex and the complexity demands that relays employed for transmission line protection be reliable, secure, accurate and take less time to make decisions. Electro-mechanical and static relays are presently being used for transmission line protection. Several researchers and organizations [2], however, have been conducting substantial research in the area of computer relaying for the last two decades.

Early research in the field of computer relaying [4] considered the use of a central computer for all the relaying functions in a substation. In the event of computer breakdowns, the use of a single computer would result in a complete failure of the entire substation protection. The need would, therefore, arise for a different computer to act as a backup. The use of two main-frame computers, a main and a standby, for a substation protection appeared too expensive to be commercially viable. Recent advances in microelectronics have resulted in the availability of low cost processors with enhanced capabilities. This has helped in the present view to use individual micro-computers dedicated to specific relaying functions.

This chapter discusses the functional details of a digital relay and the advantages of using digital technology and micro-processor based relays. The chapter also outlines briefly the previously proposed digital relaying algorithms, digital coding of signals and the errors arising from this procedure.

4.2. Functional Details of a Digital Relay

The major functional blocks of a micro-processor based relay are shown in Figure 4.1. The interconnections between the blocks depend on the actual hardware used to form the relay. Some blocks may not exist and some may be more significant than others depending on the functions to be performed by the relay. A digital relay monitors one or more operational parameters of the power system. Voltages and currents are the operational parameters generally used in protective relays. These parameters are time dependent continuous signals with magnitudes of several hundreds of kilovolts and several thousands of kiloamperes. The levels of these signals are mostly reduced to lower values.

The analog input sub-system receives low levels of voltages and currents provided by voltage transformers and current transformers respectively. The purpose of this system is to isolate the relay from the power system, provide protection from transient overvoltages, attenuate high frequencies sufficiently to minimize the consequences of aliasing, reduce the level of voltages and convert currents to equivalent voltage signals. Power system voltages and currents include high frequency components during faults. The voltage and current signals are sampled since digital devices accept discrete data. Depending on the rate at which a signal is sampled, some of the high frequency components may appear to be components of power frequency. Consider that the signal in Figure 4.2(a) [1] is a 660Hz voltage which is sampled 600 times per second. The result of the sampling process is shown in Figure 4.2(b). It could be seen from Figure 4.2(c) that, in the absence of additional information, the sampled voltage appears to have a frequency of 60Hz. This incorrect representation can cause digital relays to produce in-

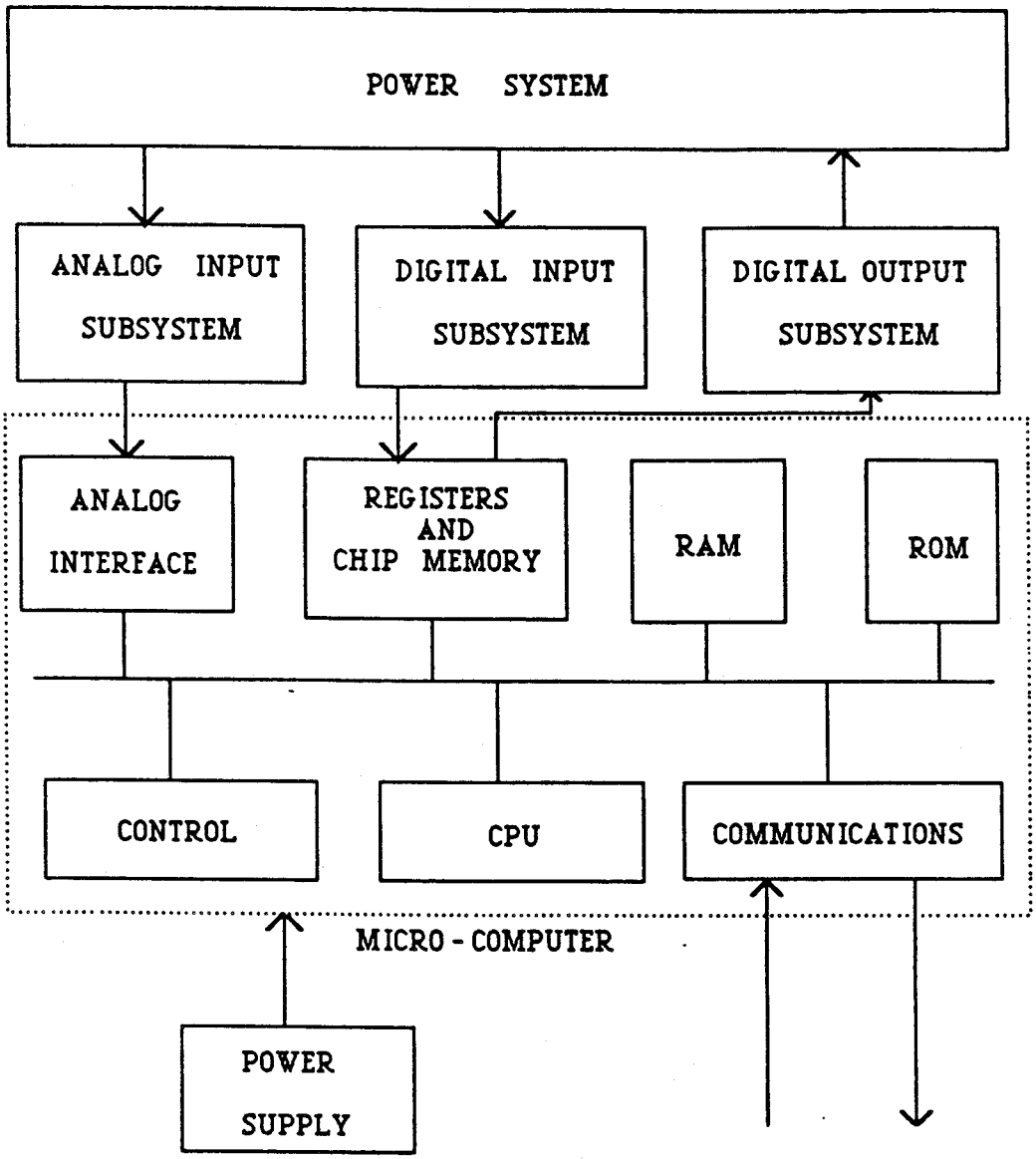

Figure 4.1: The functional block diagram of a digital relay.

correct results. To alleviate this problem, antialiasing filters are used. These filters should effectively attenuate frequencies equal to and more than one half the sampling rate.

The outputs of the analog input subsystem are applied to the analog interface subsystem. This subsystem includes sample and hold (S/H), analog to digital conversion (A/D) and multiplexing (MUX) hardware. The S/H hardware samples the signals at uniform intervals. Voltages, representing the instantaneous values of the inputs are held across capacitors for some time. A multiplexer applies each voltage in turn to an A/D converter which converts the levels of sampled voltages to equivalent digital numbers.

The digital input sub-system conveys to the relay the status of the power system circuit breakers, isolators and contacts. Relay targets and voltage sense information from the power system are also provided to the relay via the digital input sub-system. Input wiring must be properly shielded to protect the relay from transient voltages that may be experienced on the wiring.

The output of a digital relay is transmitted to the power system through the digital output sub-system. A relay may have several digital outputs. Some of these outputs provide signals for tripping circuit breakers and for annunciations. Proper isolation of the micro-processor output circuits from the power system and protection from transients must be included.

The digitized data are then entered into the Random Access Memory (RAM). The RAM keeps records of special events both on the power system and within the relay as historical files. A local computer accepts the data in the historical files as soon as possible to make the RAM free for the next occurrence of a transient. The programs of the relay reside in a non-volatile Read Only Memory (ROM). The controllers, central processing unit (CPU) and the registers work together to execute the programs, one statement at a time.

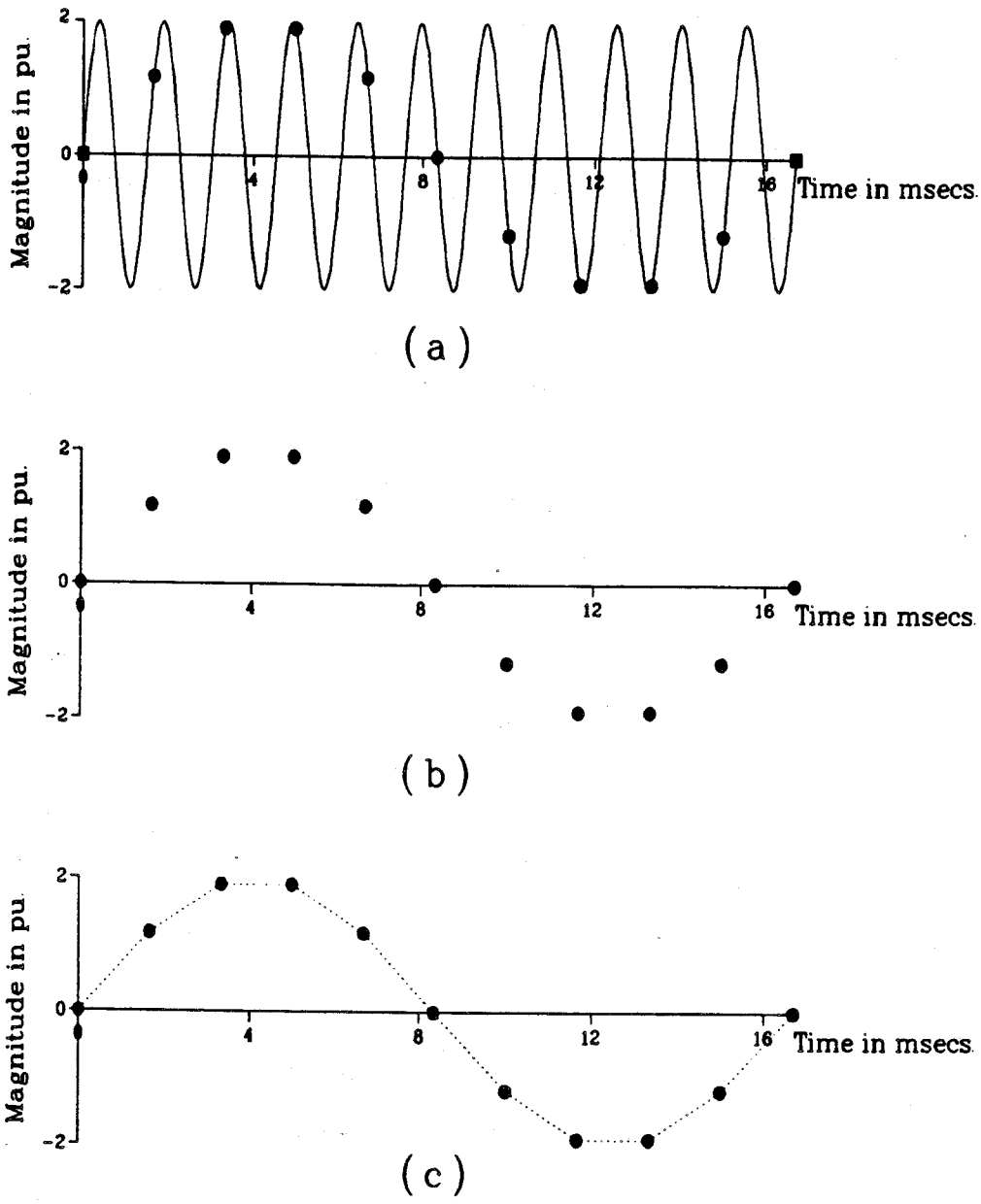

Figure 4.2: (a) A 660Hz voltage sampled 600 times per second. (b) The sampled information as a function of time. (c) Interpretation of the sampled information.

A digital relay requires uninterrupted supply of power. The power is supplied by a battery through a dc to dc converter. A battery charger or ac to dc converter keeps the battery fully charged at all times. In the event of ac failure the battery should be able to withstand the load for a considerable length of time.

4.3. Benefits of Digital Relaying

Recent advances in the field of micro-processors have enabled digital relays to be a viable alternative to electro-mechanical and static relays. The cost of conventional relays has been increasing during the last two decades, however, the cost of digital devices has been decreasing during the same time. It seems therefore, that digital relays will in future be more economical to use in a power system than electro-mechanical or static relays.

In addition to its relaying functions, a digital relay has the ability to perform other tasks, such as self diagnosis and data analysis. The benefits of these additional features can offset, to some degree, the higher cost of presently available digital relays. This section presents a summary of the specific advantages of using digital relays.

4.3.1. Flexibility

Digital relays are more flexible than the conventional relays. They are programmable devices and include multiple characteristics. Revision and modifications in digital relay characteristics, necessitated by changes in the operating conditions, can be made through pre-programmed modules. A single general purpose hardware based relay can be designed to perform a variety of protection and control functions with change of the programming only. Several of these functions can be called upon as needed. This would ultimately reduce the inventory required for repair and maintenance of relays as the presently used relays are replaced by their digital counterparts.

4.3.2. Reliability

The failure rate of digital equipment is higher than the components of conventional relays. Most digital relays are, however, designed to monitor themselves at regular intervals by executing the software together with pre-specified data and comparing the results with those expected from a properly functioning device. In the event of the results deviating from the expected values, the digital relay alerts an operator of the device failure. System reliability can be further increased by the relay checking its hardware at all times and flagging any failures. These features increase the reliability but, also increase the hardware and software costs.

4.3.3. Data-interface Access

A digital relaying system can always be equipped with input/output ports through which data and control commands can be exchanged. The pre-fault and post-fault signals can be stored in the relay memory and later transmitted to a central computer through a data link. This information can be used for further investigation that might lead to improved operating practices and relay design.

4.3.4. Adaptive Capabilities

A digital relay can be programmed to automatically change its behavior depending upon external circumstances which change with time. The basis for the change can be either local information available directly to the relay, such as load flow in the protected apparatus; or the change can be initiated from an external source of intelligence, such as a substation operator or a data link from a central system control computer. The change may only be in a specific setting of the relay or a whole new protection routine can be selected when needed.

4.3.5. Mathematical Capabilities

Designs of conventional relays are constrained by the characteristics and limitations of the electro-mechanical or solid state components. A digital relay can, however, be programmed to provide almost any function within the limits of imagination or understanding of the designer. Specific protection problems can be broken down into fine details, and each handled separately. A simple example related to distance protection of transmission lines is the ease with which arbitrary operating characteristic shapes on the impedance plane can be provided.

Many researchers of computer relaying have recognized and proposed possible equations which can serve as bases for distance protection of transmission lines. Brief analysis of these varied approaches is the principal subject of the next section.

4.4. Relaying Algorithms

In the previous sections the specific details of the sub-systems which constitute a digital relay were described. These sub-systems convert ac signals into digital form for processing. Also discussed are the benefits of using digital technology in power system protection.

This section presents algorithms which estimate parameters of interest for protection from samples of voltages and/or currents. The algorithms are combinations of mathematical equations and logic implemented on microprocessors. Digital relaying algorithms can be divided in two classes, those using nonrecursive and recursive filters. The nonrecursive filters use a finite number of data samples to obtain the estimates. The time period that contains these samples is called a data window. The outputs of the filters depend solely on the values of the samples in a data window. The outputs of the recursive filters are functions of the present inputs as well as all the previous inputs. This section presents only the nonrecursive algorithms which can be classified as

1. trigonometric algorithms,
2. least error square algorithms,
3. correlation algorithms and
4. others.

This review assumes that the signals under consideration are voltages. The same procedure, however, holds for current signals.

4.4.1. Trigonometric Algorithm

The trigonometric algorithms assume that the input voltages and currents are sinusoids of the nominal frequency. These signals can be expressed as

$$v = V_q \ sin(\omega_0 \ t \ + \ \theta_v) \tag{4.1}$$

where:

v is the instantaneous value,

V_q is the peak value,

θ_v is the phase angle,

ω_0 is the nominal frequency and

t is time in seconds.

The first derivative of the voltage with respect to time provides Equation 4.2.

$$v' = \omega_0 \ V_q \ cos(\omega_0 \ t \ + \ \theta_v) \tag{4.2}$$

Dividing both sides of this equation with ω_0 provides Equation 4.3.

$$\frac{v'}{\omega_0} = V_q \ cos(\omega_0 \ t \ + \ \theta_v) \tag{4.3}$$

Using Equations 4.1 and 4.3, the peak value and phase angle of the voltage signal can be obtained as follows:

$$V_q^2 = v^2 + (\frac{v'}{\omega_0})^2 \tag{4.4}$$

$$\omega_0 t + \theta_v = arctan(\omega_0 \frac{v}{v'}) \tag{4.5}$$

Mann and Morrison [14] estimated the first derivative v' from three consecutive samples. The sampling of the waveforms is done after every interval of ΔT seconds. If actual sampling times are $(k-1)\Delta T$, $k\Delta T$ and $(k+1)\Delta T$ seconds, then estimate of the first derivative at time $k\Delta T$ is mathematically expressed as,

$$v_k' = \frac{(v_{k+1} - v_{k-1})}{2\ \Delta T}. \tag{4.6}$$

Gilcrest et al [15], Rockefeller and Udren [16] used the first and second derivatives of the voltage equation to estimate its peak value and phase angle. The second derivative of the voltage equation is derived as

$$v'' = -\ \omega_0^2\ V_q\ sin(\omega_0\ t + \theta_v) \tag{4.7}$$

Equations 4.8 and 4.9 give the expressions which were used in References [15] and [16] to estimate the peak values and phase angles.

$$V_q^2 = (\frac{v'}{\omega_0})^2 + (\frac{v''}{\omega_0^2})^2 \tag{4.8}$$

$$\omega_0\ t + \theta_v = arctan(\frac{-v''}{\omega_0\ v'}) \tag{4.9}$$

Equations 4.6 and 4.10 are the mathematical expressions for the first and second derivatives of the voltage signal.

$$v_k'' = (\frac{1}{\Delta T})^2\ (v_{k+1} - 2\ v_k + v_{k-1}) \tag{4.10}$$

Makino and Miki [17] used two samples to determine the peak value and the phase angle of a sinusoid.

4.4.2. Least Error Squares Algorithm

Luckett et al [18] proposed the least error squares algorithm. The algorithm determines the peak values of voltages and currents and their phase angles. Brooks [19] also used this method assuming that the input signal is a combination of a dc component and a fundamental frequency component. Sachdev and Baribeau [20], investigated further and demonstrated that most of the computations can be done off line. The procedure to implement the least error squares technique consists of the following steps.

1. Select a suitable model for representing the signal,
2. linearize the model,
3. select a sampling rate,
4. select a data window size,
5. express the process in matrix form,
6. determine the left pseudoinverse of the coefficient matrix and
7. estimate the values of the elements in the vector of unknowns.

A voltage signal can be expressed by a mathematical model of the form of Equation 4.11.

$$v(t) = K_0\, e^{-t/\tau} + \sum_{m=1}^{N} K_m\, sin(m\omega_0 t + \theta_m) \tag{4.11}$$

where:

K_0 is the magnitude of the decaying dc component at t=0,

τ is the time constant of the dc component,

K_m is the magnitude of the mth harmonic component and

θ_m is the phase angle of the mth harmonic component.

The model represents a voltage that contains a decaying dc component, a fundamental frequency component and harmonics. Assume that the voltage is composed of the fundamental frequency component and a decaying dc component only. Its equation can be defined as follows:

$$v(t) = K_0\, e^{-t/\tau} + K_1\, sin(\omega_0\, t + \theta_1) \tag{4.12}$$

The exponential of the above equation can be replaced by the first two terms of its Taylor series expansion. Another substitution which is made is $\cos(\theta_1)\sin(\omega_0\ t) + \sin(\theta_1)\cos(\omega_0\ t)$ replacing $\sin(\omega_0\ t + \theta_1)$. The resulting equation after these substitutions is

$$v(t) = K_0 - (\frac{K_0}{\tau})\ t + (K_1\ cos\theta_1)sin(\omega_0\ t) + (K_1\ sin\theta_1)cos(\omega_0\ t) \tag{4.13}$$

At time $t=t_1$, the voltage equation becomes

$$v(t_1) = K_0 - (\frac{K_0}{\tau})\ t_1 + (K_1\ cos\theta_1)sin(\omega_0\ t_1) + (K_1\ sin\theta_1)cos(\omega_0\ t) \tag{4.14}$$

In linear form the representation of Equation 4.14 is given as

$$v(t_1) = a_{11}\ x_1 + a_{12}\ x_2 + a_{13}\ x_3 + a_{14}\ x_4 \tag{4.15}$$

where:

$$x_1 = K_0 \qquad a_{11} = 1$$

$$x_2 = -K_0/\tau \qquad a_{12} = t_1$$

$$x_3 = K_1\ cos(\theta_1) \qquad a_{13} = sin(\omega_0\ t_1)$$

$$x_4 = K_1\ sin(\theta_1) \qquad a_{14} = cos(\omega_0\ t_1)$$

The next voltage sample arrives at $t_2 = t_1 + \Delta T$. The linear representation of this voltage is given by Equation 4.16.

$$v(t_1 + \Delta T) = a_{21}\ x_1 + a_{22}\ x_2 + a_{23}\ x_3 + a_{24}\ x_4 \tag{4.16}$$

For a preselected time reference and known sampling rate, the values of the 'a' coefficients become specified. Assuming there are 'p' samples, the matrix equation is

$$\underset{p\times 4}{[A]}\ \underset{4\times 1}{[X]} = \underset{p\times 1}{[V]} \tag{4.17}$$

The unknown vector $[X]$ is determined as follows if 'p' is greater than four.

$$\underset{4\times 1}{[X]} = \underset{4\times p}{[A]^{+}}\ \underset{p\times 1}{[V]} \tag{4.18}$$

where:

$[A]^{+}$ is the left pseudo-inverse of $[A]$.

Its mathematical model is

$$\underset{4\times p}{[A]^{+}} = \underset{4\times p}{[[A]^{T}}\ \underset{p\times 4}{[A]]^{-1}}\ \underset{4\times p}{[A]^{T}} \tag{4.19}$$

The elements of $[A]^{T}$ can be determined off-line. This reduces substantially the on-line calculations necessary for estimating the real and imaginary components of the phasors.

4.4.3. Correlation Algorithm

A signal can be correlated with itself, with other signals, or with some selected functions. This will lead to the extraction of the real and imaginary parts of the fundamental frequency component of the signal. Ramamooty [21] suggested that the information concerning the fundamental frequency voltage and current phasors can be extracted from the fault transients by correlating one cycle of data samples with the samples of sine and cosine waves of that frequency. Figure 4.3 [22] shows the correlation process. It can be expressed mathematically as follows:

$$v_r = (\frac{2}{m}) \sum_{n=0}^{m-1} V_{k+n-m+1}\ sin(\frac{2\pi n}{m}) \tag{4.20}$$

$$v_i = (\frac{2}{m}) \sum_{n=0}^{m-1} V_{k+n-m+1}\ cos(\frac{2\pi n}{m}) \tag{4.21}$$

where:

m is the number of samples per second,

v_r is the real part of the fundamental frequency component of the signal and

v_i is the imaginary part of the fundamental frequency component of the signal.

Equations 4.22 and 4.23 determine the peak value and phase angle of the voltage using the correlation approach.

$$V_q = \sqrt{V_r^2 + V_i^2} \tag{4.22}$$

$$\theta_v = arctan(\frac{v_i}{v_r}) \tag{4.23}$$

Implementing the correlation approach Phadke et al [23] used a data window of half cycle plus one sample.

Another group of functions that use the correlation algorithms are even and odd rectangular waves [24]. Figure 4.4 shows these two functions. In mathematical form they are expressed as follows:

$$W_r(t) = signum(sin(\omega_0\ t)) \tag{4.24}$$

$$W_i(t) = signum(cos(\omega_0\ t)) \tag{4.25}$$

where:

$$signum(x) = -1\ for\ x < 0,$$

$$= 0\ for\ x = 0,$$

$$= 1\ for\ x > 0,$$

$W_r(t)$ is the odd rectangular wave and

$W_i(t)$ is the even rectangular wave.

The real and imaginary components of the fundamental frequency voltage phasor are represented by the following equations.

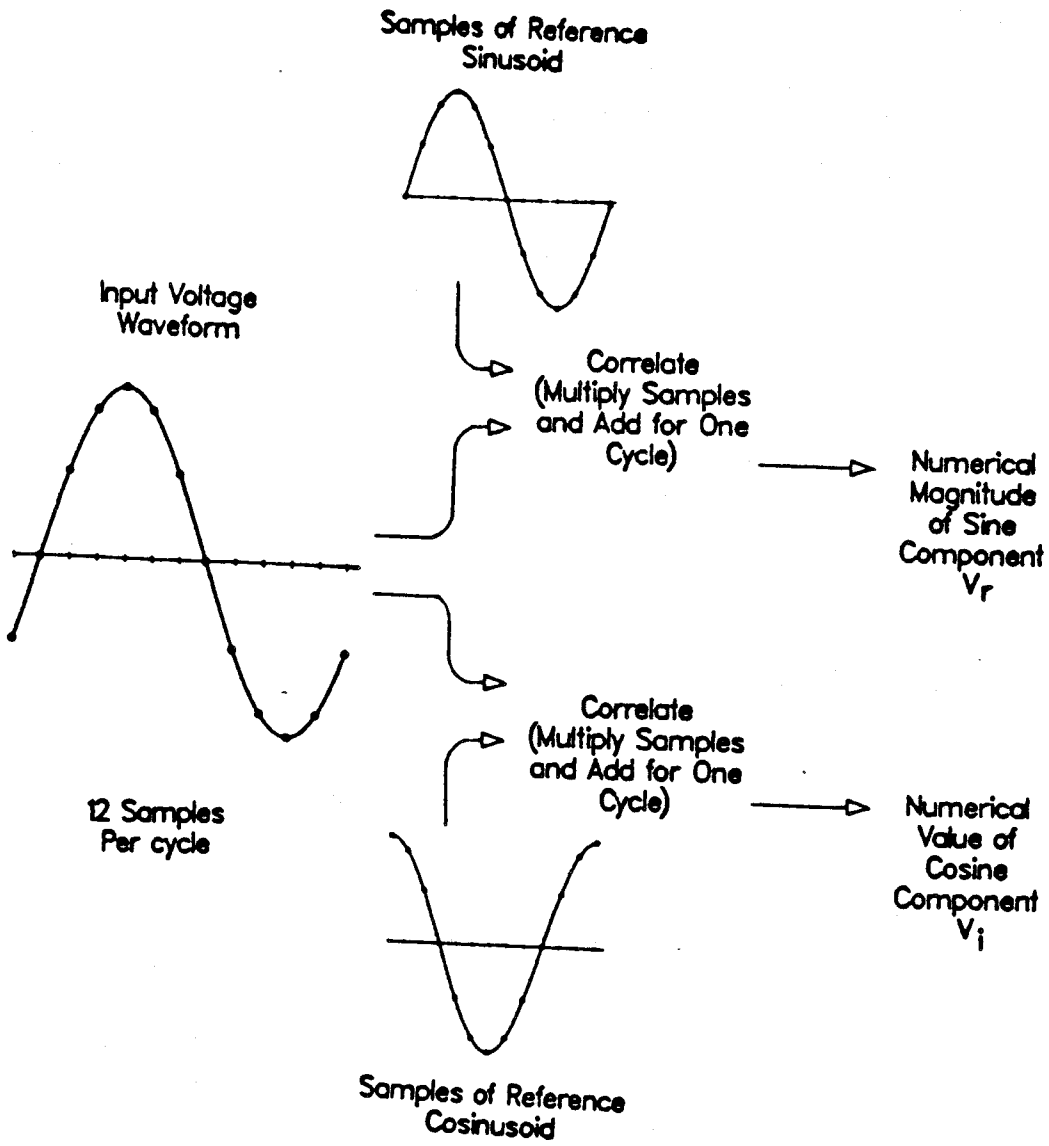

Figure 4.3: The correlation of an input waveform with sine and cosine functions.

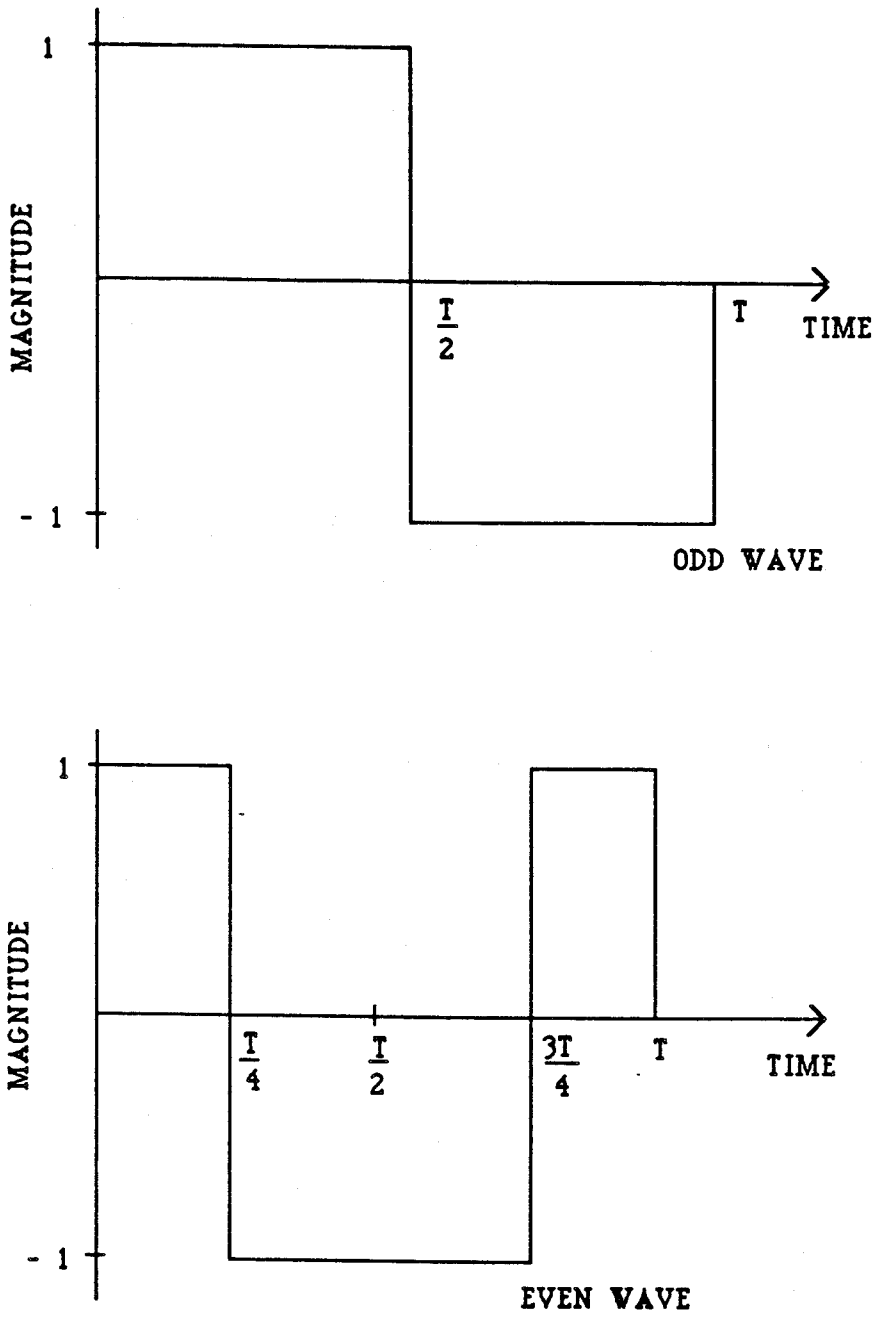

Figure 4.4: Even and odd rectangular waves.

$$v_r = (\frac{1}{A}) \sum_{n=0}^{m-1} V_{k+n-m+1} signum(sin(\frac{2\pi n}{m})) \tag{4.26}$$

$$v_i = (\frac{1}{A}) \sum_{n=0}^{m-1} V_{k+n-m+1} signum(cos(\frac{2\pi n}{m})) \tag{4.27}$$

where:

A is the scaling factor.

The computations involved in these equations are only additions and subtractions and, therefore, it becomes advantageous to use this technique. Schweitzer et al [25] used this approach to calculate the fundamental and harmonic frequency components of signals. For transmission line protection, Hope et al [26] used cross-correlation and auto-correlation of currents and voltages. Equations 4.28 and 4.29 represent mathematically the procedure they suggested.

$$\psi_1(t) = (\frac{1}{N}) \sum_{n=1}^{N} i_{k+n} i_{k+n+m} \tag{4.28}$$

$$\psi_2(t) = (\frac{1}{N}) \sum_{n=1}^{N} i_{k+n} v_{k+n+m} \tag{4.29}$$

where:

ψ_1(t) and ψ_2(t) are the auto-correlation and cross-correlation functions respectively and

m is the lag.

4.4.4. Others

McInnes and Morrison [27] used a differential equation approach for modelling a digital distance relay. They assumed an R-L lumped-parameter model of the transmission line. With the aid of sampled data the line impedance as seen by the relay was determined. Further modifications were suggested by Breingan et al [28] to this approach. Phadke et al [29] suggested the use of symmetrical components for digital distance relay-

ing algorithms. They demonstrated that a single criterion can be developed for detecting all types of short circuit faults that are likely to occur on transmission lines. Carr and Jackson [30] also demonstrated the use of frequency domain analysis in digital transmission line protection.

4.5. Digital Coding of Signals

Digital signals in digital relaying systems are usually represented by digital words or codes [31]. The information carried by a digital word is generally in the form of discrete bits (logic pulses of '0' or '1') coded in a serial or parallel format. The numerical value of a digital word then represents the magnitude of the information in the variable which this word represents. This is the binary form of number representation.

Each of the binary digits (0 or 1) is referred to as a bit. Bits are strung together (from 8 to 32) to form larger units. In this way a byte is obtained. Also, several of the bytes can be placed together to form a word. Figure 4.5 illustrates the relation between word, byte and bit. Digital words in a computer are represented as fixed-point numbers or floating point numbers.

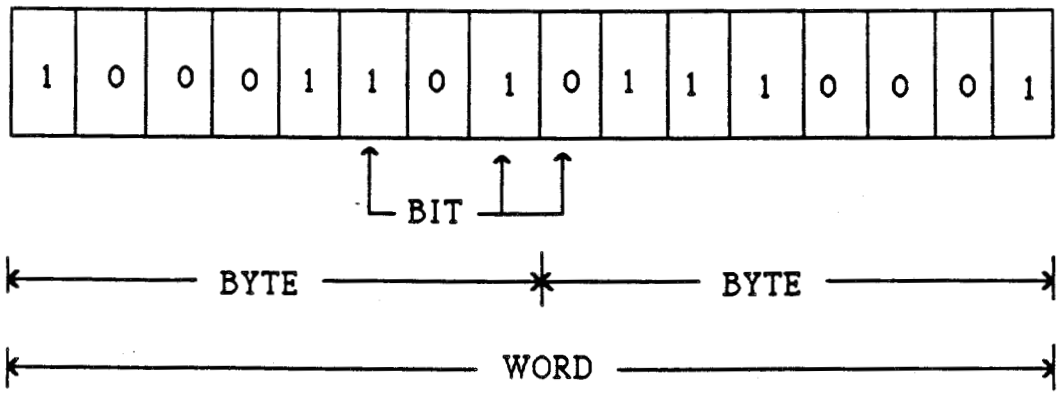

Figure 4.5: The relation between a word, a byte and a bit.

4.5.1. Fixed-Point Number Representation

If all the 16 bits of the word shown in Figure 4.5 are used to represent a number, where each bit can be a 0 or a 1, the fixed-point number representation is obtained. In general, an n-bit binary word representing a fixed-point integer number is written as

$$N = a_{n-1}2^{n-1} + \ldots + a_2 2^2 + a_1 2^1 + a_0 2^0 \tag{4.30}$$

where:

the coefficients $a_i (i = 0,1,2, \ldots ,n-1)$ are either 0 or 1.

The digits of the number in Equation 4.30 are ordered from left to right with the most significant bit (MSB) being a_{n-1} on the left and the least significant bit (LSB), a_0, on the right.

Fixed point representation can also be used to represent fractional numbers. An $n-bit$ fraction can in general be represented as

$$N = a_{-1}2^{-1} + a_{-2}2^{-2} + \ldots + a_{-n}2^{-n} \tag{4.31}$$

where:

the coefficients $a_i (i = -1,-2, \ldots ,-n)$ assume the value of 0 or 1.

The first coefficient a_{-1} represents the MSB and the LSB is a_{-n}.

Negative numbers may be represented by assigning the first bit of the binary word as a sign bit; ie., 0 for '+' and 1 for '-'. An alternative method of representing negative numbers is to use the two's complement and one's complement algorithms. In general an integer is represented by an n-bit word and lies between $(2^{n-1} - 1)$ and $-(2^{n-1} - 1)$; the limits included [31]. In a similar fashion a sign bit can be used for the representation of a non-integer or fraction. The fractional number can be represented by an n-bit word with a sign bit and m fractional bits. The binary number lies between $(2^{n-1} - 1)2^{-m}$ and $-(2^{n-1} - 1)2^{-m}$, inclusively [31].

4.5.1.1. Floating-Point Number Representation

The numbers are sometimes represented using the floating-point number representation. The first part of the data is used to store a number called the mantissa, and the second part is the exponent. In digital computers and systems, binary floating-point numbers are usually represented as

$$N = M \times 2^E \tag{4.32}$$

where:

M is the mantissa and

E is the exponent of the number N.

M is usually scaled to be a fraction whose decimal value lies in the range of 2^{-1} and 1. Figure 4.6 shows a floating point representation of an $8-bit$ word with a $5-bit$ mantissa and $3-bit$ exponent. Since the mantissa and the exponent can be both positive and negative, the first bits of the mantissa and the exponent are the sign bits. The first two bits of the entire word can, however, be used as the sign bits of the mantissa and exponents, respectively.

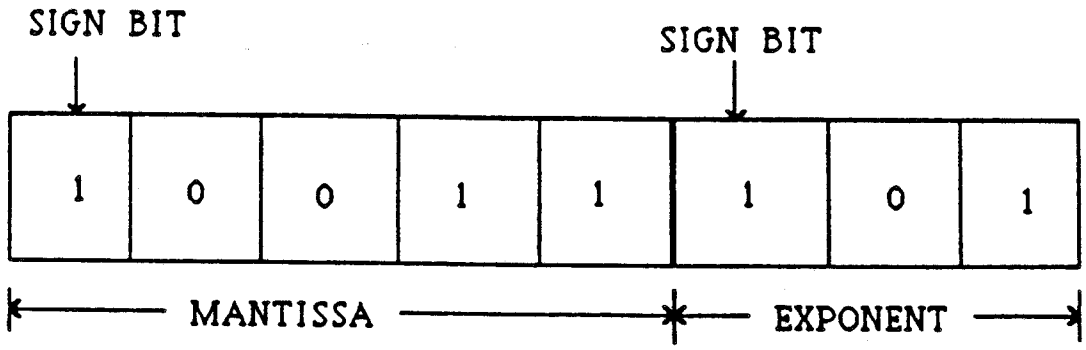

Figure 4.6: The floating-point representation of an 8-bit number.

4.6. Errors in Digital Relays

The advantages of using digital relays have been discussed in Section 4.2. Due to binary representation of the input signals, relays have inherent problems which limit the accuracy of the estimates computed by the algorithms of Section 4.3. The coefficients of digital filters (relay algorithms) cannot be represented precisely in processors. The responses of these filters implemented on micro-processors, therefore, differ from those of the precise implementations. Errors in computations are also introduced when the results of arithmetic operations are stored in words of finite sizes. The effects of finite word sizes in digital filters are described in References [32] and [33]. The design of an A/D converter is for an input of a specified range. When this input is out of this range, the A/D converter saturates, resulting in an incorrect representation of the input. This section briefly describes the sources of errors associated with digital relays.

4.6.1. Analog to Digital Converter Errors

Assume that an A/D converter has b+1 bits. If an analog voltage, v, is applied to this converter, then the binary output is $Q(v)$. In most instances the binary representation is not equal to the true value of the analog input. Ideally, an infinite number of bits may be required to accurately represent some analog inputs within the specified range. For actual implementations, these numbers are either truncated or rounded to fit into a selected word length.

4.6.1.1. Truncation Errors

For a truncated binary representation, the difference between a quantized number and the true number, $Q(v) - v$, is the truncation error. For positive numbers, this error is negative or zero. The largest error is when all the discarded bits are unity. Thus for truncation of numbers

$$0 \geq \epsilon \geq -2^{-b} \tag{4.33}$$

where:

ϵ is the truncation error and

b is the number of bits in the word of the processor.

The truncation error for negative numbers depends on the type of binary arithmetic used. For the sign and magnitude, and one's complement methods,

$$0 \leq \epsilon \leq 2^{-b}. \tag{4.34}$$

If two's complement method of representing binary numbers is used, the truncation errors are negative. The mathematical expression which describes this is

$$-2^{-b} \leq \epsilon \leq 0. \tag{4.35}$$

4.6.1.2. Rounding Errors

An alternate method to truncation is rounding. This process consists of choosing the closest quantization level. A number lying exactly halfway between two quantization levels either rounds up or down. This number is generally rounded up if its value differs from the quantized value by one half the least significant bit (LSB) or more, else it is rounded down. Assuming that a number lying exactly halfway between two steps always rounds up, the following inequality describes the rounding error.

$$-\frac{1}{2}2^{-b} < \epsilon \leq \frac{1}{2}2^{-b} \tag{4.36}$$

Rounding errors are independent of the method of representing negative numbers. Figure 4.7 [32] shows the quantized value as a function of input signal for both truncation and rounding.

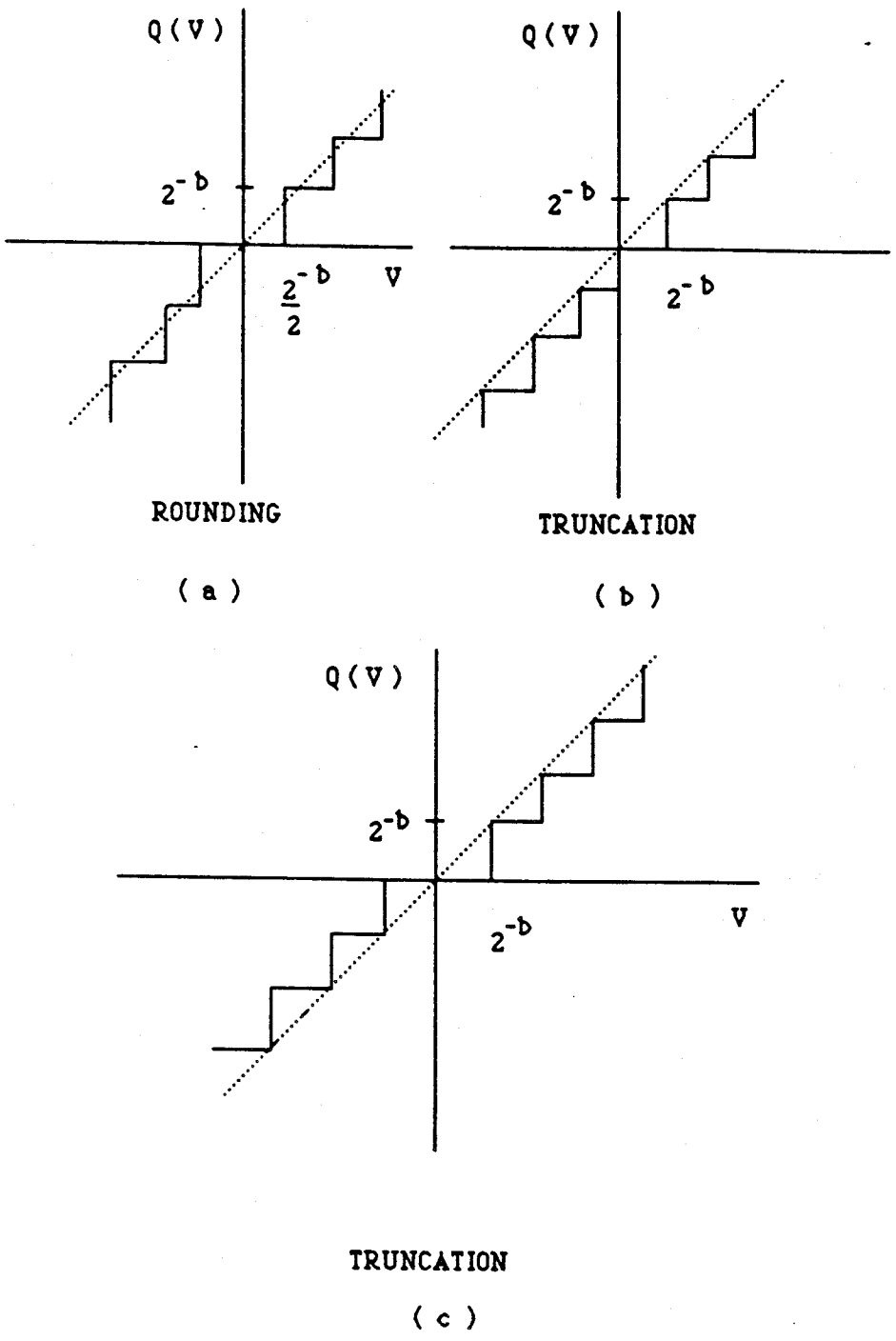

Figure 4.7: The nonlinear relationships representing: (a) rounding, (b) truncation (two's complement) and (c) truncation (sign and magnitude, and one's complement).

4.6.1.3. Saturation Errors

An A/D converter accepts input voltages in a specified range. If the voltage exceeds this range the converter saturates. As a consequence the digital representation will not truely represent the analog signal. Figure 4.8 [22] shows the digital representation of a sinusoidal signal with a 12V peak value that an A/D converter designed for ± 10V range provides. The output of a digital relay will not be certain when such a clamped signal is processed.

4.6.2. Digital Processor Errors

The results of arithmetic operations such as additions, subtractions, multiplications and divisions cannot always be stored in the finite word size of the processor. An example is the evaluation of two numbers with b+1 bits each. The result is a number which cannot be stored in a word of b+1 bits. Truncation or rounding is needed at such instances. Errors due to truncation or rounding will accrue as the computations proceed. The use of multiple word lengths of processors will, however, reduce these errors.

4.6.3. Software Errors

Errors arising from the software could be due to several factors. Two major sources of errors are identified in this section. One factor is the way filter coefficients are represented by their equivalent binary numbers. The second factor is due to the use of bit shifting approach for multiplications and divisions.

4.6.3.1. Effects of Inaccuracies in Coefficient Representation

When implementing a relaying algorithm on a micro-processor, equivalent binary numbers are used to represent filter coefficients. A binary number, equivalent to b+1 bits represents each coefficient due to the finite word length of the processor. The difference between the binary representations and the true values will adversely affect the filter characteristic. This consequently affects the accuracy of the results.

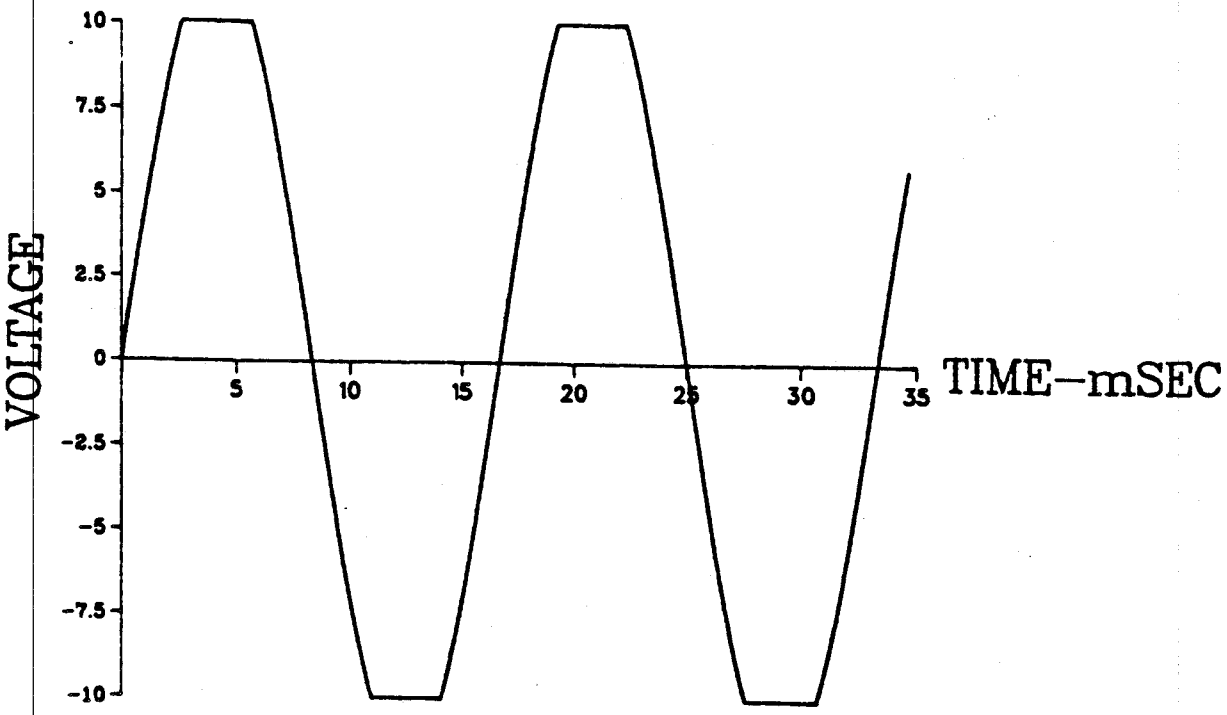

Figure 4.8: Representation of a signal as interpreted by a saturated A/D converter.

4.6.3.2. Errors Due to Bit Shift Approach of Multiplications

Designers of digital relays use the bit shift approach to implement multiplications on micro-processors that do not have the multiplication facility. In some situations this approach reduces software execution time. The filter coefficients which are fractional values multiplies the digitized values of the input. This is achieved by representing each filter coefficient as a series function. The multiplications are then implemented by a set of bit shift, add and subtract instructions. This approach introduces computation errors since the series may not precisely represent the filter coefficients. These errors also depend on whether the arithmetic operation uses rounding or truncation. The errors accumulate for multiple shift operations.

4.7. Summary

The chapter has presented the functional blocks of a typical digital relay. Also presented are the advantages of digital relays over conventional relays (electro-mechanical and static). Digital relays use a set of mathematical equations or relaying algorithms to estimate the parameters of interest in a power system protection. Some of these algorithms and the errors that are introduced due to the characteristics of the relay hardware have been discussed. In the next chapter the voltage and current estimates from the relaying algorithms are used to model digital distance and directional relays.

5. MODELLING DIGITAL DISTANCE AND DIRECTIONAL RELAYS

5.1. Introduction

Distance and directional relay comparators are presented in Chapter 2. These comparators have characteristics which are represented on the impedance plane either as curves or straight lines. The method of representing these characteristics on the impedance plane was also discussed. Comparators accept signals which are proportional to power system voltages and currents. The procedure for obtaining the signals and the scaling that should be used are discussed in Chapter 3. Chapter 4 discusses the hardware of a digital relay and the algorithms used by the relays to estimate the peak values of voltages and currents. The effects of rounding, truncation and A/D converter saturation on the estimated values are also discussed in Chapter 4.

This chapter is concerned with the modelling of digital distance and directional relays. Digital distance and directional relays considered are the

1. mho relay,
2. composite mho/reactance relay,
3. quadrilateral relay,
4. single phase directional relays and
5. directional/impedance relay.

Each relay operates as an amplitude comparator or as a phase comparator. The input signals to these comparators were discussed in Chapter 2. They are reproduced here in Tables 5.1 and 5.2.

Table 5.1: The input signals for an amplitude comparator.

RELAY TYPE	OPERATING SIGNAL	RESTRAINING SIGNAL
Impedance	$I_L Z_R$	V_L
Mho	$I_L Z_R/2$	$V_L - I_L Z_R/2$
Offset Mho	$I_L(Z_R - Z_{R1})$	$2V_L - I_L(Z_R - Z_{R1})$
Reactance	$I_L X_R - V_L$	V_L
Directional	$0.5(V_L + I_L Z_R)$	$0.5(V_L - I_L Z_R)$

Table 5.2: The input signals for a phase comparator.

RELAY TYPE	MEASURING SIGNAL	POLARIZING SIGNAL
Impedance	$I_L Z_R - V_L$	$I_L Z_R + V_L$
Mho	$I_L Z_R - V_L$	V_L
Offset Mho	$I_L Z_R - V_L$	$V_L - I_L Z_{R1}$
Reactance	$I_L Z_R - V_L \sin \theta$	$I_L Z_R$
Directional	$I_L Z_R$	V_L

5.2. Modelling of a Mho Relay

The author of this thesis developed models for mho relays which use

1. amplitude comparison,
2. phase comparison,
3. direct impedance estimation and
4. memory mapped targeting techniques.

The operation of amplitude and phase comparators has been discussed in Chapter 2. The direct impedance estimation technique calculates the impedance seen from a relay location and compares it with the desired characteristic of the relay. Memory mapped targeting uses the same procedure except that the characteristic of the relay is segmented into squares. Each segment is assigned with a value of one and stored as a matrix. The impedance seen from the relay location is also assigned with either a one or zero depending on its location on the impedance plane. The value assigned to the line impedance is compared with the elements of the matrix.

5.2.1. Amplitude Comparison Technique

The developed model performs amplitude comparison by computing the magnitudes of the operating and restraining signals and comparing them. The model provides a trip output if the magnitude of the operating signal is greater than the magnitude of the restraining signal.

5.2.2. Phase Comparison Technique

The developed model performs phase comparison using two methods. The first method consists of computing the phase angles of phasors representing the measuring and polarizing signals. The model provides a trip output if the difference between the angles is within the limits set for the comparator, which is $\pm$ 90 $^{\circ}$ in the software. The second method consists of computing the dot product of the phasors representing the measuring and

polarizing signals. If the product is positive, the model provides a trip output.

5.2.3. Direct Impedance Estimation Technique

The direct impedance estimation technique uses a model of the characteristic of the relay. Figure 5.1 shows the relay characteristic drawn on the impedance plane.

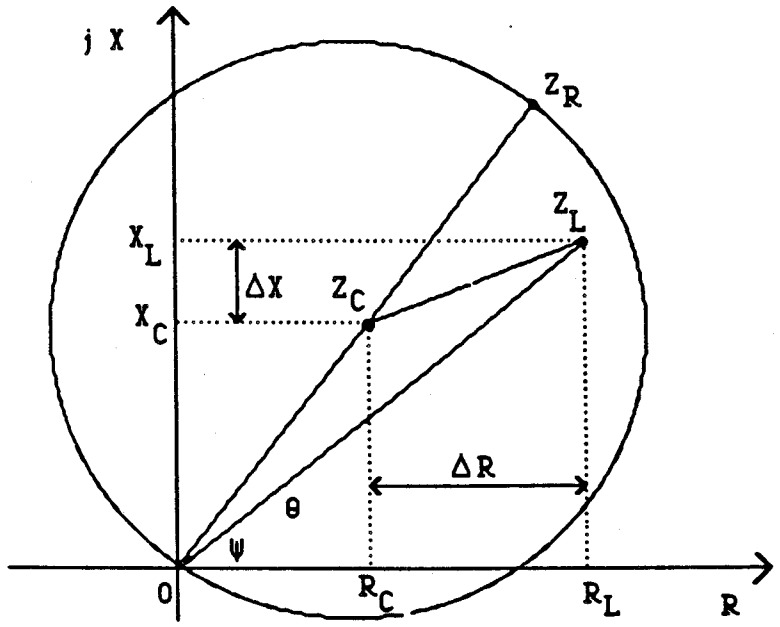

Figure 5.1: The operating characteristic of a mho relay.

The magnitude and angle of Z_R, the relay setting, is known. The radius of the characteristic and the coordinates of the center of the circle are, therefore, known. If the impedance seen by the relay is $Z_L \angle \psi$, its real and imaginary components define the coordinates of Z_L. The coordinates of Z_C and Z_L can be expressed as

$$R_C = Z_C \cos\theta \tag{5.1}$$

$$X_C = Z_C \sin\theta \tag{5.2}$$

$$R_L = Z_L \cos\psi \tag{5.3}$$

$$X_L = Z_L \sin\psi \tag{5.4}$$

where:

Z_C is the radius of the mho circle,

R_C and X_C are the coordinates for the center of the mho circle,

R_L and X_L are the coordinates of the fault impedance,

θ is the maximum torque angle of the relay and

ψ is the phase angle of the fault impedance.

The magnitude of the vector from the center to Z_L is determined in the developed model using the following equations.

$$\Delta R_{CL} = R_L - R_C \tag{5.5}$$

$$\Delta X_{CL} = X_L - X_C \tag{5.6}$$

$$|Z_{CL}| = \sqrt{\Delta R^2_{CL} + \Delta X^2_{CL}} \tag{5.7}$$

where:

$|Z_{CL}|$ is the magnitude of the vector from the center of the circle to the fault location.

$|Z_{CL}|$ and the radius of the circle are compared in the model. A trip output is provided if $|Z_{CL}|$ is less than the radius of the circle.

5.2.4. Memory Mapped Targeting Technique

Memory mapped targeting [34] can be used to model a distance relay characteristic. The technique consists of segmenting the characteristic of the relay. Figure 5.2 shows the characteristic of the mho relay segmented into a mesh of squares with sides of dimension ΔS. A matrix whose dimensions are equal to the number of segments along the sides AB and AD of the square $ABCD$, is formed and stored in the memory of a micro-processor. The elements of the matrix are assigned one to one correlation with the seg-

ments of the square $ABCD$. If a segment is in the operating zone of the relay, its corresponding element in the matrix is assigned a value of one. The elements of the matrix that correspond to the segments outside the relay characteristic are assigned a value of zero. This procedure provides one to one correspondence between the segments of the relay and the matrix used for modelling the characteristic.

The coordinates of each segment define the position of an impedance on the impedance plane. The coordinates of some of the segments are negative. For example, the impedance at A, in Figure 5.2, has coordinates of $(-2,-2)$. The rows and columns of an $N \times N$ matrix are assigned values from one to N. To allow a one to one correspondence between the segmented characteristic and the matrix, linear transformation is used. Adding $3 + j3$ to all values of Z in Figure 5.2 provide the transformed characteristic shown in Figure 5.3. Now rotating this characteristic clockwise through 90° provides the characteristic shown in Figure 5.4. In this manner, the impedance value corresponding to the lower left hand segment $(-2,-2)$ in Figure 5.2 appears in Figure 5.4 at the upper left corner as element (1,1). This is the location of the element in the matrix that should contain information concerning $Z = -2 - j2$. The elements of the matrix that can be used to implement a mho relay characteristic are shown in Figure 5.5.

The coordinates of a line impedance, $R_L + jX_L$, on the impedance plane are converted by the model to $m + jn$ by dividing R_L and X_L by ΔS. Both m and n are integers. The element (m,n) of the matrix corresponds to the impedance $m + jn$. If both elements are less than or equal to the dimensions of the matrix, the line impedance is inside the square $ABCD$, otherwise it is outside this square. In case the line impedance is outside the square, the model does not provide any trip output. If the coordinates of the line impedance correspond to the coordinates of a segment in the square, a second check is performed to ascertain if the impedance is inside the operating characteristic of the relay. This is done by checking if

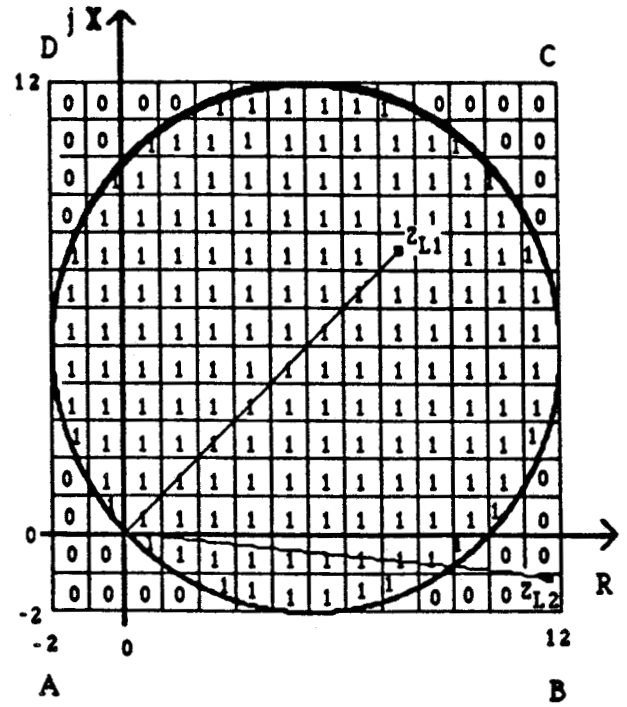

Figure 5.2: The segmented mho relay characteristic.

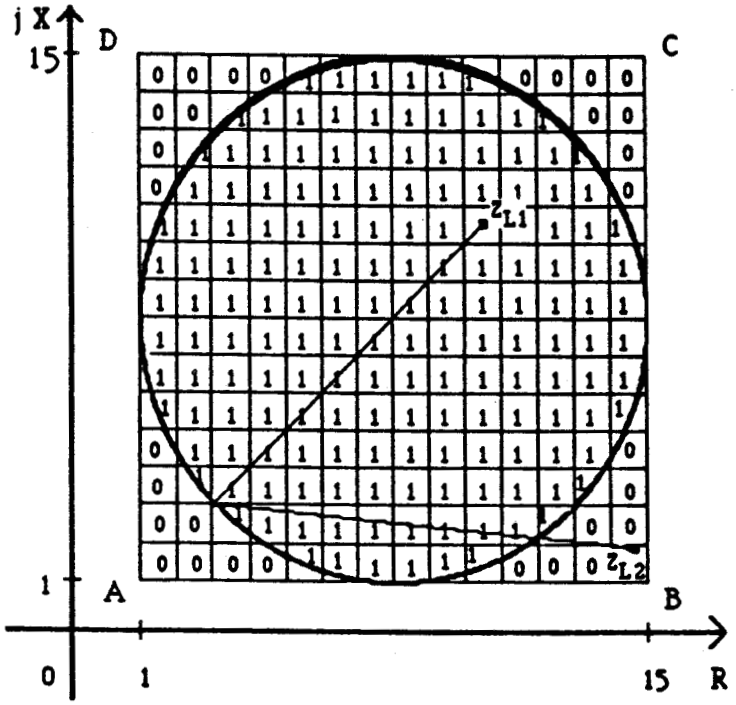

Figure 5.3: The transformed mho relay characteristic.

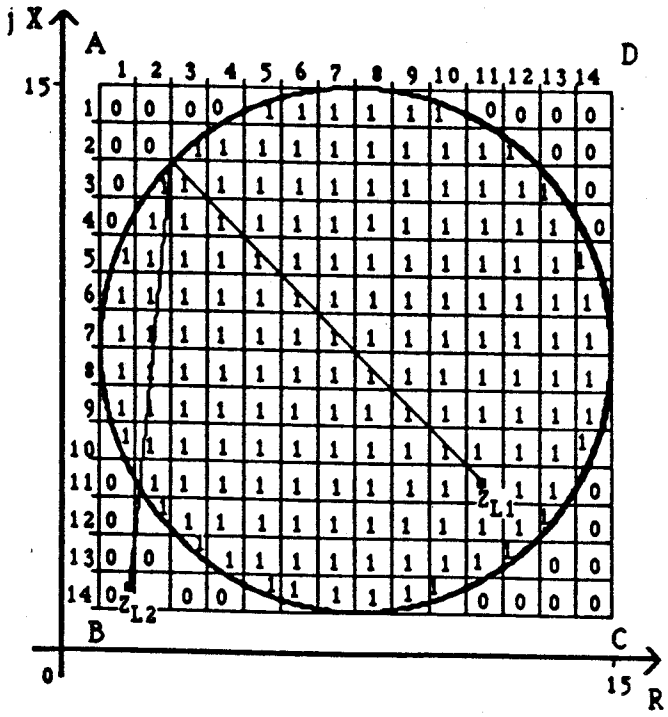

Figure 5.4: The rotated mho relay characteristic.

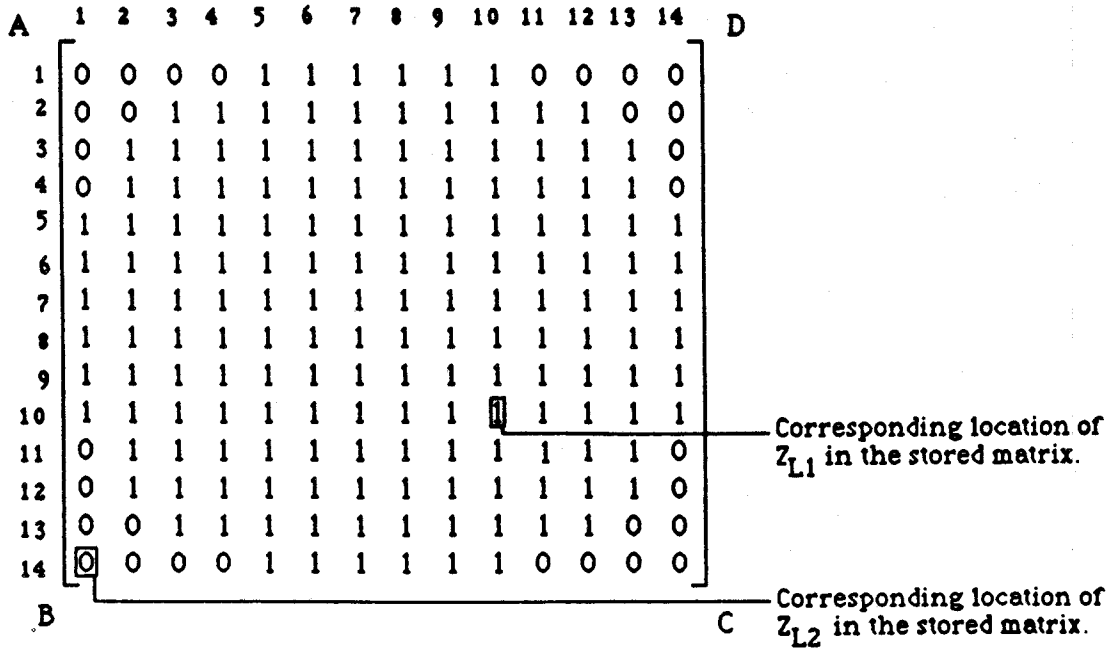

Figure 5.5: The matrix derived from a segmented mho relay characteristic.

the corresponding location in the matrix has been assigned a value of one or zero. If the value is one, the model provides a trip output but if it is zero no output is provided.

For example an impedance $Z_{L1} = 7 + j7$ is in the operating zone of the relay whose characteristic is shown in Figure 5.2. The characteristic is segmented in 14 × 14 segments as shown in Figure 5.3. The matrix for memory mapping given in Figure 5.5 has, therefore, dimensions of 14 × 14. The coordinates of this impedance on the segmented characteristic are (7,7). These coordinates when modified by adding (3,3) and rotating through 90° provide (10,10). These coordinates are less than the dimensions of the matrix. The element (10,10) in the matrix of Figure 5.5 has a value of one. The model, therefore, concludes that the calculated impedance is in the operating zone of the relay. The impedance $Z_{L2} = 11 - j2$ is outside the operating zone of the relay characteristic shown in Figure 5.2. The coordinates of this impedance on the segmented characteristic are (11,−2). These coordinates when modified by adding (3,3) and rotating through 90° provide (14,1). These coordinates are less than or equal to the dimensions of the matrix. The element (14,1) in the matrix of Figure 5.5 has a value of zero. The model, therefore, concludes that the calculated impedance is outside the operating zone of the relay. Figure 5.6 illustrates the steps followed in the model to provide an output.

5.3. Modelling of a Composite Mho/Reactance Relay

The models of the composite mho/reactance relay developed in the software use four techniques. These are

1. amplitude comparison,
2. phase comparison,
3. direct impedance estimation and
4. memory mapped targeting techniques.

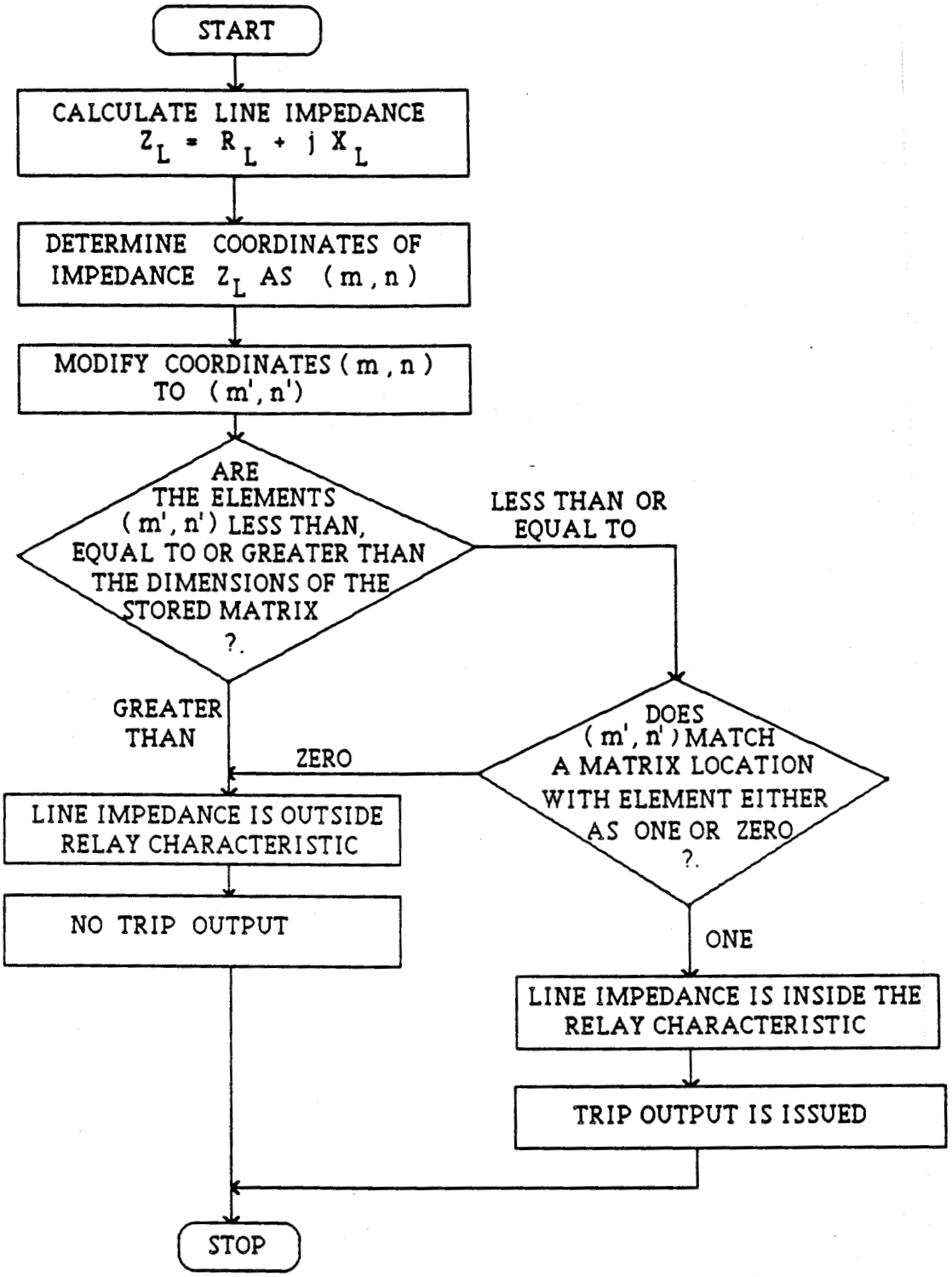

Figure 5.6: The flow chart of steps followed in the software to provide an output when memory mapped targeting technique is used.

5.3.1. Amplitude Comparison Technique

The mho/reactance relay is a combination of two comparators, one providing the mho characteristic and the other providing the reactance characteristic. Each comparator is fed with two signals, one operating signal and one restraining signal. The details of the inputs provided to each comparator are given in Section 2.5 and are listed in Table 5.1. The model developed for this project performs amplitude comparison by computing the magnitudes of the signals and comparing each operating signal with the corresponding restraining signal. The model provides a trip output if the magnitudes of both operating signals are greater than the magnitudes of the corresponding restraining signals.

5.3.2. Phase Comparison Technique

As stated in Section 5.3.1, the composite mho/reactance relay is a combination of two comparators. Each comparator is fed with two signals. The details of the inputs are given in Section 2.5 and are listed in Table 5.2.

The phase comparison technique of modelling the composite mho/reactance relay uses two approaches. The first approach consists of computing the phase angles of the phasors representing the measuring and polarizing signals. The differences between the phase angles of each pair of signals are calculated. A trip output is provided by the model if each difference is within $\pm 90^{\circ}$, the limits set for the comparators of this relay. The second approach consists of computing the dot products of the phasors of each pair of the inputs. The model provides a trip output if both dot products are positive.

5.3.3. Direct Impedance Estimation Technique

The direct impedance estimation technique uses a model of the relay characteristic. Figure 5.7 shows this characteristic drawn on the impedance plane. The model determines the coordinates of Z_C and Z_L and the magnitude of the vector $Z_L - Z_C$.

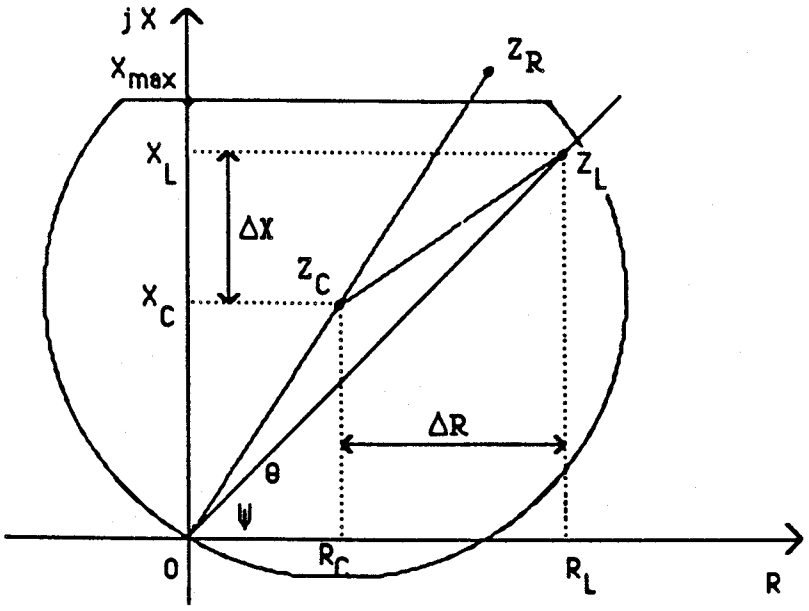

Figure 5.7: The operating characteristic of a mho/reactance relay.

X_{max} in Figure 5.7 is the reactance setting of the model developed in this project. The magnitude of the vector $(Z_L - Z_C)$ is compared with the radius of the mho circle and X_{max} is compared with the fault reactance. A trip output is provided if $|Z_L - Z_C|$ and X_{max} are less than the radius of the mho circle and the fault reactance respectively.

5.3.4. Memory Mapped Targeting Technique

Figure 5.8 shows the segmented characteristic of the composite mho/reactance relay. The procedure for modelling the composite relay in this project using memory mapped targeting technique is similar to the method described in Section 5.2.4.

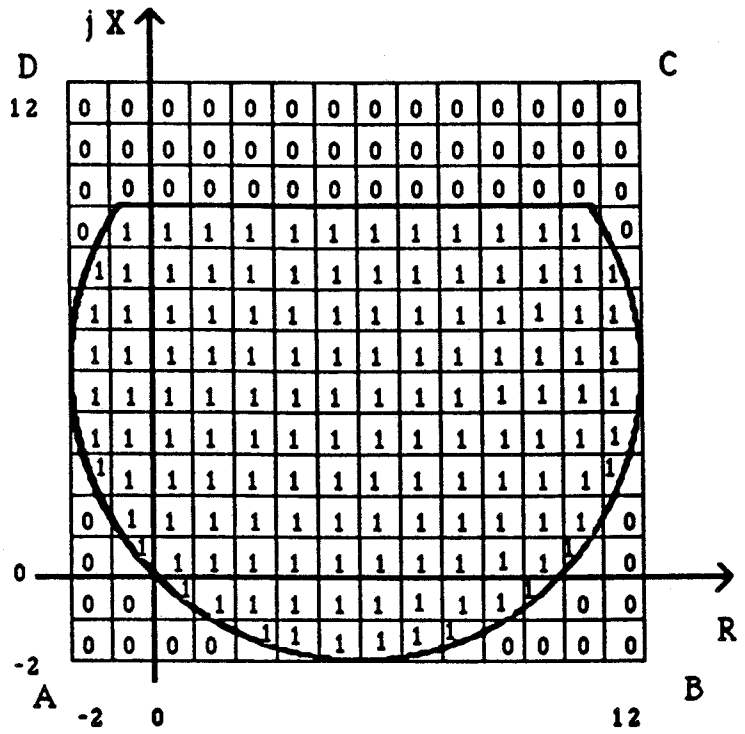

Figure 5.8: The segmented characteristic of a mho/reactance relay.

5.4. Modelling of a Quadrilateral Relay

The models of the quadrilateral relay use four techniques. These are

1. amplitude comparison,
2. phase comparison,
3. direct impedance estimation and
4. memory mapped targeting techniques.

5.4.1. Amplitude Comparison Technique

The quadrilateral relay if modelled as an amplitude comparator uses either a combination of three comparators or a combination of four comparators. The model which uses three comparator arrangement is implemented in this project. Each comparator is fed with a pair of signals. The details of the input signals are described in Section 2.5.

The model developed in this project performs amplitude comparison by computing the magnitudes of the operating and restraining signals of each pair of inputs. A trip output is provided by the model if the magnitude of all operating signals are greater than the magnitudes of the corresponding restraining signals.

5.4.2. Phase Comparison Technique

The quadrilateral relay if modelled as a phase comparator uses either a combination of three comparators or a combination of four comparators. The model which uses three comparator arrangement is implemented in this project. Each comparator is applied two inputs; the details of the inputs are given in Section 2.5.

The modelling procedure consists of computing the phase angles of the phasors representing the input signals. The differences, β_1 and β_2 between the phase angles of each pair of signals are calculated and compared with the limits set for the comparators of the relay. The model provides a trip output if the differences between the phase angles are within the limits of the comparators. These limits are discussed in Section 2.5.1.

5.4.3. Direct Impedance Estimation Technique

The direct impedance estimation technique uses a model of the characteristic of the relay. Figure 5.9 shows this characteristic drawn on the impedance plane. The lines forming the characteristic have been numbered as 1, 2, 3 and 4. The equations for these lines are

$$X_{L1} = C_1 \tag{5.8}$$

$$X_{L2} = m_2 \, R_{L2} \tag{5.9}$$

$$X_{L3} = m_3 \, R_{L3} \tag{5.10}$$

$$X_{L4} = m_4 \, R_{L4} + C_4 \tag{5.11}$$

where:

$(0,X_{L1})$, (R_{L2},X_{L2}), (R_{L3},X_{L3}) and (R_{L4},X_{L4}) define the locations of points Z_{L1}, Z_{L2}, Z_{L3} and Z_{L4},

m_2, m_3 and m_4 are the slopes of lines 2, 3 and 4 respectively and

C_1 and C_4 are points of intersection on the reactance axis for lines 1 and 4.

The inputs to the model are the angles ϕ_1, ϕ_2 and ϕ_3, the intercepts C_1 and L_1. The model calculates the slopes m_2, m_3 and m_4 and the intercept C_4.

Consider that the calculated impedance during a fault is $R_L + jX_L$. The model substitutes the value of R_L for R_{L2}, R_{L3} and R_{L4} in Equations 5.8 to 5.11 and calculates the values for X_{L2}, X_{L3} and X_{L4}. The model issues a trip command if the following conditions are satisfied.

$$X_{L1} > X_L > X_{L2} \tag{5.12}$$

$$X_{L3} < X_L > X_{L4} \tag{5.13}$$

The projections of the impedance Z_L onto the characteristics of the comparators to achieve the above limits are illustrated in Figure 5.10.

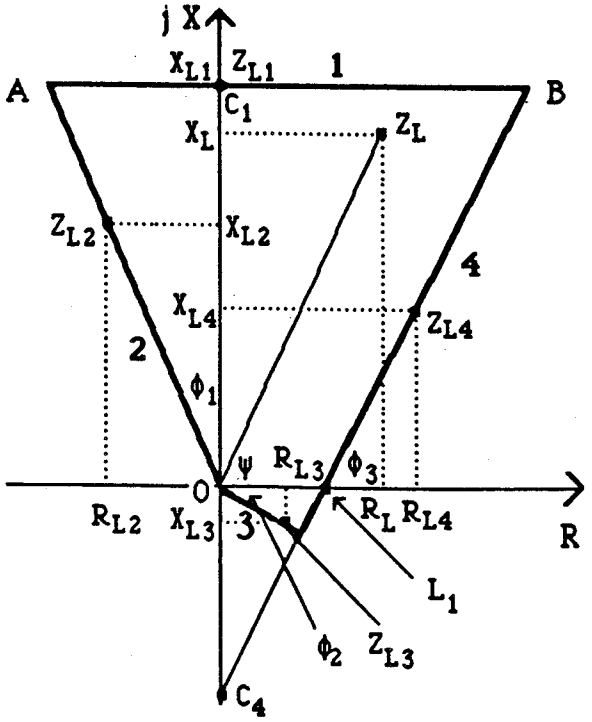

Figure 5.9: The operating characteristic of a quadrilateral relay.

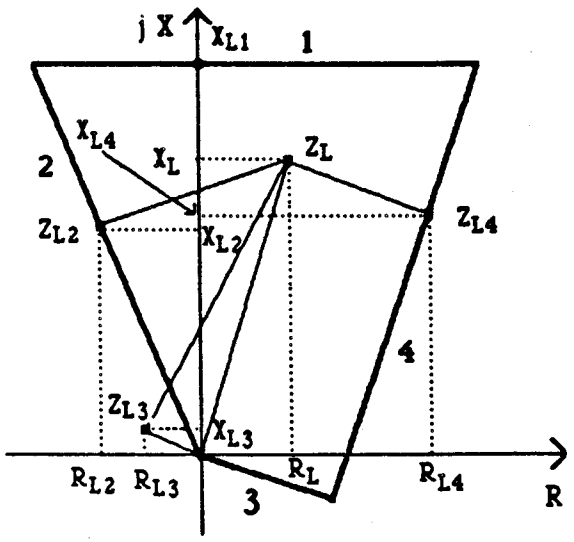

Figure 5.10: Projections on the quadrilateral relay characteristic to achieve its comparator limits.

5.4.4. Memory Mapped Targeting Technique

Figure 5.11 shows the segmented characteristic of the quadrilateral relay. The procedure used for modelling this characteristic is similar to the method described in Section 5.2.4.

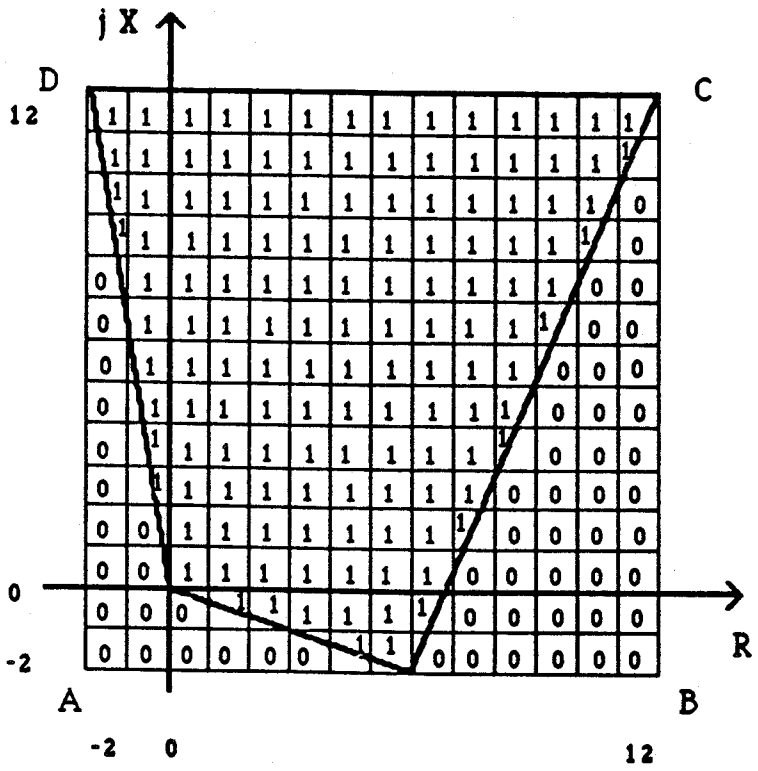

Figure 5.11: The segmented characteristic of a quadrilateral relay.

5.5. Modelling of a Directional Relay

The models of directional relays use two techniques. These are

1. phase comparison and
2. impedance estimation techniques.

5.5.1. Phase Comparison Technique

The phase comparison technique described in Section 2.3.1 is used to model the directional relays. The details of the inputs depend on the desired connection angles and are reported in Section 3.7.

The model correlates the voltage and current inputs of each relay element over one cycle of the power system frequency. The results are compared with a threshold value that is selected by the user. A trip output is provided if the resultant of the correlated functions is greater than the threshold.

5.5.2. Impedance Estimation Technique

The impedance estimation technique uses a model of the relay characteristic. Figure 5.12 shows the characteristic drawn on the impedance plane. Since the characteristic is a straight line passing through the origin of the impedance plane the equation of the characteristic is

$$X_{L1} = mR_{L1} \tag{5.14}$$

where:

(R_{L1},X_{L1}) defines the impedance Z_{L1} which is in the boundary of the characteristic and

m is the slope of the characteristic.

The angle θ and the impedance Z_{L1} are the inputs provided by the user to the model. The model calculates the slope m from the inputs.

Consider that the impedance calculated during a fault is $R_L + jX_L$. The model substitutes R_L for R_{L1} in Equation 5.14 and calculates the value for X_{L1} and issues a trip command if X_{L1} is less than X_L.

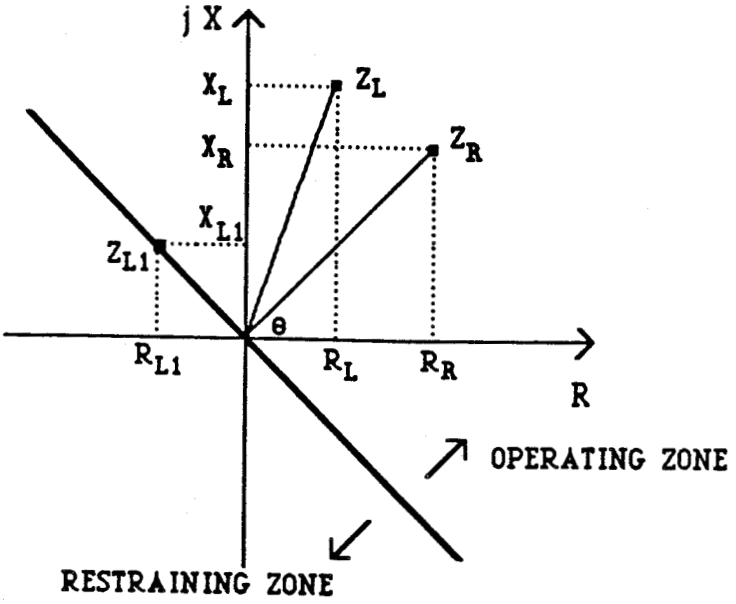

Figure 5.12: The operating characteristic of a directional relay.

5.6. Modelling of a Directional/Impedance Relay

The composite directional/impedance relay uses four techniques for its models. These are

1. amplitude comparison,
2. phase comparison,
3. direct impedance estimation and
4. memory mapped targeting techniques.

5.6.1. Amplitude Comparison Technique

The directional/impedance relay is a combination of two comparators, one providing the directional characteristic and the other providing the impedance characteristic. Each comparator is fed with two signals, one operating signal and one restraining signal. The details of the inputs provided to each comparator are given in Section 2.5 and are listed in Table 5.1. The model developed in this project performs amplitude comparison by computing the magnitudes of the signals and comparing each operating signal with the corresponding restraining signal. The model provides a trip output if the magnitudes of the operating signals are greater than the magnitudes of the corresponding restraining signals.

5.6.2. Phase Comparison Technique

As stated in Section 5.6.1, the composite directional/impedance relay is a combination of two comparators. Each comparator is fed with two signals. The details of the inputs are given in Section 2.5 and are listed in Table 5.2.

The phase comparison technique uses two methods for the model. The first method consists of computing the phase angles of the phasors representing the measuring and polarizing signals. The differences between the phase angles of each pair of signals are calculated and compared with the limits set for the comparators. The model provides a trip output if the differences are within $\pm$ 90°, the limits set for the comparators of this relay. The second method consists of computing the dot products of the phasors of each pair of the inputs. The model provides a trip output if both dot products are positive.

5.6.3. Direct Impedance Estimation Technique

The direct impedance estimation technique uses a model of the relay characteristic. Figure 5.13 shows this characteristic drawn on the impedance plane. The model determines the coordinates of Z_C and Z_L and the magnitude of the vector $Z_L - Z_C$. The directional characteristic of this relay is modelled as discussed in Section 5.5.2. The model provides a trip output if $|Z_L - Z_C|$ is less than Z_C and also when the condition stated in Section 5.5.2 is satisfied.

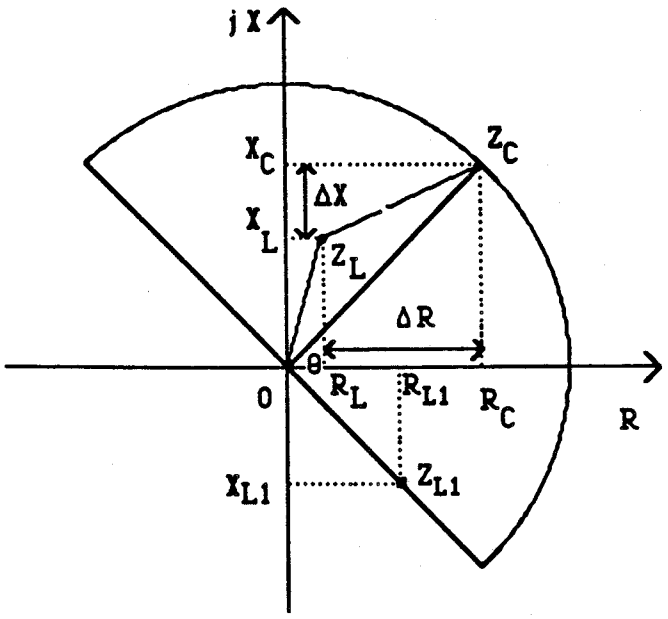

Figure 5.13: The operating characteristic of a directional/impedance relay.

5.6.4. Memory Mapped Targeting Technique

Figure 5.14 shows the segmented characteristic of the composite directional/impedance relay. The procedure used for modelling this characteristic is similar to the method described in Section 5.2.4.

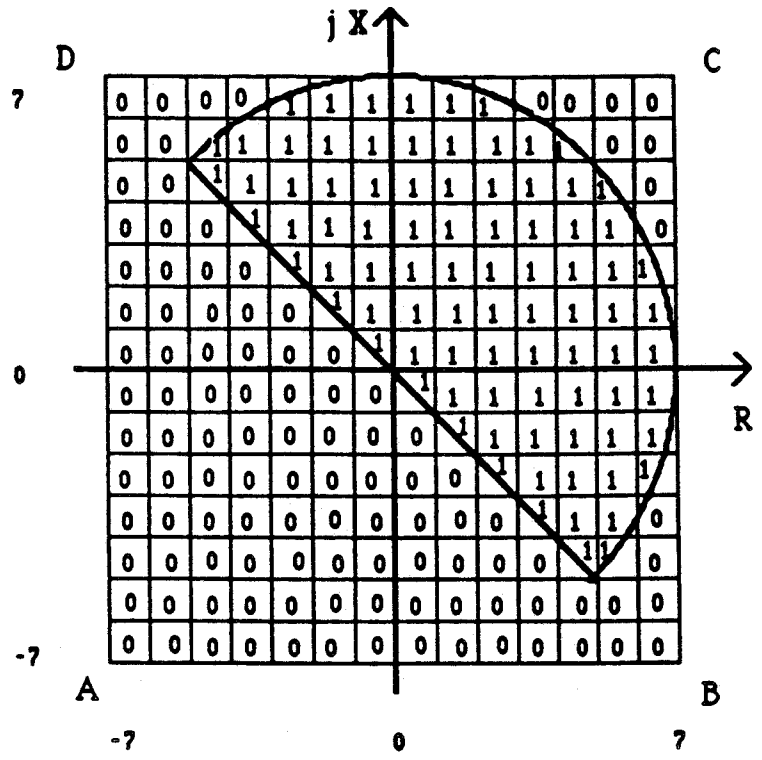

Figure 5.14: The segmented characteristic of a directional/impedance relay.

5.7. Summary

This chapter has presented the techniques used in this project for modelling digital distance and directional relays. Apart from the single phase directional relays the models of the other relays were implemented using four techniques. Two of the techniques use the signals fed to the comparators of the relays. The remaining two techniques model the relays using their characteristics. The techniques presented in this chapter have been implemented on a main frame computer. The details of the computer programs are described in the next chapter.

6. INTERACTIVE SOFTWARE FOR DIGITAL DISTANCE AND DIRECTIONAL RELAYS

6.1. Introduction

The principles needed for the development of digital distance and directional relay models have been discussed in the preceding chapters. Analog to digital converters, micro-processors and relay algorithms introduce errors in a digital relay due to quantization and truncation. The selection of an inappropriate algorithm and hardware can also cause significant errors in computations performed by a digital relay.

Before finalizing the design of a digital relay, its performance should be examined. Two approaches are available for this purpose. The first is to design and build a prototype of the relay and evaluate its performance. The second approach is to model the digital relay on a main frame computer and investigate the performance that might be expected. This chapter describes an interactive software that models and evaluates the performance of digital distance and directional relay algorithms.

6.2. Background Work

An interactive software package which evaluates digital relay algorithms was previously developed by Sachdev et al [22, 35]. The package includes programs for determining peak values of voltages and currents. The software can calculate the impedances of transmission lines as seen by digital distance relays. This package also contains a program that can generate data for voltages and currents of a power system. The following components can be included in the data.

1. A fundamental frequency component.
2. A decaying or constant dc component.
3. Components of harmonic frequencies.
4. Components of non-harmonic frequencies.
5. Random noise.

A Fortran program, PLOTER.FOR uses the CALCOMP plotting package on the VAX-11 computer at the University of Saskatchewan to plot the output of the software package.

6.3. Reorganization and Extension of Software

The purpose of this work was to develop an interactive software package that will evaluate the performance of digital distance and directional relay algorithms. To realize this objective, the following functions were performed.

1. The previous software developed by Sachdev et al [22, 35] was revised.
2. New programs were developed to extend the software. The extension includes programs for:
    a. incorporating polarization and memory action for distance relays as discussed in Chapter 3.
    b. modelling digital distance and directional relays using amplitude comparison, phase comparison, impedance estimation and memory mapped targeting techniques. These techniques are described in Chapter 5.

The upgraded and augmented programs provide a complete software package for digital distance and directional relay models.

6.3.1. Software Specifications

The following specifications were set out for the software package.

1. The user should be able to interact with the software. Inputs should be checked for errors and user allowed to make corrections. The software should be able to direct the user through the programs with prompts that are easy to understand.

2. The software should include programs that can generate instantaneous values of sampled data.

3. The software should incorporate the existing relay algorithms which estimate peak values and phase angles of voltages and currents.

4. The user should be able to calculate impedances of transmission lines as seen by a digital distance relay.

5. The software should facilitate the execution of the programs in two modes. In mode one, all computations should be performed using floating point representation of numbers. The results obtained when floating point representation is used give the degree of accuracy of the algorithms. In mode two, the effect of A/D converters, truncation or rounding and the finite word size of micro-processors should be considered. All computations should be implemented as are done by a digital processor. This mode of operation is useful for evaluating the performance of digital distance and directional relay algorithms.

In general the software should be written and organized such that difficulties encountered by users are minimal. It should also be easy to modify the software in future.

6.3.2. Programming Language

A Programming Language [36, 37], (APL), is the computer language that was used for the previously developed programs. This language was also used for the new programs. APL has numerous advantages over other computer languages and this section presents some of these advantages.

APL handles the storage of data arrays dynamically; the size of an array can be changed in the course of computations. This greatly helps to free the user from advance memory allocation for data arrays.

A terminal connected to an APL system is considered as active. Associated with each active terminal is a fixed-size block of memory in the control computer termed as an active workspace. APL programs are normally referred to as functions and are not stored individually. The active workspace which contains these functions is stored. An active workspace can contain as many functions as the size of the memory can accommodate. An active workspace can be stored after an interruption of a session and the terminal deactivated. The user can later connect to the system, load this workspace and continue the session where it was interrupted.

APL is a matrix oriented language as it provides many readily available functions for mathematical manipulation of matrices. These functions are not scientific subroutines but are single APL command sets. This feature makes a program written in APL very compact. APL is the language best suited for this software as most of the computations are matrix oriented.

The software developed in this project is user interactive and therefore, requires the handling of large amounts of character information. APL has the ability to handle these character information with ease since they can be represented by alphanumeric data with no special declarations.

6.4. Software for Digital Distance and Directional Relay Models

The software package developed for evaluating the performance of digital distance and directional relay algorithms resides in eight APL workspaces. Figure 6.1 shows the overall structure and functional details of this software. The workspaces of the software package are:

1. PROLIB.APL,
2. INDATG.APL,
3. ALLCMP.APL,
4. ALLPKV.APL,
5. POLARIZ.APL,
6. RELC.APL,
7. DISTANCE.APL and
8. DIRECT.APL.

6.4.1. PROLIB.APL

In the workspace PROLIB.APL is a collection of functions which are referred to as subroutines. This collection forms a function library for use by other functions of the software package. The functions contained in PROLIB.APL are INPTFILE, RDFILE, PRFILE, WRFILE, ADCON, MUL, MULSGP, MULDBP, CMUL, SQRT, ACCURACY, BLOCK and TEST. The functions BLOCK and TEST were developed by the author of this thesis. The rest were developed in the previous software by Sachdev et al [22, 35]. The following paragraphs describe the functions contained in this workspace.

(a) INPTFILE

The purpose of this function is to take data from a data file and convert it into a form that can be read by the major functions of the software package. INPTFILE, apart from rearranging the input data compares the key parameters entered by the user, such as, system frequency and sampling frequency, with those read from the file header. It notifies the user if any discrepancy is detected. The function INPTFILE calls two other functions, RDFILE and PRFILE. RDFILE reads a specified number of data samples

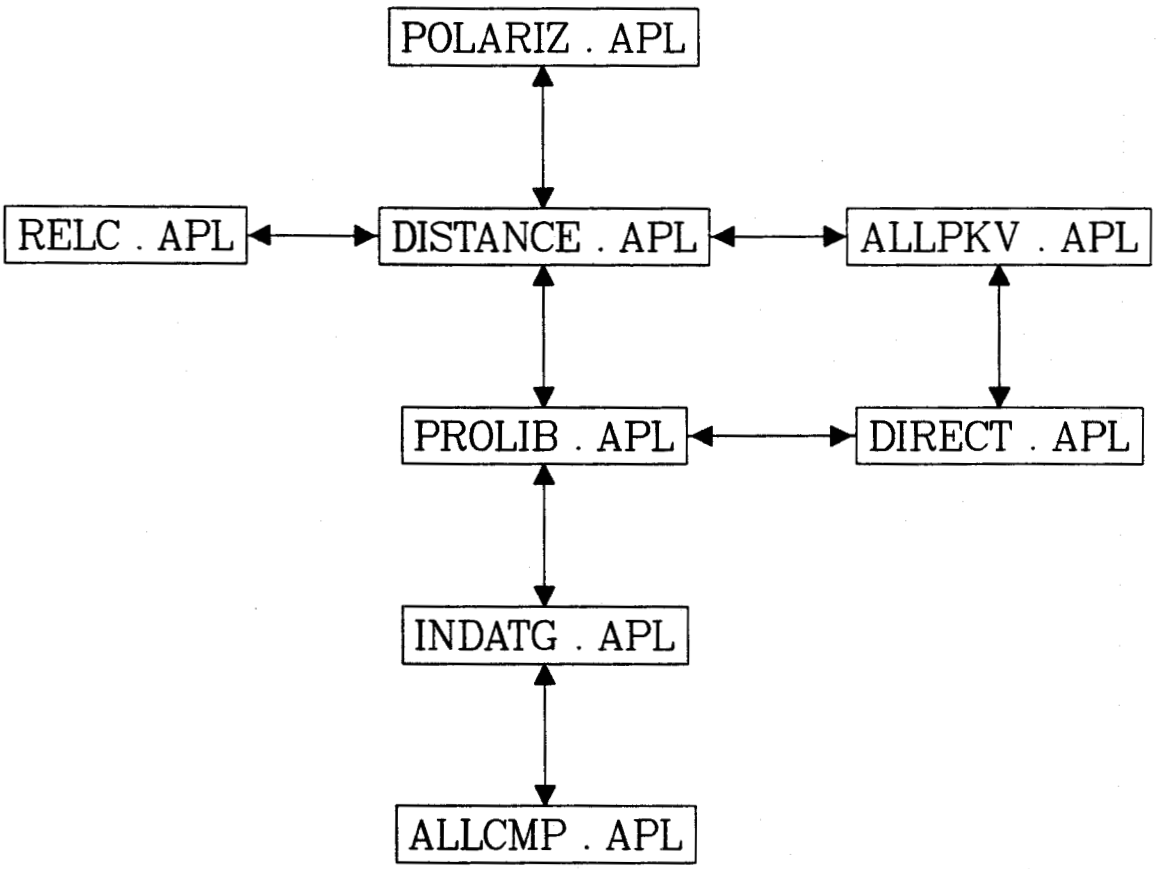

Figure 6.1: An overall software structure for the digital distance and directional relays.

from a file. PRFILE prints information of the data file on the terminal after this file has been read by RDFILE.

(b) WRFILE

This function creates an output file for the results obtained from the main functions of the software package. The data files created by WRFILE are in a form readable by INPTFILE. The data contained in these files can be plotted using the Fortran program PLOTER.FOR.

(c) ADCON

ADCON is a function which simulates the effect of limited word size in digital relays. Appendix A describes the modelling procedure used in this function.

(d) MUL

MUL is a function which calculates the product of an integer number and a decimal number. It uses the bit shift approach for performing multiplications. The use of this function allows the user to demonstrate how multiplications are performed by micro-processors. MUL calls one of two functions, MULSGP or MULDBP. MULSGP implements the ordinary bit shift approach and MULDBP implements the extended bit shift approach. Appendix B discusses the bit shift approaches used by the functions of the software package. MUL also calls the function CMUL if the product of two complex numbers are to be determined.

(f) SQRT

In digital relaying, most computations involve estimating the magnitudes and phase angles of phasors from their real and imaginary com-

ponents. The realization of this requires two squaring operations and one square root operation. These operations are computationally inefficient. The function SQRT provides a piecewise linear approximation to replace the squaring and square root operations. Details of the procedure are discussed in Appendix C.

(g) ACCURACY

This function allows the user to select

1. the type of quantization, either truncation or rounding, in analog to digital converters and micro-processors,
2. the number of bits for the analog to digital converters and micro-processors,
3. the bit shift multiplication, either ordinary or extended approach and
4. the number of regions of approximation implemented when using the function SQRT.

(h) BLOCK

The purpose of creating the function BLOCK is to process the voltage and current inputs to directional relays as discussed in Sections 2.5 and 3.7. The user is required to provide the following inputs to the function BLOCK.

1. The code for the type of directional relay.
2. The replica impedance needed for the model.
3. The maximum torque angle required for the relay model.

(i) TEST

This function accepts inputs from the function BLOCK and uses these inputs to model directional relays as discussed in Section 5.5.1. The following are to be entered by the user during the execution of TEST.

1. The window size over which trip decision is to be made by the model.
2. The threshold of the model's integrator.

After modelling, the function TEST displays the output in a tabular form. The output includes:

1. the type of directional relay connection,
2. the date of fault occurrence,
3. the fault occurrence time and
4. the trip and reset times of the relay model.

6.4.2. INDATG.APL

The workspace INDATG.APL contains the function INDATGEN which generates sampled data that represent power system voltages and currents. INDATGEN interacts with some of the functions in the workspaces PROLIB.APL and ALLCMP.APL. The function INDATGEN and the functions residing in the workspace ALLCMP.APL were developed by the authors of References [22] and [35]. Figure 6.2 shows the structure of the workspace INDATG.APL.

The function INDATGEN, residing in the workspace INDATG.APL has five blocks; the input, decision making, calculation, display and output blocks. The input block accepts data that includes the system frequency, sampling frequency and the number of samples required. INDATGEN then gives the user the option of generating the data or entering the data from

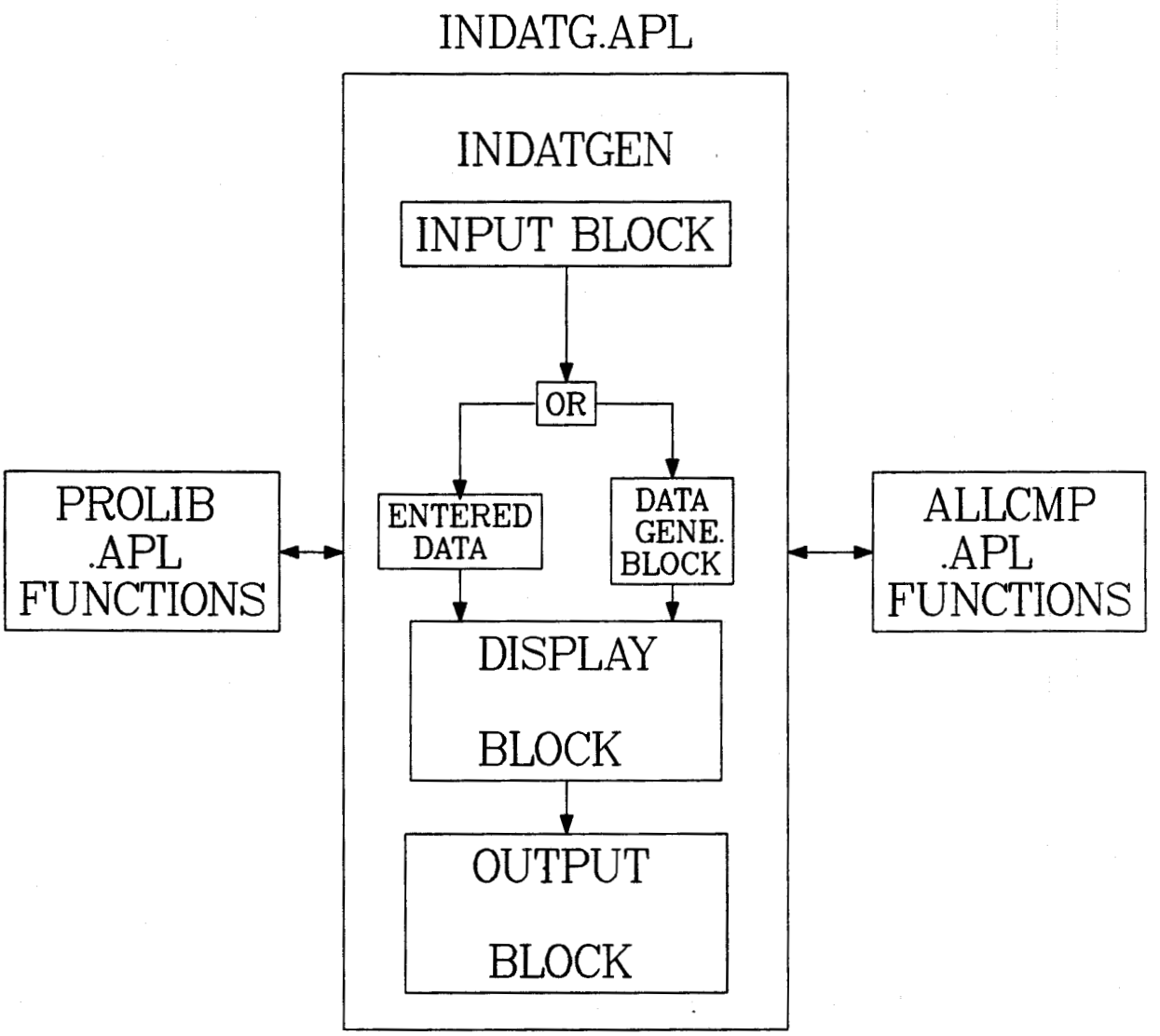

Figure 6.2: A functional block diagram of the workspace INDATG.APL.

the terminal. The calculation block calls some of the functions residing in the workspace ALLCMP.APL if data generation by the program is selected. The specifications of the data determine which functions are called. A power system voltage and current can include the following components.

(i) The fundamental frequency component of

  (a) constant amplitude,

  (b) decaying amplitude and

  (c) rising amplitude.

(ii) The dc component of

  (a) constant amplitude,

  (b) decaying amplitude and

  (c) rising amplitude.

(iii) The harmonic components of

  (a) constant amplitude,

  (b) decaying amplitude and

  (c) rising amplitude.

(iv) Components of non-harmonic frequencies with

  (a) constant amplitude,

  (b) decaying amplitude and

  (c) rising amplitude.

(v) Pseudo-random noise of specified mean and standard deviation.

The function INDATGEN allows the user to optionally select the above components, in succession, that are to be included in the required signal. The function for the selected component is copied into the active workspace from ALLCMP.APL. The copied function is then executed to compute the sampled data that represent the selected component. The function called from the workspace ALLCMP.APL is erased from the active workspace after its execution. This procedure is repeated until the user enters a stop command. The sampled data representing the selected components are added to obtain the required signal.

The user can enter the data directly from the terminal instead of generating them by the program. The display block displays the data generated by the programs or entered through the terminal. The output block directs the data into files by calling the function WRFILE which resides in the workspace PROLIB.APL. The data contained in the files created with the help of WRFILE can be used by the major functions of the software package and can also be plotted using the Fortran program PLOTER.FOR.

6.4.3. ALLPKV.APL

The workspace ALLPKV.APL contains functions which estimate peak values and phase angles of power system voltages and currents. The functions of the workspace ALLPKV.APL can use sampled data generated by the function INDATGEN as well as data from other sources. The workspace ALLPKV.APL contains functions for the following algorithms.

(i) Trigonometric Algorithms [14, 15, 16, 17]:

(a) Makino and Miki algorithm.

(b) Mann and Morrison algorithm.

(c) Gilcrest, Rockefeller and Udren algorithm.

(ii) Least Error Squares (LES) Algorithms [18, 19, 20]:

(a) Three-sample LES algorithm assuming that the input signal consists of a fundamental frequency component only.

(b) Five-sample LES algorithm assuming that the input signal consists of a fundamental frequency component only.

(c) The LES algorithm assuming that the input signal consists of a fundamental frequency component only. The user selects the data window size.

(d) Three-sample LES algorithm assuming that the input signal consists of a fundamental frequency component which adds to a constant dc component.

(e) Five-sample LES algorithm assuming that the input signal consists of a fundamental frequency component which adds to a constant dc component.

(f) The LES algorithm assuming that the input signal consists of a fundamental frequency component which adds to a constant dc component. The user selects the data window size.

(g) The LES algorithm assuming that the input signal consists of components of the fundamental frequency and second harmonic which add to a constant dc value. The user selects the data window size.

(h) The LES algorithm assuming that the input signal consists of components of the fundamental frequency and second harmonic which add to a decaying dc value. The user selects the data window size.

(i) The LES algorithm assuming that the input signal comprises of the components of fundamental frequency, second harmonic, third harmonic, fourth harmonic and fifth harmonic which add to a decaying dc value. The user selects the data window size.

(iii) Correlation Algorithms [21, 23, 24, 25, 26]:

(a) Full cycle Fourier analysis algorithm.

(b) Half cycle Fourier analysis algorithm.

(c) Full cycle even and odd rectangular waves algorithm.

(d) Gilbert and Shovlin algorithm.

The functions which implement the above listed algorithms were developed by the authors of References [22] and [35].

6.4.4. POLARIZ.APL

The workspace POLARIZ.APL contains the function POLAR which was developed by the author of this thesis. The function POLAR is only an input block. During the execution of POLAR, the user is prompted to select the type of polarization scheme for the distance relay models from available options. POLAR also prompts the user to enter the polarization constants and the maximum torque angles of the models.

6.4.5. RELC.APL

The workspace RELC.APL contains two functions, CHAR and MEMOR which were developed by the author of this thesis. Figure 6.3 shows the structure of the workspace RELC.APL. The functions CHAR and MEMOR implement the models of digital distance relays using the techniques discussed in Chapter 5. CHAR uses amplitude comparison, phase comparison and direct impedance estimation techniques to implement the models of distance relays.

The function MEMOR is called by CHAR when memory mapped targeting technique is selected. CHAR has three blocks as indicated in Figure 6.3. These are the input, calculation and display blocks. The input block prompts the user to select a code for the type of digital distance relay. It also prompts the user to select a technique for implementing the relay

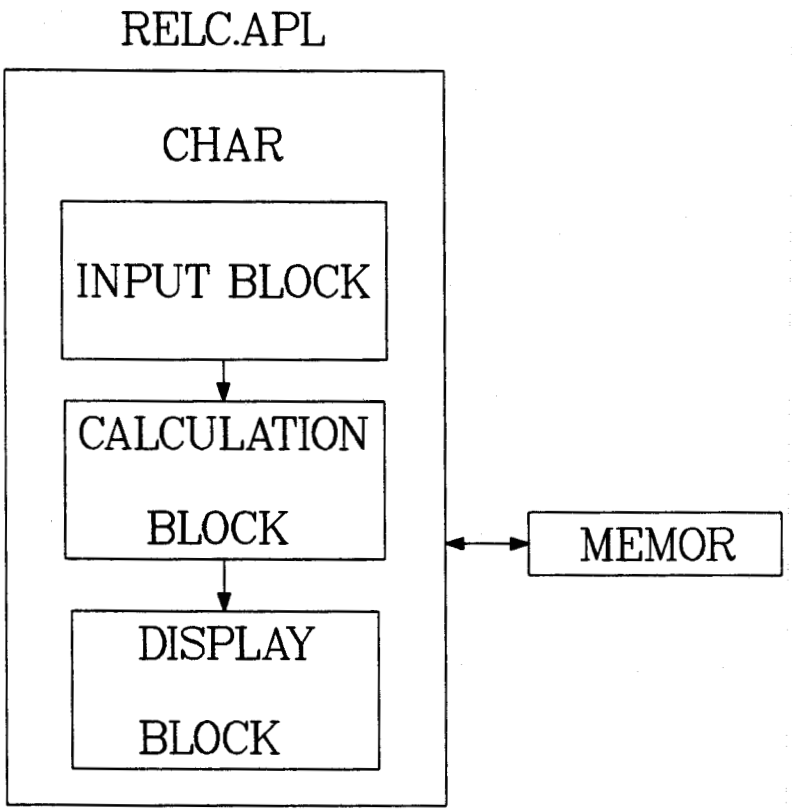

Figure 6.3: A functional block diagram of the workspace RELC.APL.

model. The calculation block models the relay using the procedures described in Chapter 5. The display block displays the type of fault, fault occurrence time, trip time and reset time of the relay model.

6.4.6. DISTANCE.APL

This workspace, in the previous software was created as ZVALUE.APL that contained functions ZVALUE and IMPVAL. The name was changed to DISTANCE.APL by the author of this thesis and a new function, IMPVALB added to its contents. This function incorporates polarization in the distance relay models as discussed in Chapter 3. The functions ZVALUE and IMPVAL were also modified so that they can be used with the new function and other functions contained in other workspaces. Figure 6.4 shows the structure of the workspace DISTANCE.APL. The functions in the workspace DISTANCE.APL interact with some functions residing in PROLIB.APL. They also interact with the functions of the workspaces POLARIZ.APL and RELC.APL. ZVALUE is the major function of DISTANCE.APL and it calls IMPVAL during its execution. The function IMPVAL processes the input data before the functions in ALLPKV.APL use it. IMPVALB does not interact with ZVALUE but does so with IMPVAL.

The function ZVALUE which resides in this workspace has four blocks; the input, calculation, display and output blocks. Figure 6.5 shows a functional block diagram of ZVALUE. The input block of ZVALUE prompts the user to enter the input data that includes sampled voltages and currents and the distance relay connections. For rearranging and reading the input data, ZVALUE calls the function INPTFILE from the workspace PROLIB.APL. The input block of ZVALUE copies the function POLAR from the workspace POLARIZ.APL into the active workspace. POLAR is the function that allows the user to enter the polarization parameters. The input block also allows the user to incorporate effects of limited word size in digital relays by calling the functions ADCON and ACCURACY from the workspace PROLIB.APL. It then prompts the user to select a code for the type of

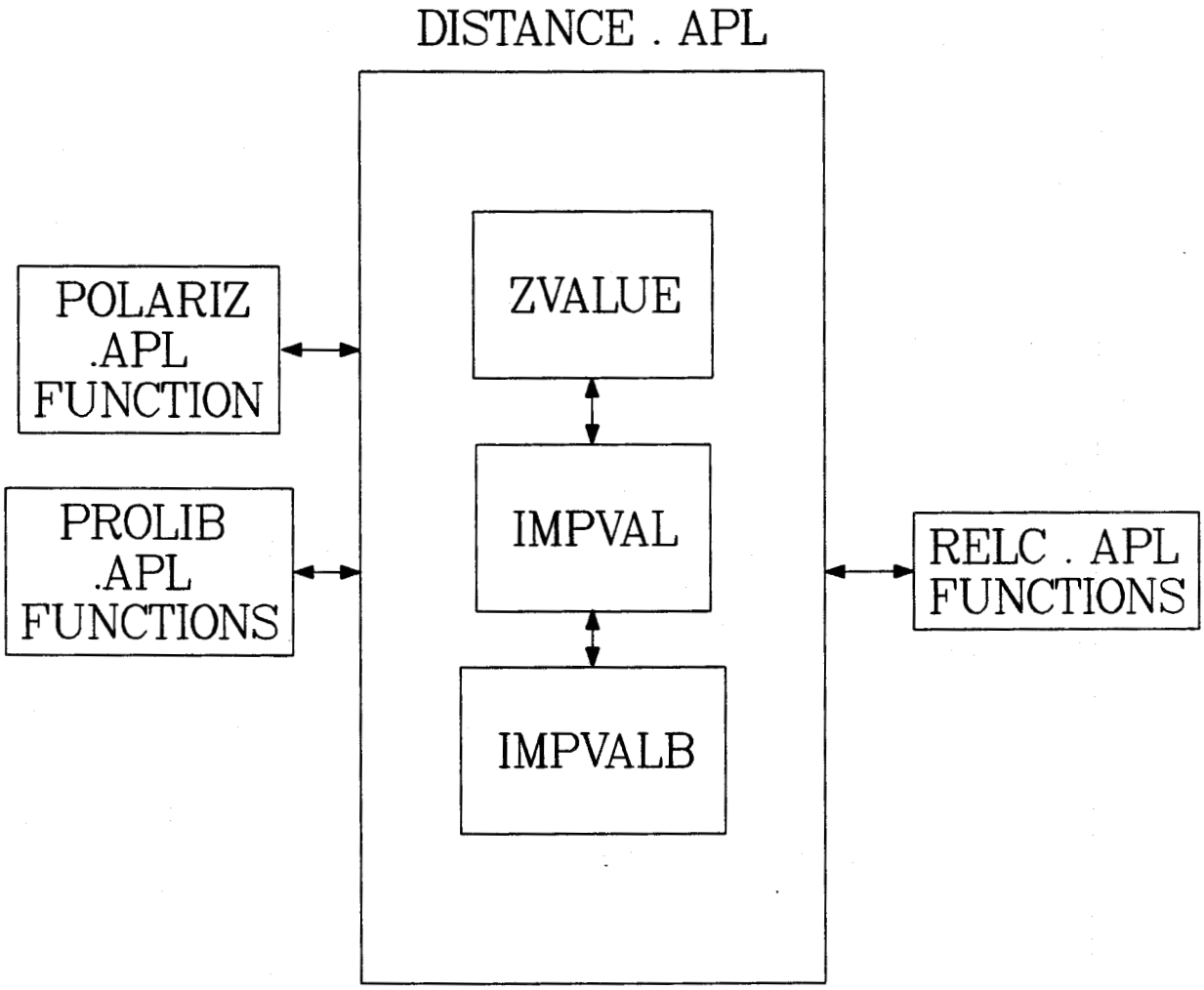

Figure 6.4: A functional block diagram of the workspace DISTANCE.APL.

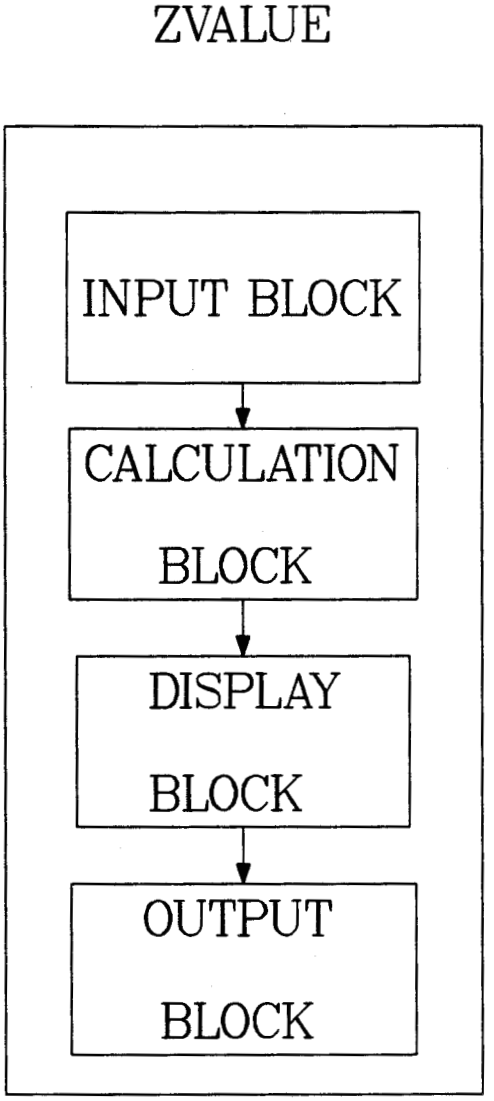

Figure 6.5: A functional block diagram of the function ZVALUE.

relay algorithm. The calculation block of ZVALUE calls IMPVAL and executes it. The function IMPVAL copies three functions into the active workspace during its execution. One of these functions is for implementing the selected relay algorithm. The outputs of this function are estimates of voltage and current phasors in the Cartesian form. The second function called by IMPVAL is IMPVALB. This function uses the selected polarization scheme to compose the inputs for use in the relay model. The third function, called from the workspace RELC.APL, is CHAR. This function models digital distance relays as discussed in Chapter 5. IMPVAL also computes the impedance of a transmission line as seen from the relay location. It uses the following equations.

$$Z_{Lr} = \frac{V_{Lr}\ I_{Lr} + V_{Li}\ I_{Li}}{I_{Lr}\ I_{Lr} + I_{Li}\ I_{Li}} \tag{6.1}$$

$$Z_{Li} = \frac{V_{Li}\ I_{Lr} - V_{Lr}\ I_{Li}}{I_{Lr}\ I_{Lr} + I_{Li}\ I_{Li}} \tag{6.2}$$

where:

V_{Lr} is the real part of the voltage phasor,

I_{Lr} is the real part of the current phasor,

V_{Li} is the imaginary part of the voltage phasor and

I_{Li} is the imaginary part of the current phasor.

The display block of ZVALUE gives the user an option to display the impedances either in the Cartesian or the polar form. Output files of the impedances can be created by using the function WRFILE that resides in the workspace PROLIB.APL. The data in the created files can be plotted using the Fortran program PLOTER.FOR. ZVALUE erases all the functions called from the other workspaces after they have completed their intended tasks.

6.4.7. DIRECT.APL

This workspace was originally created as PEAKVALUE.APL but was changed to DIRECT.APL by the author of this thesis. Its function, PEAKVALUE was modified so that it can be used with the functions BLOCK and TEST residing in PROLIB.APL. The function PEAKVALUE also interacts with some of the other functions residing in PROLIB.APL and the functions residing in ALLPKV.APL. Figure 6.6 shows the structure of the workspace DIRECT.APL.

The function PEAKVALUE, which resides in DIRECT.APL, has four blocks; the input, calculation, display and output blocks. The input block requests for the inputs, checks their validity and allows the user to make corrections. It also allows the user to select the parameters of the A/D converter and micro-processor and the code for the desired relay algorithm. The calculation block copies the function for the selected relay algorithm from the workspace ALLPKV.APL and estimates peak values and phase angles of the phasors. The display block prints the computed estimates on the monitor screen in a tabular form. The output block stores the computed estimates in data files with the aid of the function WRFILE. The data in the created files can be plotted using the Fortran program PLOTER.FOR.

PEAKVALUE also implements digital directional relay models. If the user opts for this, the functions BLOCK and TEST, residing in the workspace PROLIB.APL are copied into the active workspace. These functions prompt the user to enter the parameters of the directional relay models. PEAKVALUE erases all the functions copied from other workspaces after they have completed their intended tasks.

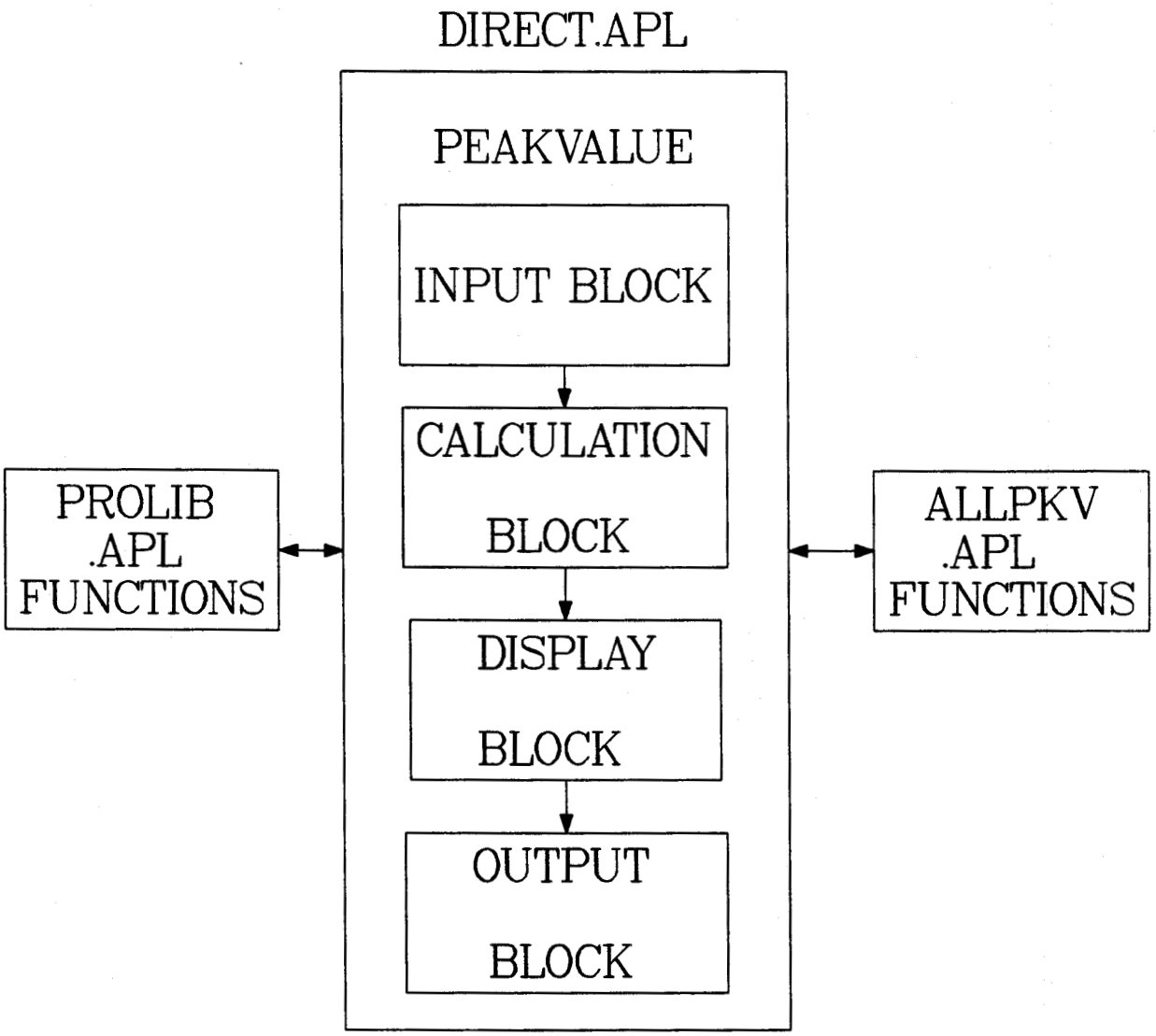

Figure 6.6: A functional block diagram of the workspace DIRECT.APL.

6.5. Summary

The software developed for evaluating the performance of digital distance and directional relay algorithms has been described in this chapter. The specifications of the software have also been outlined. An interactive approach was used and hence the software consists of "question and answer" type programs. The output of the software package is governed by the user's answers to the questions put forward by the programs. The user, therefore, has effective control over the execution of the programs. The results obtained from testing the software are reported in the next chapter.

7. TESTING THE SOFTWARE PACKAGE

7.1. Introduction

The techniques for modelling digital distance and directional relays were discussed in Chapter 5. User interactive software for implementing the techniques on a main frame computer was described in Chapter 6. This chapter presents results obtained from testing the techniques and the interactive software discussed in Chapters 5 and 6 respectively.

7.2. Model of a Power System Selected for the Studies

Figure 7.1 shows the model of a power system which was used to test the capabilities of the software. This system consists of two generators, G_1 and G_2, and two transformers, T_1 and T_2, linked by a transmission line L. Both transformers are delta connected on the generator side and wye connected on the line side. The neutrals of the wye windings are grounded. The generators are wye connected and their neutrals are solidly grounded. The figure also shows relays R_1 and R_2, which protect line L. In testing the software, only relay R_1 will be considered. Two types of faults were considered during the testing of the software. These are: phase-phase and single-phase to ground faults. These faults were assumed to have occurred at locations F_1, F_2 and F_3 of Figure 7.1. Pre-fault and post-fault voltages and currents measured at the relay location were calculated as discussed in Appendix D. From the calculated pre-fault and post-fault voltages and currents for a phase B to phase C fault at F_1, the sampled voltages and currents of Figures 7.2 and 7.3 were generated using the function INDATGEN. These sampled values were generated assuming each input contains a fundamental frequency component added to a decaying dc component. A sam-

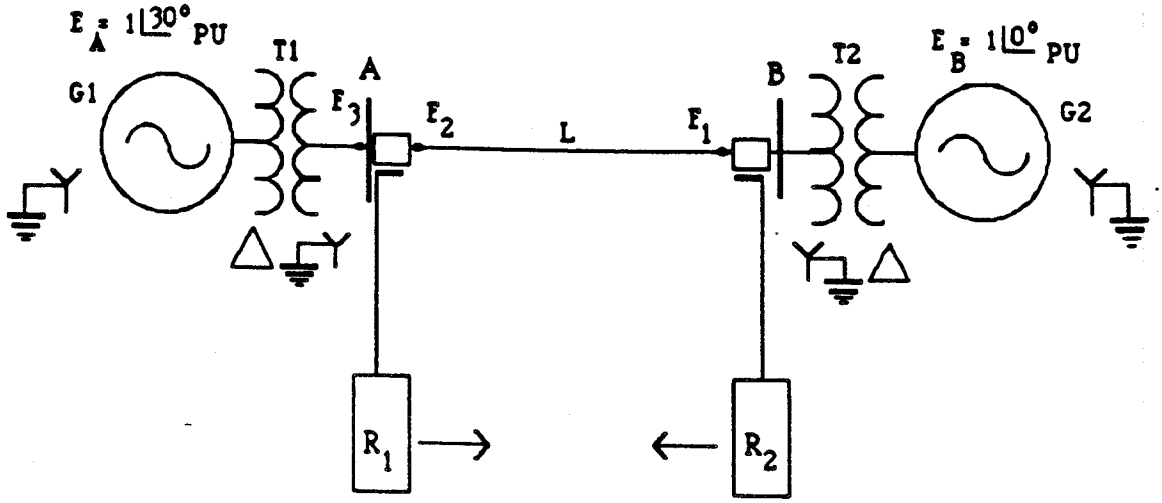

SYSTEM PARAMETERS IN PER UNIT

X	G1	G2	T1	T2	L
X_0	0.050	0.030	0.120	0.100	0.700
X_1	0.300	0.250	0.120	0.100	0.300
X_2	0.200	0.150	0.120	0.100	0.300
R_0	0.001	0.001	0.000	0.000	0.090
R_1	0.003	0.003	0.000	0.000	0.100
R_2	0.003	0.003	0.000	0.000	0.100

Figure 7.1: A sample power system used for the studies.

ponent. A sampling frequency of 720Hz was used for the data generation. Figures 7.4 and 7.5 contain sampled voltages and currents generated for a phase B to phase C fault at F_2 with the same sampling frequency. The sampled voltages and currents of Figures 7.6 and 7.7 were obtained the same way as those described earlier for the phase B to phase C fault at F_1. The sampled voltages and currents of Figures 7.8 and 7.9, Figures 7.10 and 7.11 and Figures 7.12 and 7.13 were generated for a phase A to ground fault at F_1, F_2 and F_3 respectively and in the same manner as those generated for the phase B to phase C fault at the same locations. A 10-bit analog to digital converter with dynamic range of +10V to -10V and a 16-bit microprocessor were used. The sampled data were used as inputs to the software package for investigating the manner in which the relays would respond.

The studies used algorithms discussed in Section 6.4.3 for calculating the peak values and phase angles of the phasors representing the voltages and currents. However, the results presented in this chapter are for cases in which the Fourier analysis algorithm of one cycle data window was used. The models were developed such that when five successive number of comparator outputs are within a preset range, trip commands are issued by the relays connected to the faulted phases. It was assumed that a circuit breaker takes about three cycles to clear a fault after receiving a trip command from a relay. The reset times of the models were calculated using this assumption.

7.3. Studies Conducted for Digital Distance Relays

The sampled voltages and currents of Figures 7.2 to 7.13 were used to test the polarized

1. mho,
2. mho/reactance,
3. quadrilateral and

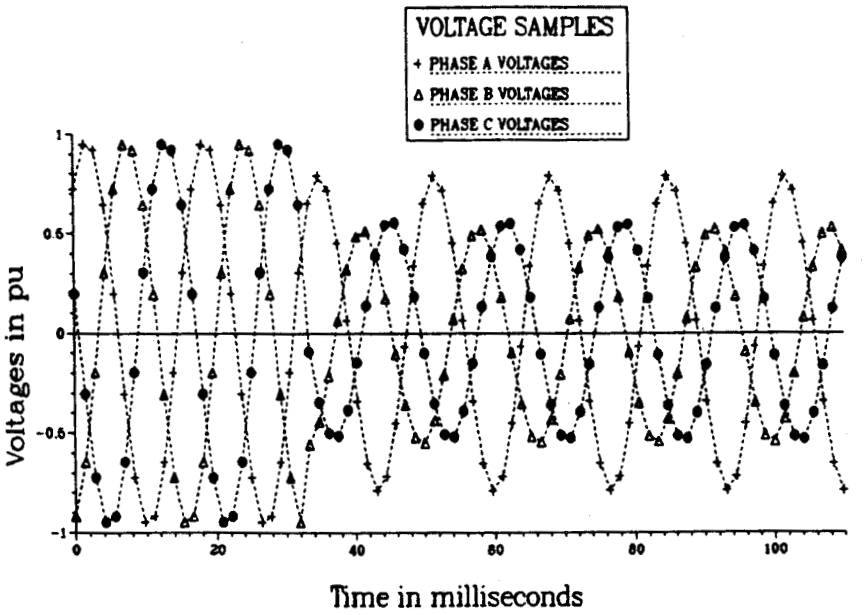

Figure 7.2: The voltage samples generated for a phase B to phase C fault at F_1.

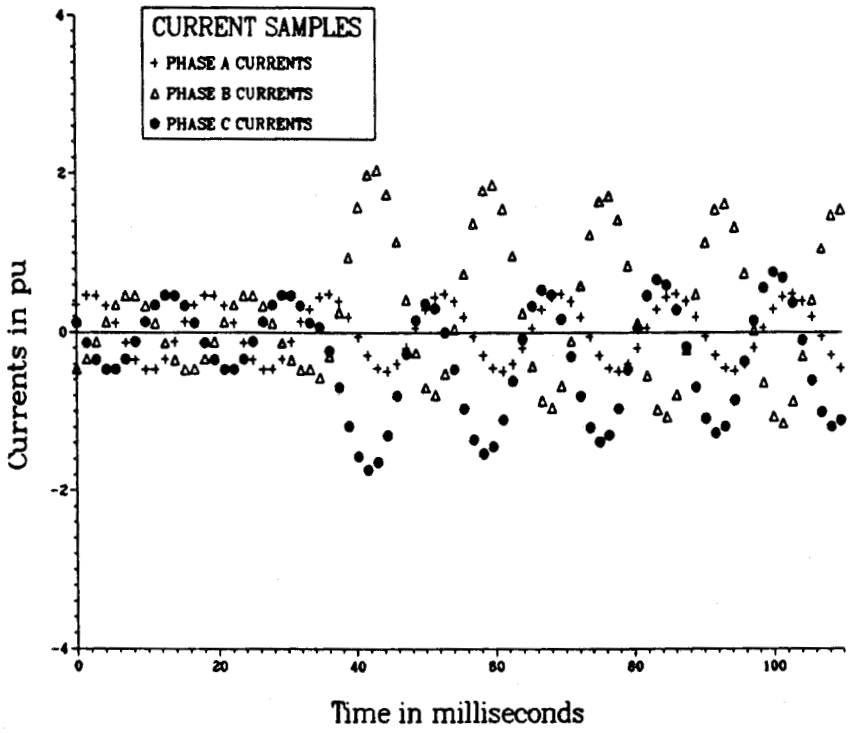

Figure 7.3: The current samples generated for a phase B to phase C fault at F_1.

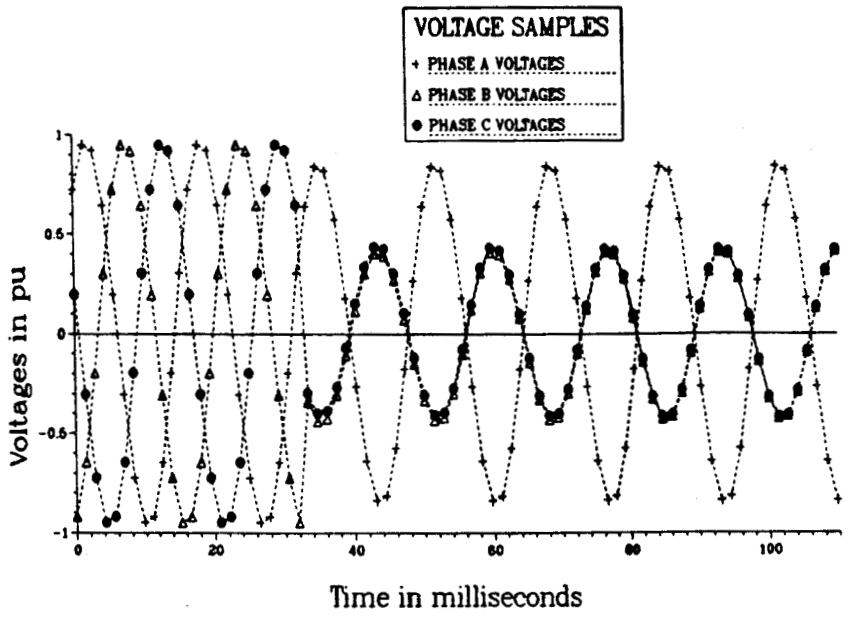

Figure 7.4: The voltage samples generated for a phase B to phase C fault at F_2.

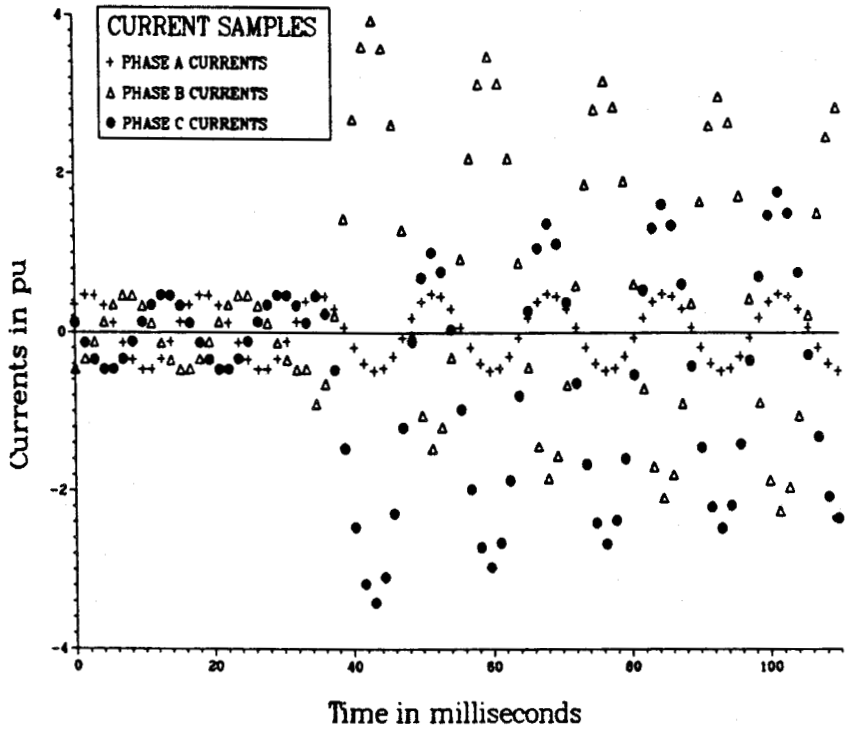

Figure 7.5: The current samples generated for a phase B to phase C fault at F_2.

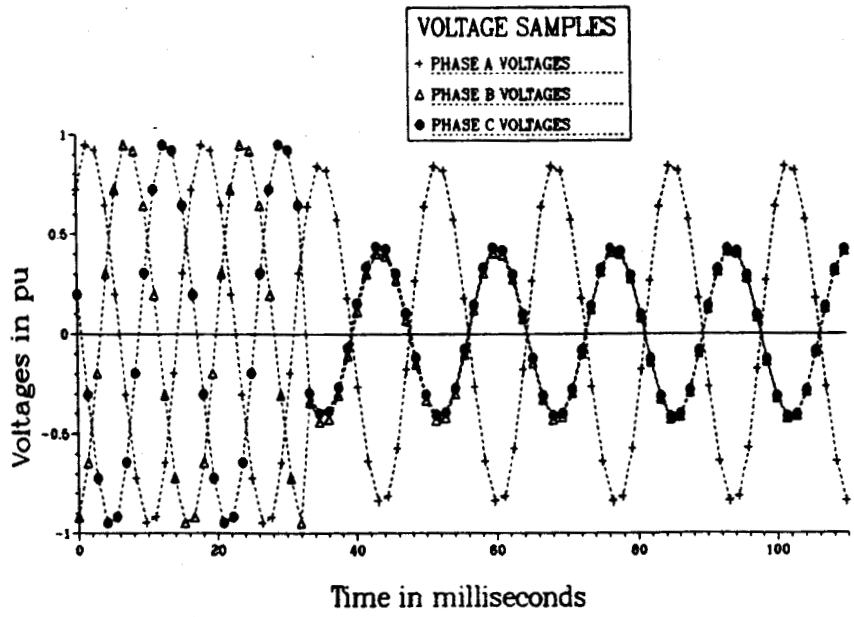

Figure 7.6: The voltage samples generated for a phase B to phase C fault at F_3.

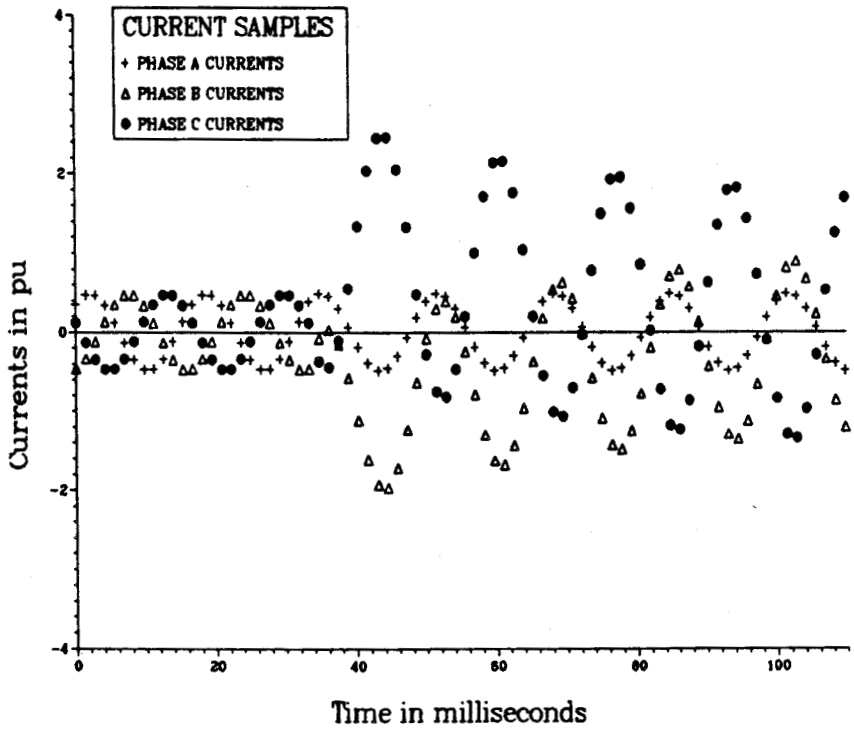

Figure 7.7: The current samples generated for a phase B to phase C fault at F_3.

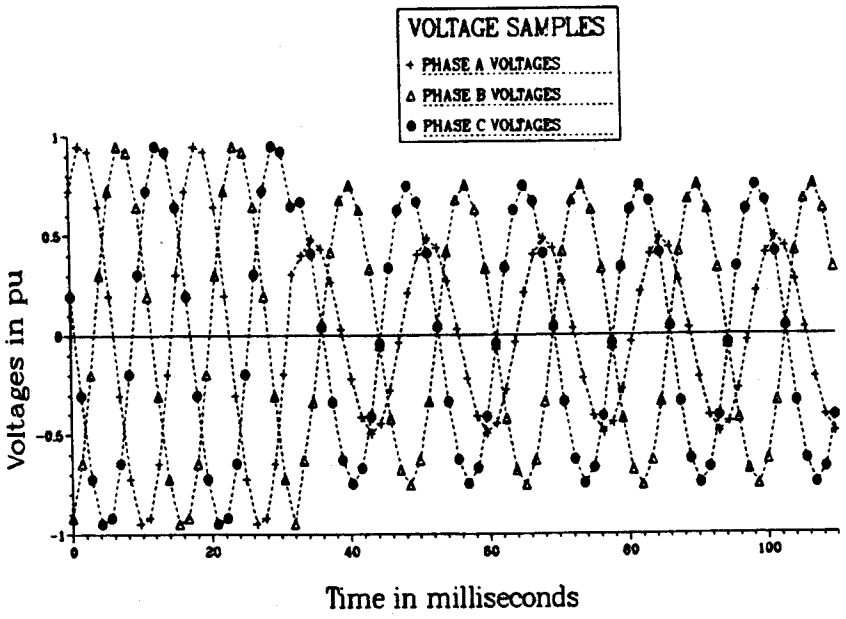

Figure 7.8: The voltage samples generated for a phase A to ground fault at F_1.

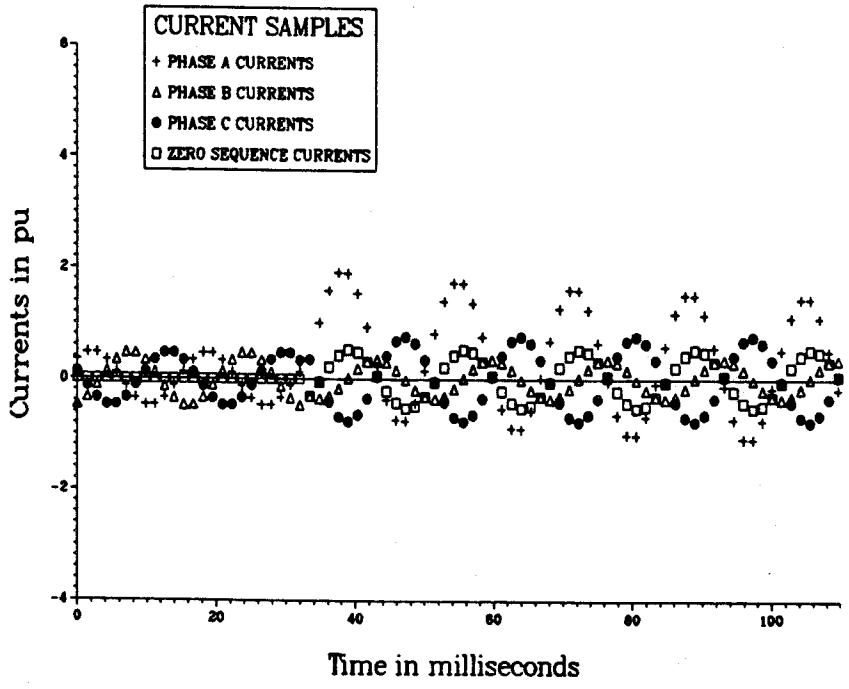

Figure 7.9: The current samples generated for a phase A to ground fault at F_1.

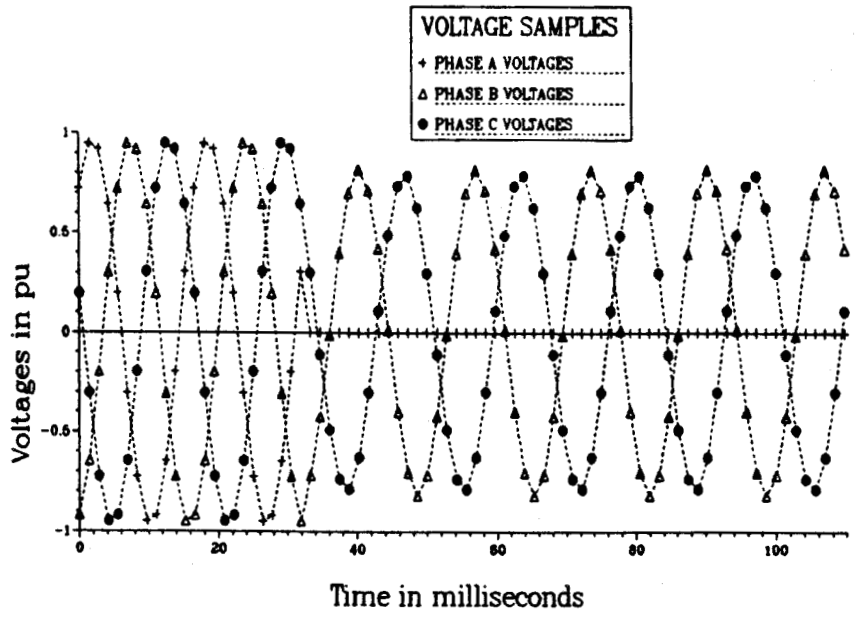

Figure 7.10: The voltage samples generated for a phase A to ground fault at F_2.

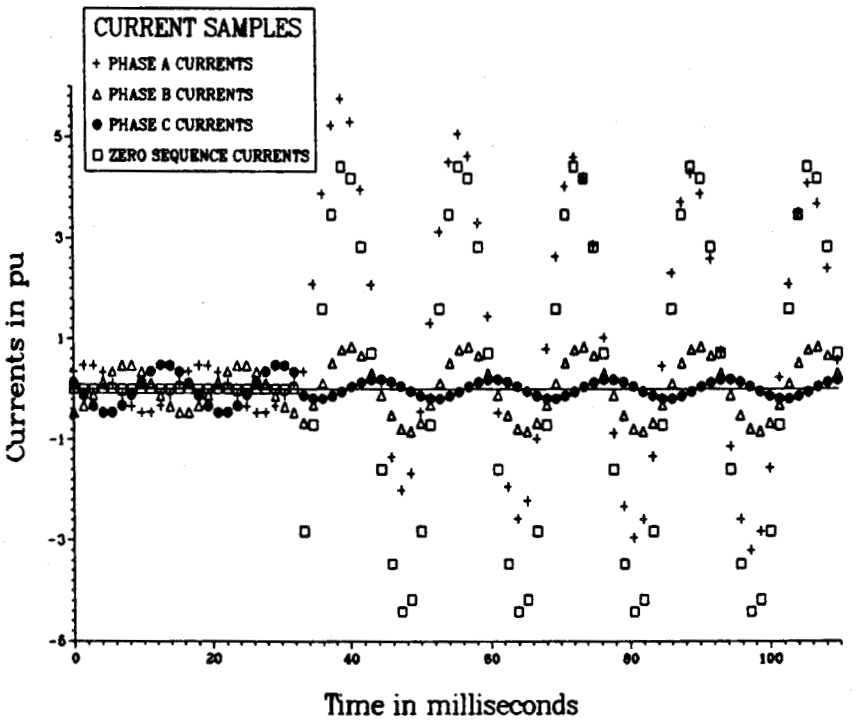

Figure 7.11: The current samples generated for a phase A to ground fault at F_2.

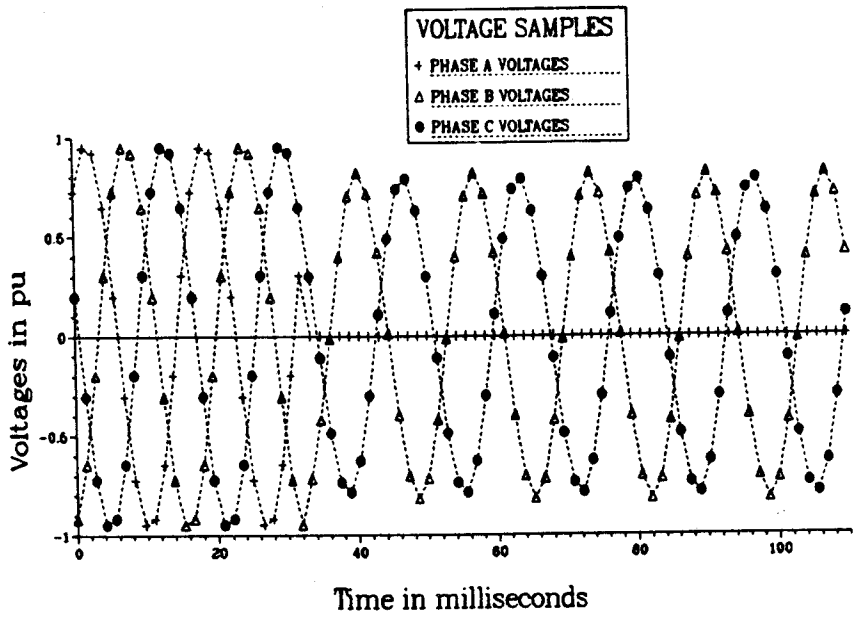

Figure 7.12: The voltage samples generated for a phase A to ground fault at F_3.

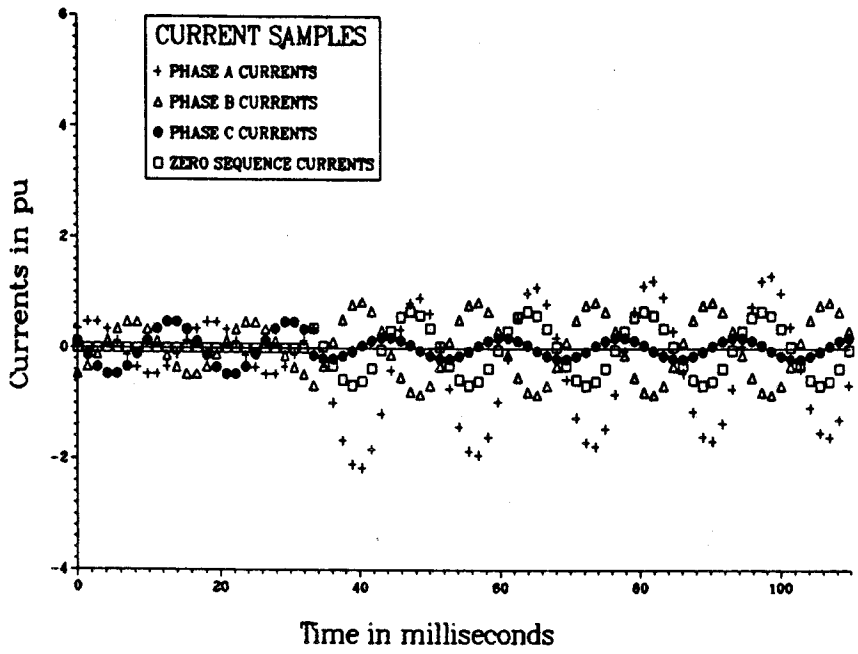

Figure 7.13: The current samples generated for a phase A to ground fault at F_3.

4. directional/impedance relays.

The relays were also tested when they were not polarized, however, the discussion in this section applies only to the polarized mho relay. The polarization coefficients $K_1 = 0.6682$ and $K_2 = 0.2\angle 13.4^\circ$ were used for the phase fault elements and $K_1 = 0.6940$ and $K_2 = 0.2\angle 59.3^\circ$ were used for the ground fault elements.

7.3.1. Phase-Phase Faults

As mentioned in Section 7.2 the phase-phase faults used for the tests in this chapter were the B phase to C phase faults. Faults involving phases A and B and phases C and A were also studied and found to give similar results. Also studied were the performance of the models of the healthy phase relays when there was a phase B to phase C fault on the line.

7.3.1.1. B-C Fault at F_1

The sampled voltages and currents shown in Figures 7.2 and 7.3 were used as inputs to the software when testing the relay algorithms for this fault. The impedances seen by the phase fault and ground fault elements are shown in Figures 7.14 and 7.15 respectively. Figure 7.14 shows that the trajectory of the phase B to phase C impedance estimates ends in the operating region of the mho relay. Figure 7.15 shows that the phase B to ground impedance estimates ends near the operating region of the mho characteristic, but these estimates did not enter the characteristic. The information provided by the software are listed in Table 7.1. Apart from the B-C relay none of the other relays issued a trip command. The fault occurred at 9 hours, 48 minutes and 8.730 seconds and the the B-C relay issued a trip command at 9 hours, 48 minutes and 8.752 seconds. Resetting of the relay took place at 9 hours, 48 minutes and 8.802 seconds. In this test the performance of all the six relays were as expected.

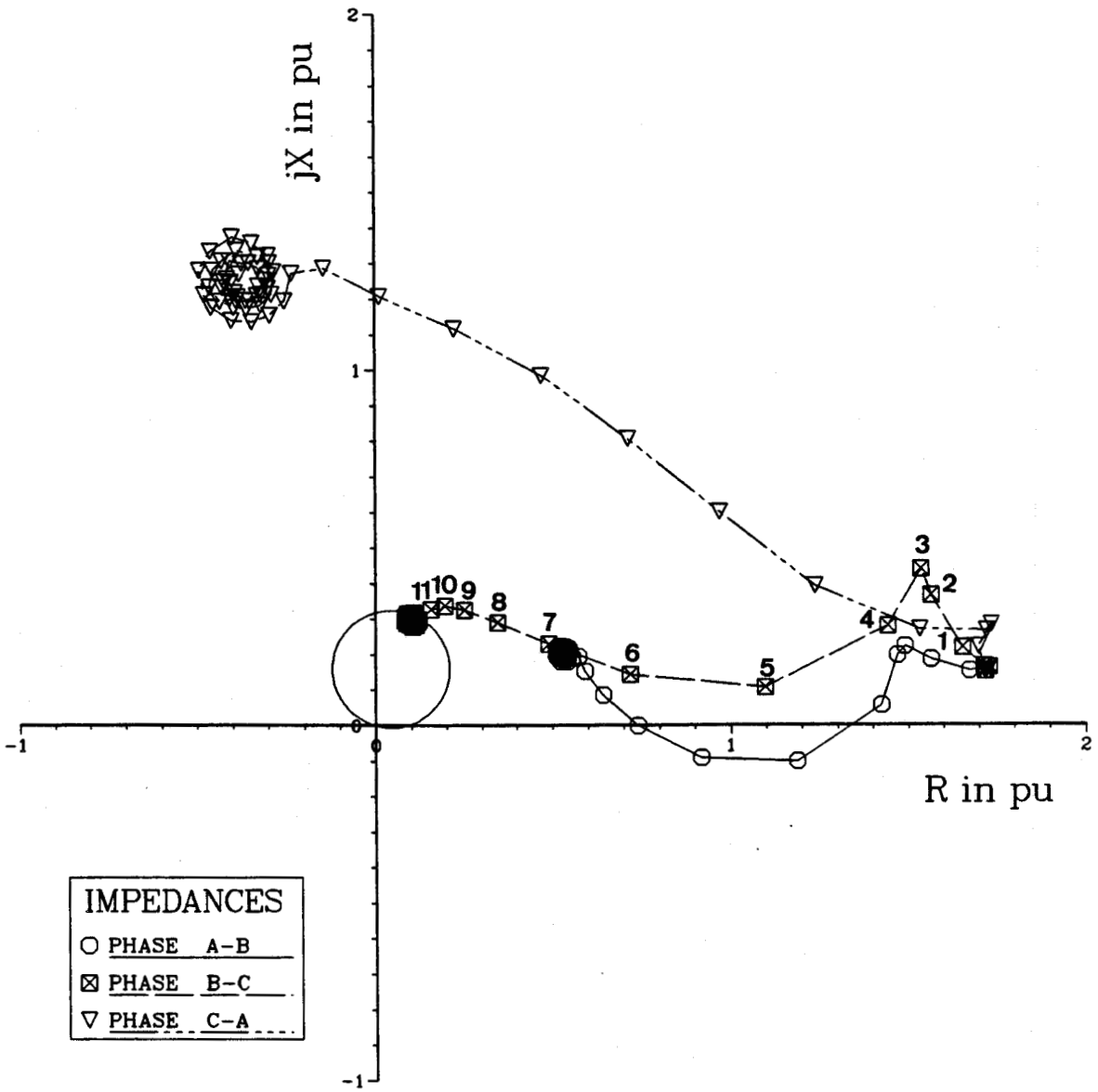

Figure 7.14: The impedances seen by the phase fault elements for a phase B to phase C fault at F_1.

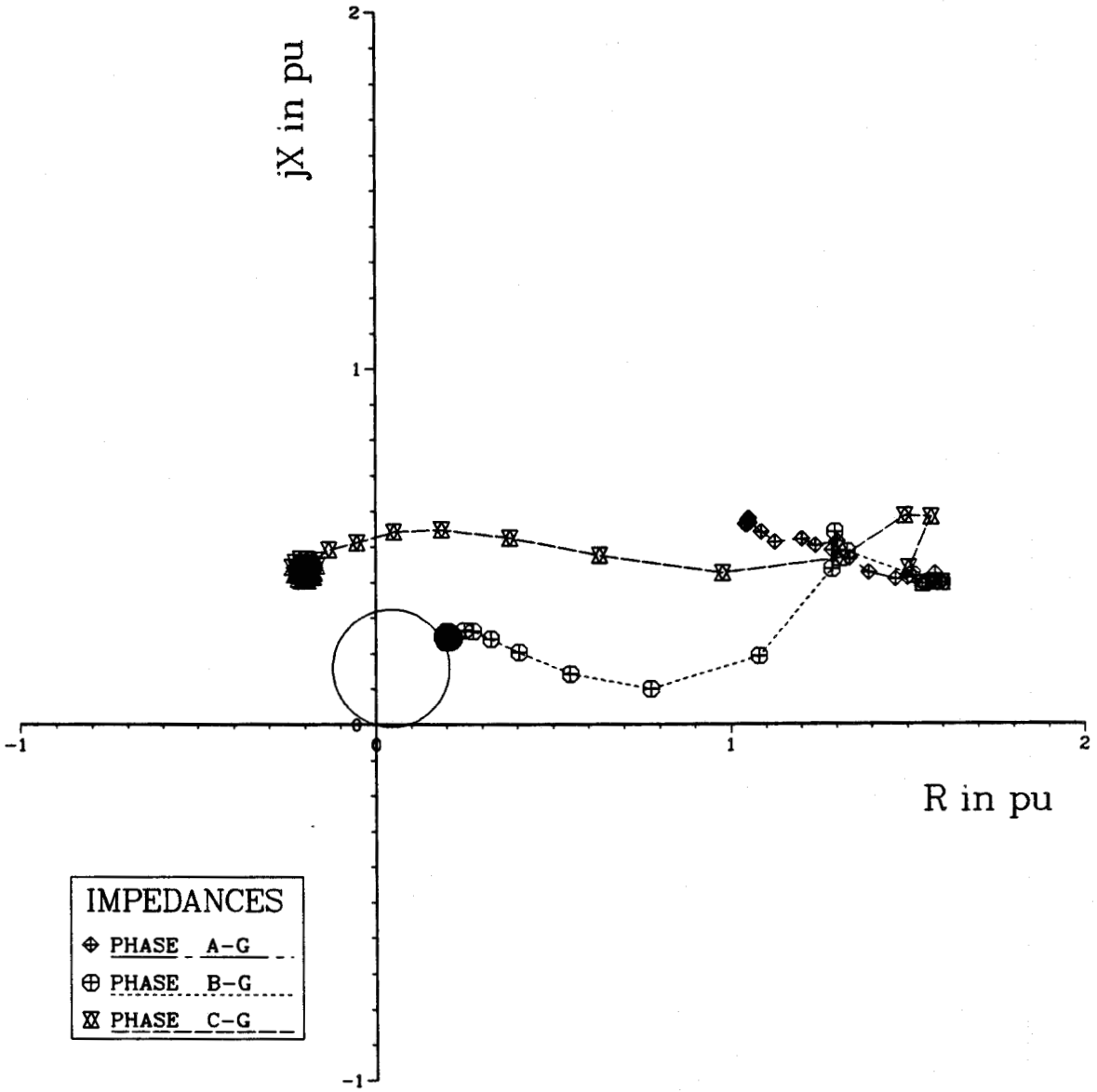

Figure 7.15: The impedances seen by the ground fault elements for a phase B to phase C fault at F_1.

Table 7.1: The output of the software for a phase B to phase C fault.

OUTPUT OF RELAY A-B	
FAULT TYPE	B-C
DATE	3/12/1988
FAULT OCCURRENCE TIME	9HRS. 48MINS. 8.730SECS.
RELAY DID NOT OPERATE	

OUTPUT OF RELAY B-C	
FAULT TYPE	B-C
DATE	3/12/1988
FAULT OCCURRENCE TIME	9HRS. 48MINS. 8.730SECS.
TRIP TIME OF RELAY	9HRS. 48MINS. 8.752SECS.
RESET TIME OF RELAY	9HRS. 48MINS. 8.802SECS.

OUTPUT OF RELAY C-A	
FAULT TYPE	B-C
DATE	3/12/1988
FAULT OCCURRENCE TIME	9HRS. 48MINS. 8.730SECS.
RELAY DID NOT OPERATE	

Table 7.1 continued.

OUTPUT OF RELAY A-G	
FAULT TYPE	B-C
DATE	3/12/1988
FAULT OCCURRENCE TIME	9HRS. 48MINS. 8.730SECS.
RELAY DID NOT OPERATE	

OUTPUT OF RELAY B-G	
FAULT TYPE	B-C
DATE	3/12/1988
FAULT OCCURRENCE TIME	9HRS. 48MINS. 8.730SECS.
RELAY DID NOT OPERATE	

OUTPUT OF RELAY C-G	
FAULT TYPE	B-C
DATE	3/12/1988
FAULT OCCURRENCE TIME	9HRS. 48MINS. 8.730SECS.
RELAY DID NOT OPERATE	

7.3.1.2. B-C Fault at F_2

For a phase-phase fault at F_2, the sampled voltages and currents of Figures 7.4 and 7.5 were used as inputs to the software. In this test the B-C and B-G relays issued trip commands. The phase C to ground impedance estimates traversed the mho characteristic, but the C-G relay did not issue a trip command since only two of the impedance estimates were in the operating region. The information provided by the software was similar to the one listed in Table 7.1 except that the B-G relay misoperated and, therefore issued a trip command. The B-C and B-G relays issued trip commands 17 and 18 milliseconds respectively after the occurrence of the fault. Figures 7.16 and 7.17 show the impedances seen by the phase fault and ground fault relays as they traverse the impedance plane.

7.3.1.3. B-C Fault at F_3

When the sampled voltages and currents of Figures 7.6 and 7.7 were applied as inputs to the software, none of the relays which were modelled issued a trip command. The behavior of all the relays which were modelled were satisfactory during this test. The trajectories of the impedances seen by the relays were all outside the tripping region of the mho relay. These are shown in Figures 7.18 and 7.19 for the phase fault and ground fault units respectively.

7.3.2. Single-Phase to Ground Faults

The studies reported in this section were done for the phase A to ground faults. However, the phase B and phase C to ground faults were also considered and the results found to be similar to those presented here.

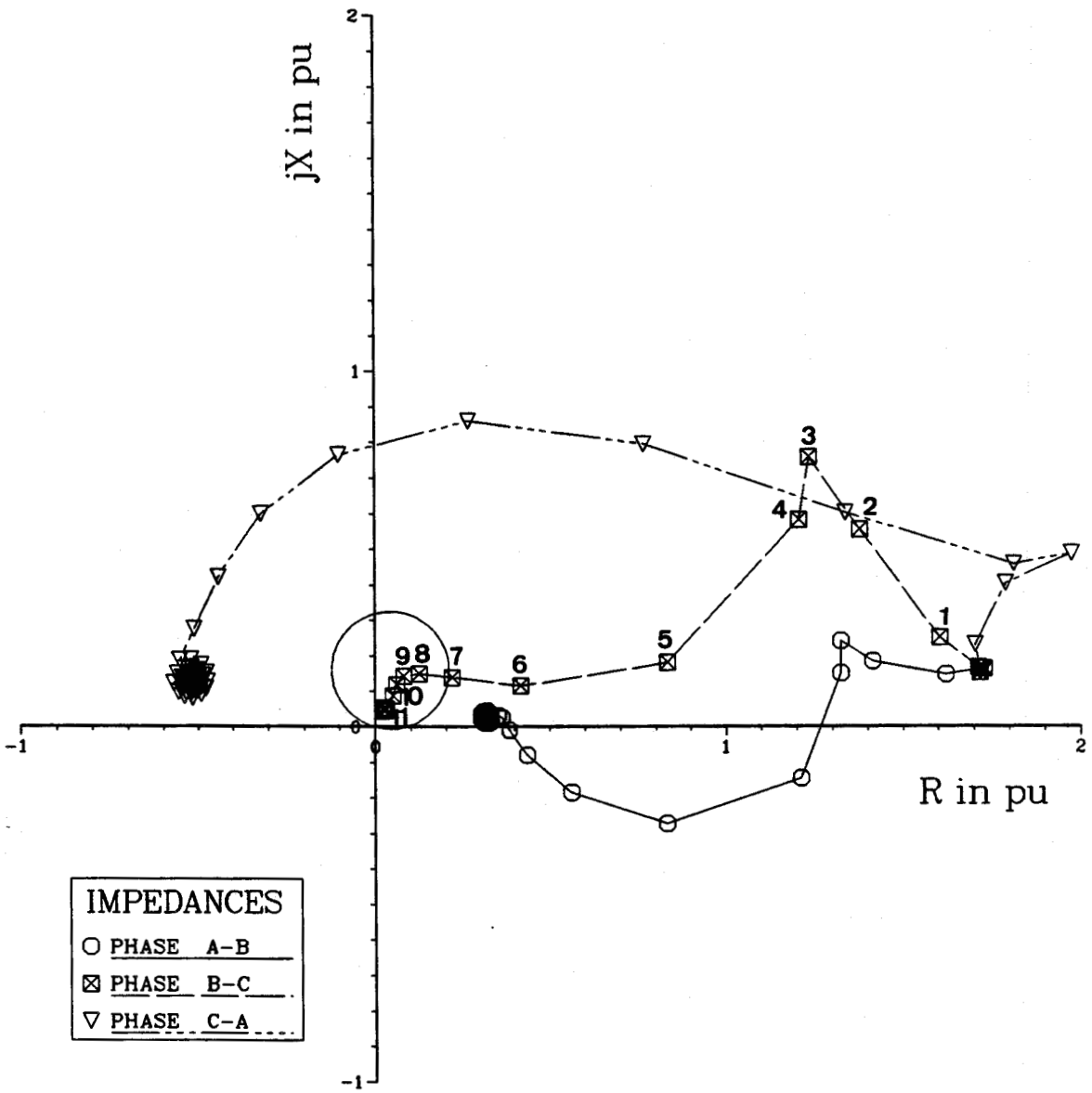

Figure 7.16: The impedances seen by the phase fault elements for a phase B to phase C fault at F_2.

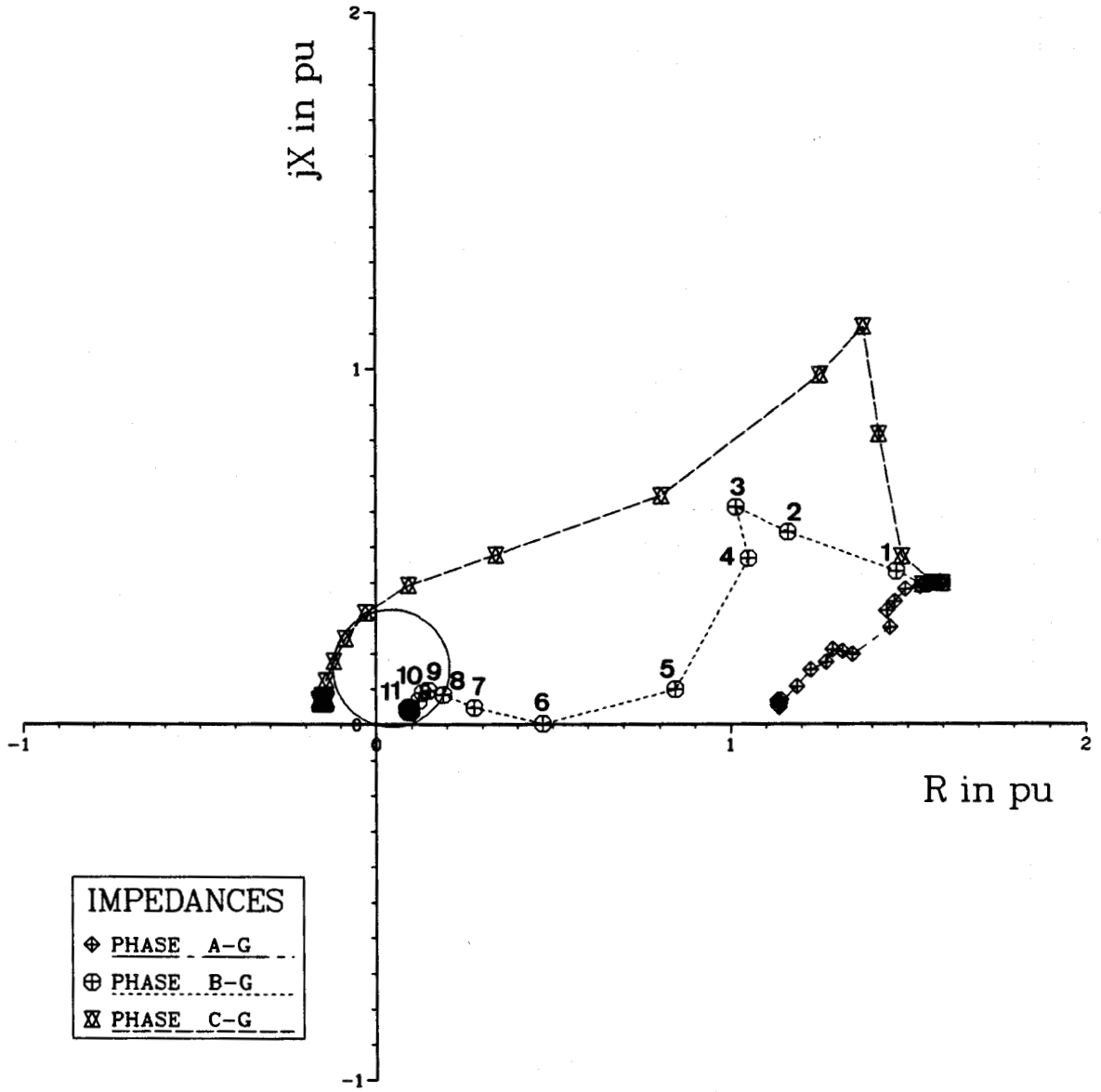

Figure 7.17: The impedances seen by the ground fault elements for a phase B to phase C fault at F_2.

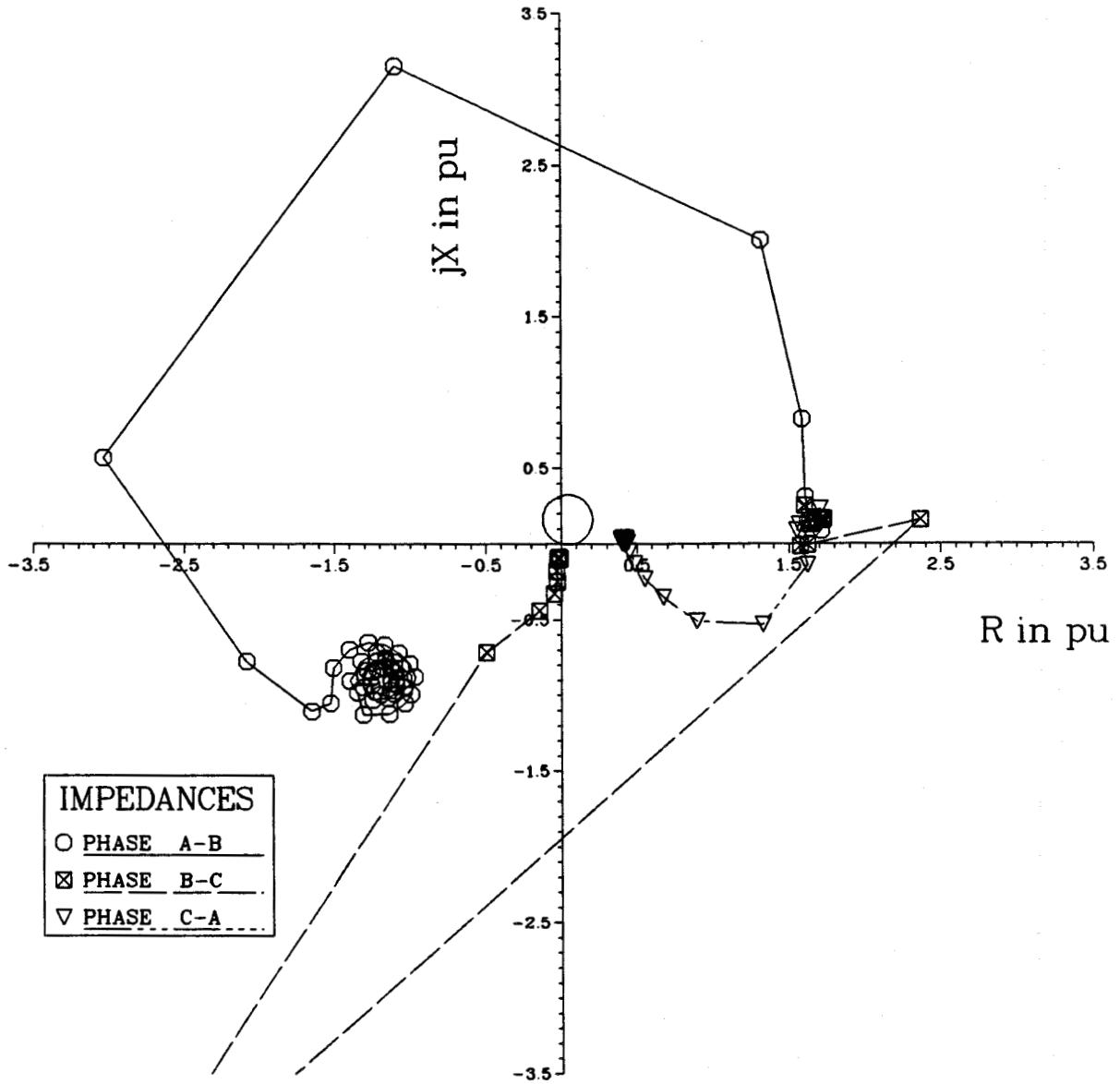

Figure 7.18: The impedances seen by the phase fault elements for a phase B to phase C fault at F_3.

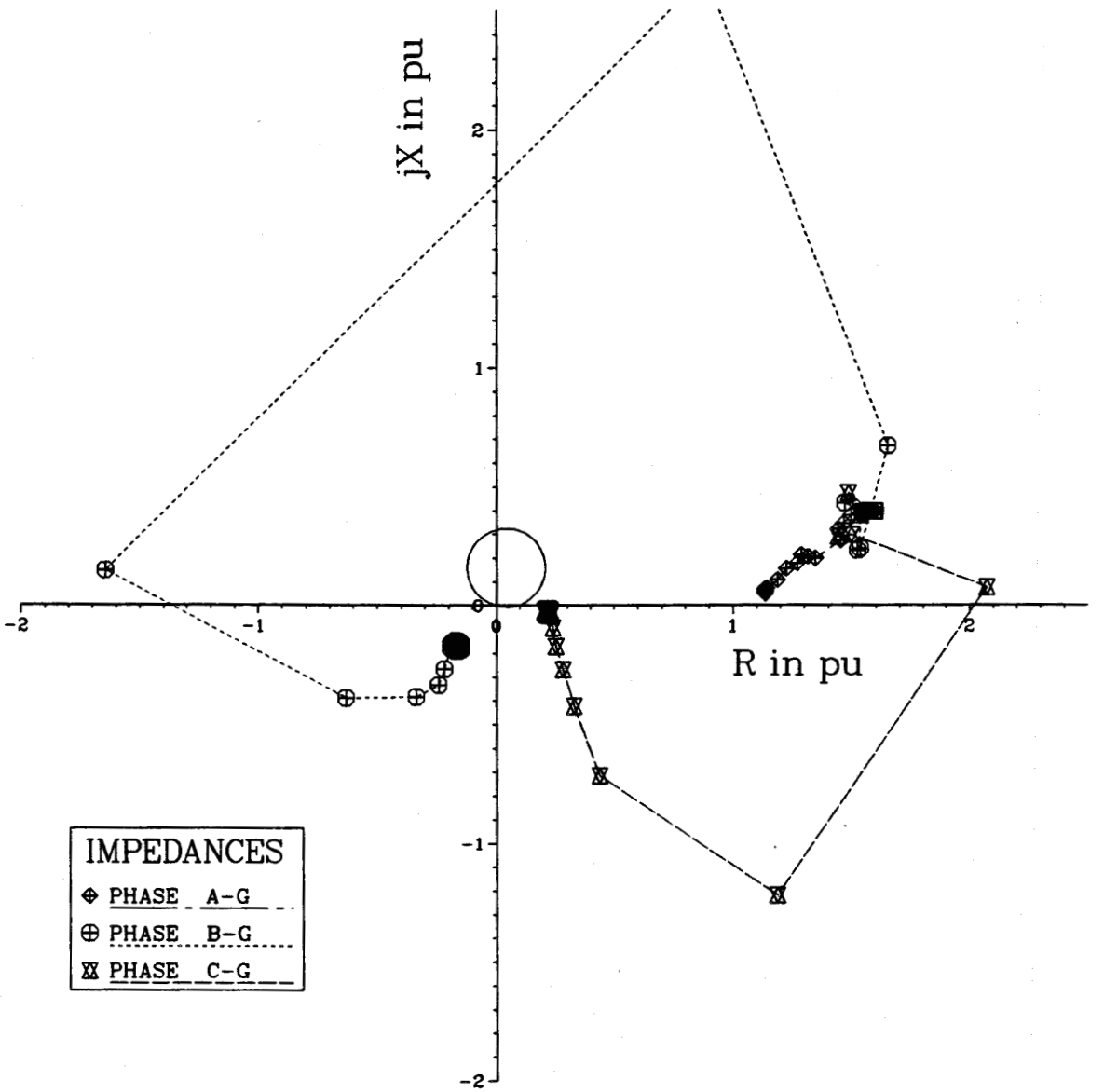

Figure 7.19: The impedances seen by the ground fault elements for a phase B to phase C fault at F_3.

7.3.2.1. A-G Fault at F_1

A phase to ground fault involving phase A and ground was assumed to have occurred at F_1. The sampled voltages and currents of Figures 7.8 and 7.9 which were generated for this fault were, therefore, applied as inputs to the software. The impedances seen by the phase fault and ground fault units are shown in Figures 7.20 and 7.21 respectively. In Figure 7.20 all the impedance trajectories end outside the operating region of the mho relay. Figure 7.21 shows that the impedance estimates of the A-G relay entered the tripping region of the mho relay characteristic. The A-G relay model, therefore, issued a trip command to the circuit breaker. The information provided by the relays are listed in Table 7.2. From the information provided by the software it is seen that all the elements performed very well for this fault.

7.3.2.2. A-G Fault at F_2

When testing for the single phase to ground fault at this location, the sampled voltages and currents of Figures 7.10 and 7.11 were used as inputs to the software. Figures 7.22 and 7.23 show the impedance estimates for the phase fault and ground fault relays respectively. The A-G relay as well as the C-A relay issued trip commands 11 and 21 milliseconds respectively after the occurrence of the fault. The C-A relay in this case misoperated. The impedances seen by the A-B relay were very near to the mho characteristic. However, it did not issue a trip command since none of the impedance estimates entered the operating region of the mho relay.

7.3.2.3. A-G Fault at F_3

The sampled voltages and currents of Figures 7.12 and 7.13 were used as inputs to the software for this fault. Under this condition none of the relays issued a trip command since all the impedance estimates were outside the operating region of the mho relay characteristic. The performance of all the units were very good for this fault. These impedances are shown in Figures 7.24 and 7.25 for the phase fault and ground fault relays respectively.

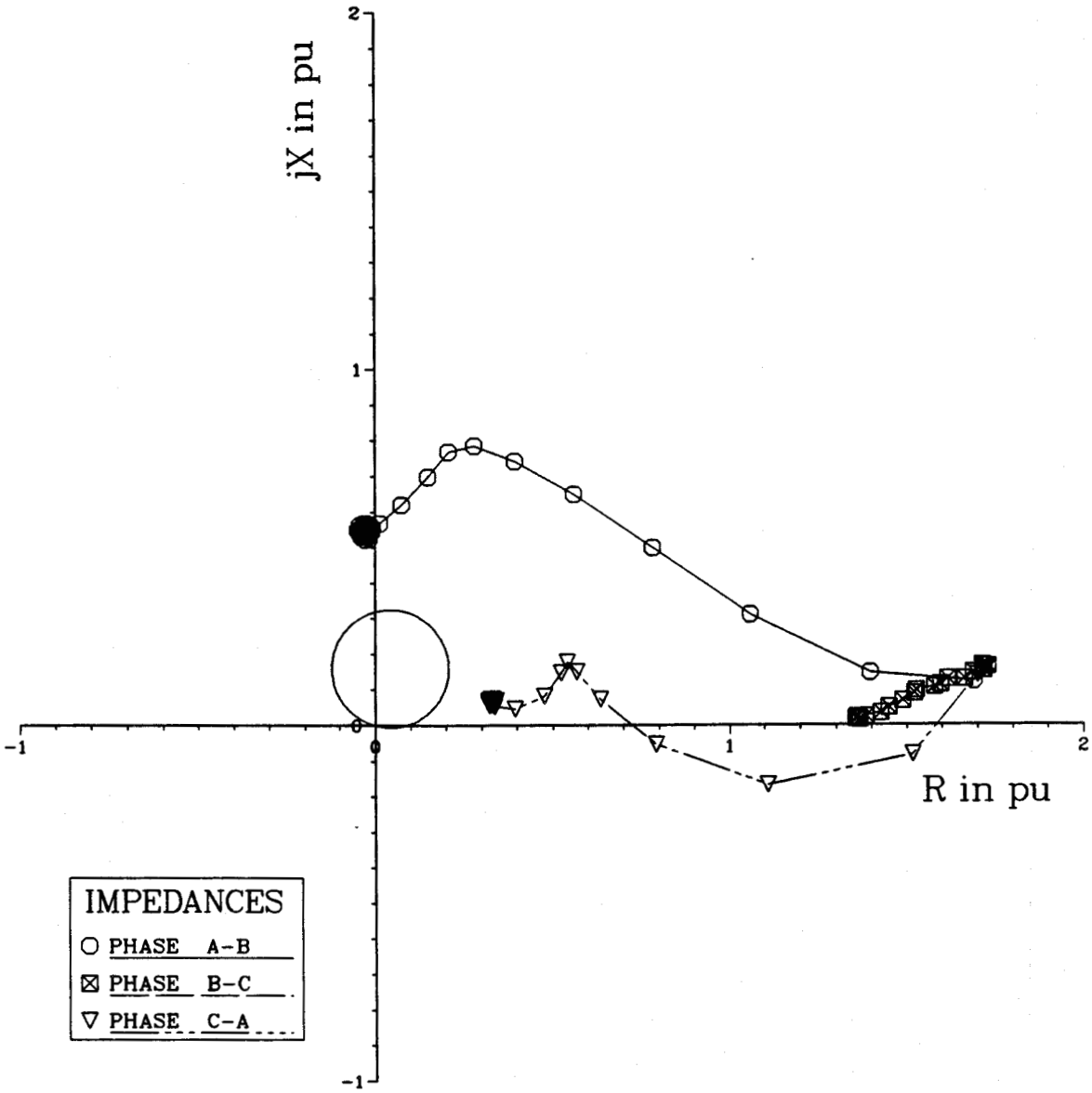

Figure 7.20: The impedances seen by the phase fault elements for a phase A to ground fault at F_1.

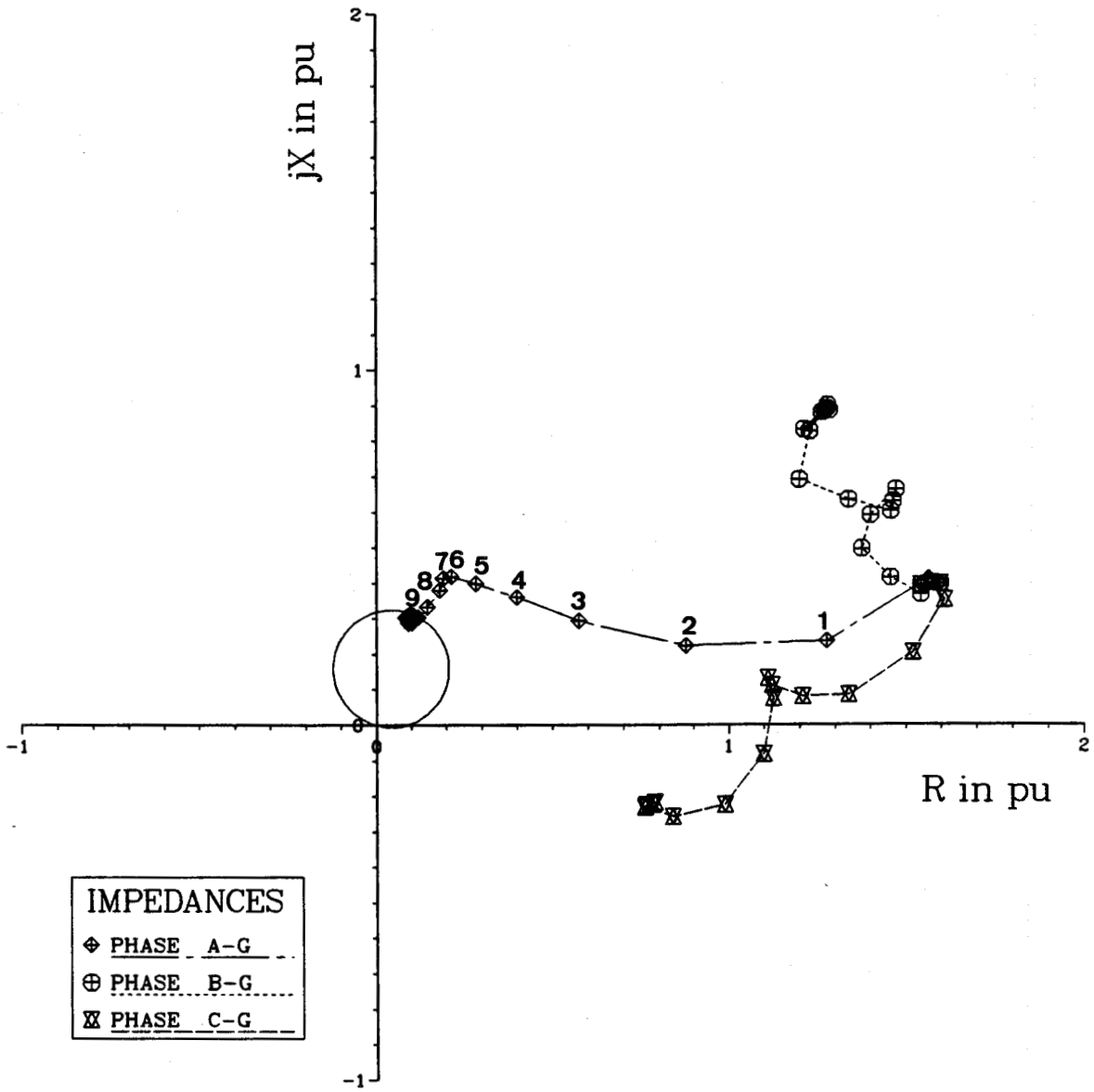

Figure 7.21: The impedances seen by the ground fault elements for a phase A to ground fault at F_1.

Table 7.2: The output of the software for a phase A to ground fault.

OUTPUT OF RELAY A-B	
FAULT TYPE	A-G
DATE	4/12/1988
FAULT OCCURRENCE TIME	10HRS. 50MINS. 26.030SECS.
RELAY DID NOT OPERATE	
OUTPUT OF RELAY B-C	
FAULT TYPE	A-G
DATE	4/12/1988
FAULT OCCURRENCE TIME	10HRS. 50MINS. 26.030SECS.
RELAY DID NOT OPERATE	
OUTPUT OF RELAY C-A	
FAULT TYPE	A-G
DATE	4/12/1988
FAULT OCCURRENCE TIME	10HRS. 50MINS. 26.030SECS.
RELAY DID NOT OPERATE	

Table 7.2 continued.

OUTPUT OF RELAY A-G	
FAULT TYPE	A-GROUND
DATE	4/12/1988
FAULT OCCURRENCE TIME	10HRS. 50MINS. 26.030SECS.
TRIP TIME OF RELAY	10HRS. 50MINS. 26.049SECS.
RESET TIME OF RELAY	10HRS. 50MINS. 26.099SECS.

OUTPUT OF RELAY B-G	
FAULT TYPE	A-G
DATE	4/12/1988
FAULT OCCURRENCE TIME	10HRS. 50MINS. 26.030SECS.
RELAY DID NOT OPERATE	

OUTPUT OF RELAY C-G	
FAULT TYPE	A-G
DATE	4/12/1988
FAULT OCCURRENCE TIME	10HRS. 50MINS. 26.030SECS.
RELAY DID NOT OPERATE	

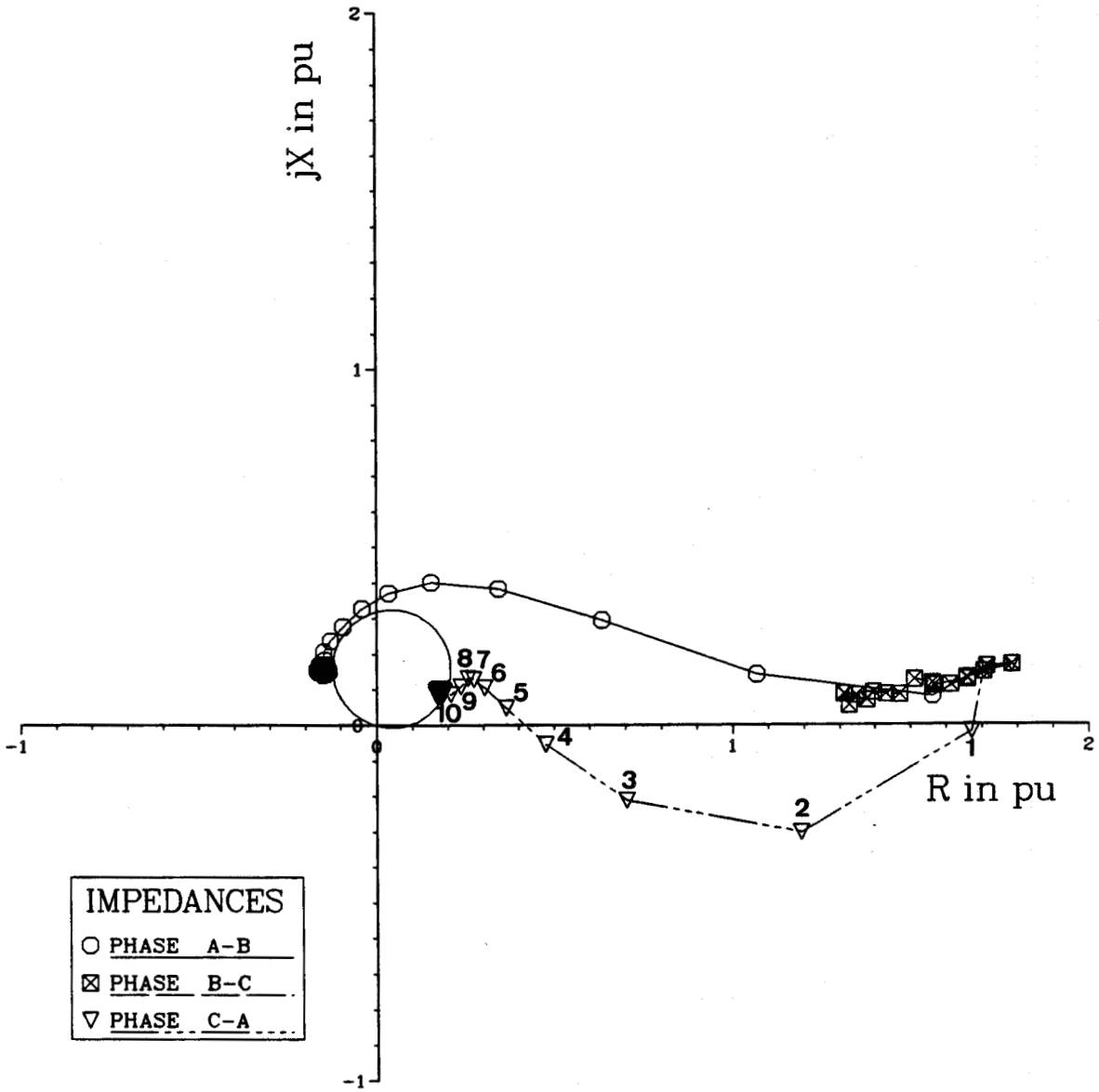

Figure 7.22: The impedances seen by the phase fault elements for a phase A to ground fault at F_2.

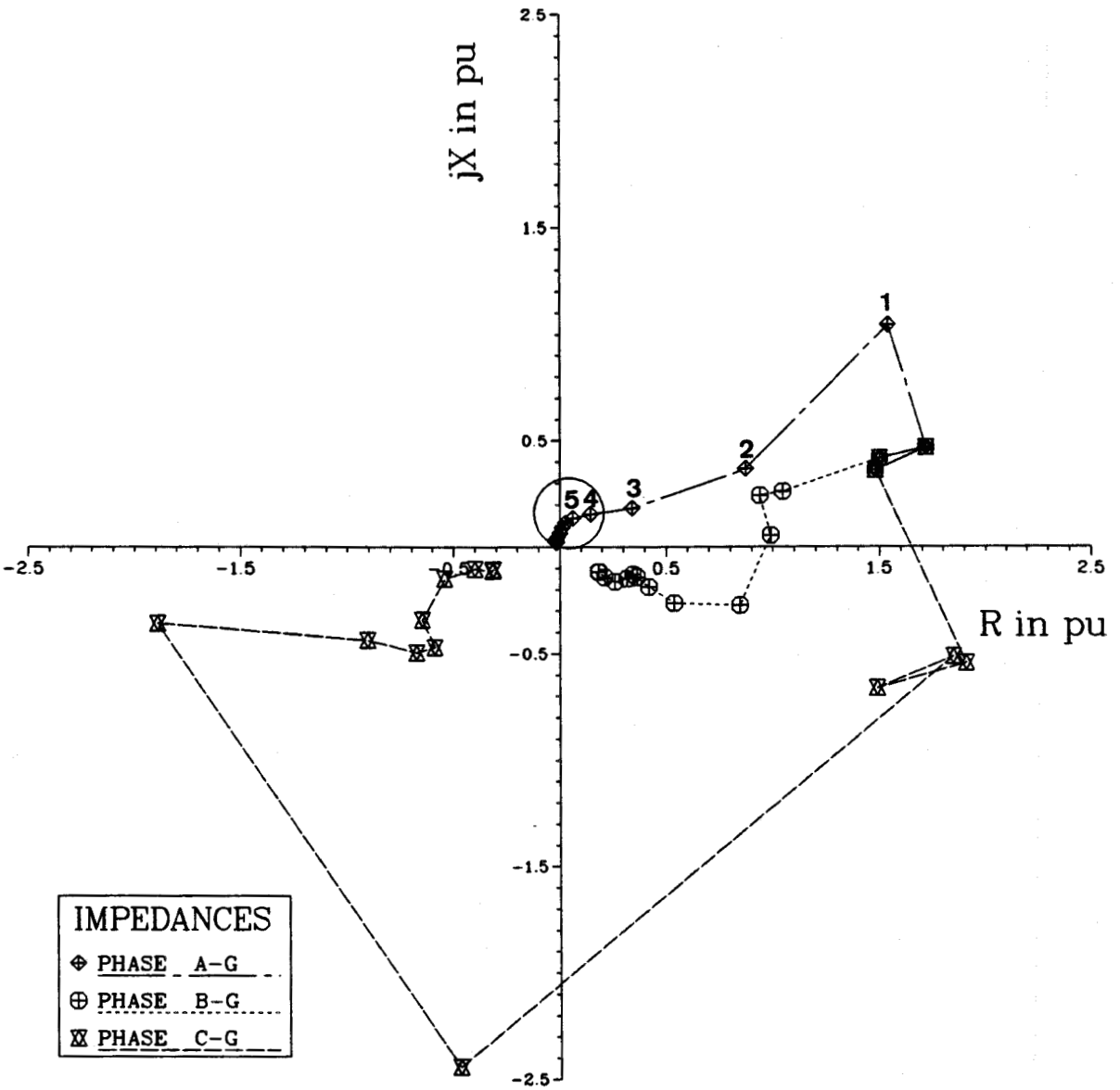

Figure 7.23: The impedances seen by the ground fault elements for a phase A to ground fault at F_2.

7.4. Studies Conducted for Digital Directional Relays

Phase-phase and single-phase to ground faults were assumed to have occurred at F_1 and F_3. The sampled voltages and currents generated at these locations were, therefore, used as inputs to the software. The relays tested were for the 90°, 60° *No.*1, 60° *No.*2 and 30° connections.

7.4.1. 90-Degree Connections

The sampled voltages and currents of Figures 7.2 and 7.3 were used as inputs to the software. The models for the B and C elements of this relay issued trip commands. The model for element B, however, took a shorter time in arriving at a trip decision. Table 7.3 contains the information supplied by the software and from this it is seen that there was no operation for the model of element A. When the sampled data of Figures 7.6 and 7.7 were used as inputs, that is fault behind the relay, none of the models for the three elements issued a trip command.

The performance of the elements were also tested for a phase A to ground fault using the sampled data of Figures 7.8, 7.9 and Figures 7.12, 7.13. Only the faulted phase element issued a trip command for the forward fault condition and none of the relays operated for the fault behind the relay.

7.4.2. 60-Degree No.1 Connections

The same sampled data used in Section 7.4.1 were used to test this relay. All the models for the three elements of this relay operated for the phase-phase fault. The model for element A in this case misoperated. It is, however, doubtful whether in practice the fault detecting element will receive enough current to enable element A to operate. None of the models for the elements operated when the fault was assumed to have occurred at F_3 and the sampled data of Figures 7.8 and 7.9 used.

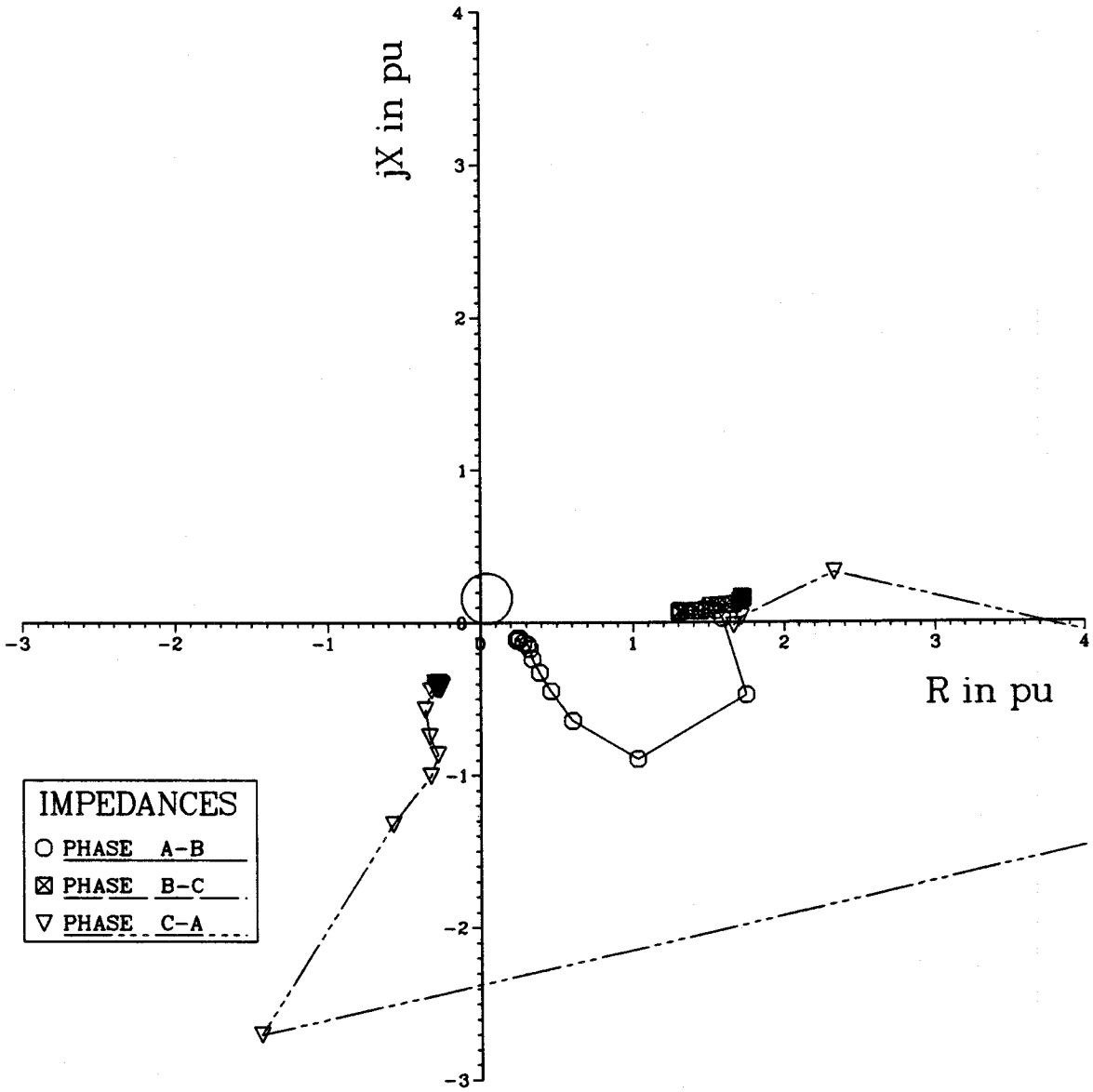

Figure 7.24: The impedances seen by the phase fault elements for a phase A to ground fault at F_3.

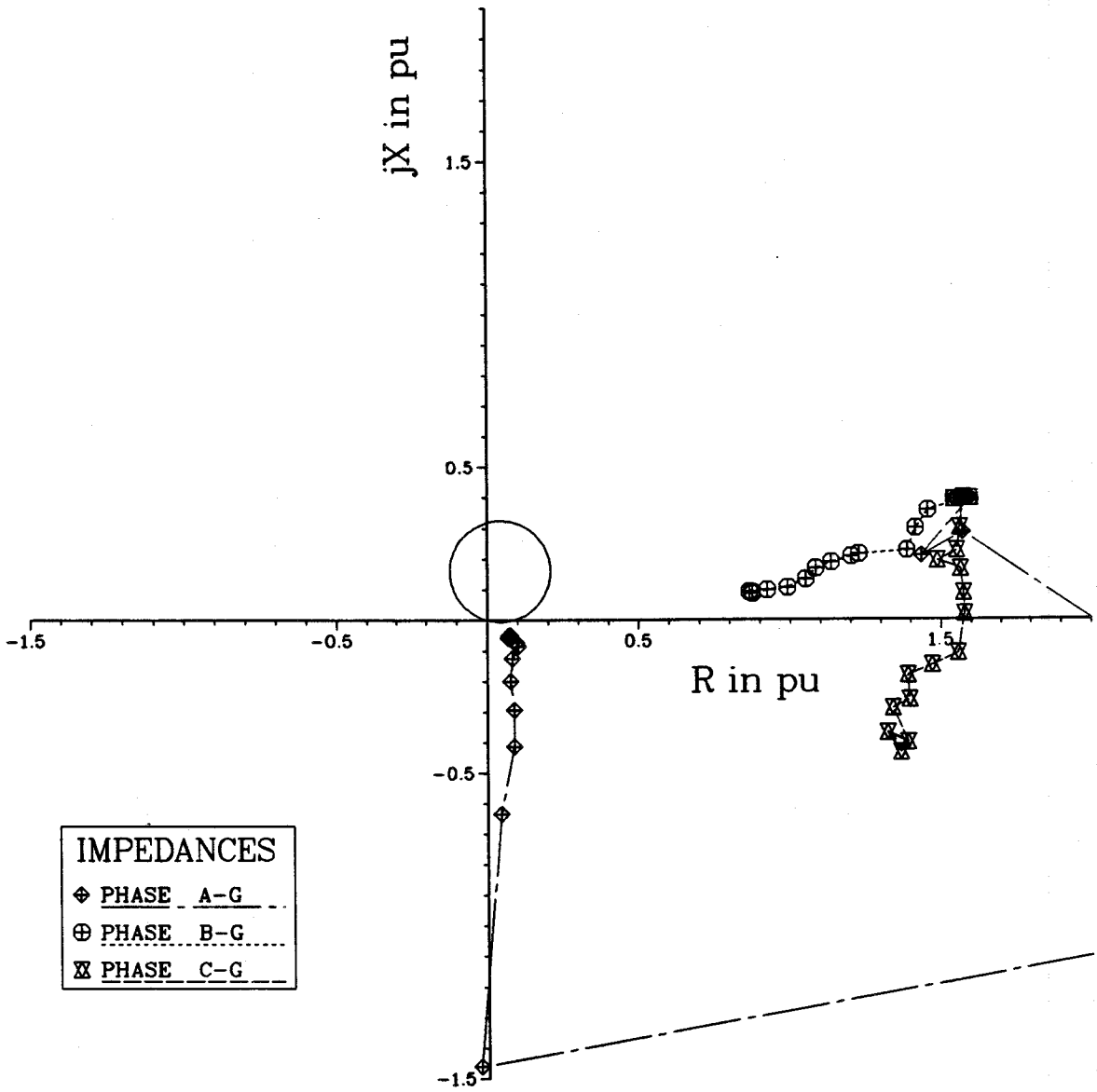

Figure 7.25: The impedances seen by the ground fault elements for a phase A to ground fault at F_3.

Table 7.3: The output of the software for a phase B to phase C fault at location F_1.

OUTPUT FROM RELAY A	
TYPE OF RELAY CONNECTION	90-DEGREES
DATE	6/12/1988
FAULT OCCURRENCE TIME	13HRS. 4MINS. 56.860SECS.
RELAY DID NO OPERATE	

OUTPUT FROM RELAY B	
TYPE OF RELAY CONNECTION	90-DEGREES
DATE	6/12/1988
FAULT OCCURRENCE TIME	13HRS. 4MINS. 56.860SECS.
TRIP TIME OF RELAY	13HRS. 4MINS. 56.886SECS.
RESET TIME OF RELAY	13HRS. 4MINS. 56.936SECS.

OUTPUT FROM RELAY C	
TYPE OF RELAY CONNECTION	90-DEGREES
DATE	6/12/1988
FAULT OCCURRENCE TIME	13HRS. 4MINS. 56.860SECS.
TRIP TIME OF RELAY	13HRS. 4MINS. 56.889SECS.
RESET TIME OF RELAY	13HRS. 4MINS. 56.939SECS.

For a phase A to ground fault in the forward direction, the models of elements A and C operated. None of the elements operated when this fault was assumed to be at the bus side.

7.4.3. 60-Degree No.2 Connections

The sampled voltages and currents of Figures 7.2 and 7.3 were used as inputs to the software. For these input data, the models for elements B and C issued trip commands. None of the elements operated when the sampled data of Figures 7.6 and 7.7 were used as inputs.

A single phase to ground fault was considered by applying as inputs, the sampled data of Figures 7.8, 7.9 and Figures 7.12, 7.13. Only the model for element A issued a trip command for the fault at F_1. In the case of bus side fault, the model for element C misoperated.

7.4.4. 30-Degree Connections

The algorithm for this relay was tested using the sampled voltages and currents of:

1. Figures 7.2, 7.3,
2. Figures 7.6, 7.7,
3. Figures 7.8, 7.9 and
4. Figures 7.12, 7.13.

In the first case, which is phase B to phase C fault at F_1, the models for elements B and C of the relay issued trip commands. No operation was recorded for any of the models in the second case, that is phase B to phase C fault at F_3. For case three , phase A to ground fault at F_1, only the model for element A issued a trip command. The model for element C issued a trip command when case four or fault behind the relay was considered.

7.5. Summary

This chapter has described some of the tests that were carried out to demonstrate the capabilities of the software package developed in this project. The studies reported for the digital distance relay models used the mho type distance relay. Studies involving the other distance relay models were conducted and the results were found to be similar to those obtained for the mho relay. The models for four types of directional relays were also tested in this chapter.

8. SUMMARY AND CONCLUSIONS

The main objective of this research was to develop an interactive software for implementing models of digital distance and directional relays on a digital computer. In achieving this objective several techniques for implementing the models were considered.

Distance and directional relays have measuring units which are basically amplitude or phase comparators. The types of comparators and the input signals have been presented in Chapter 2. These comparators exhibit characteristics which can be represented on an impedance plane. To select a model for a relay, the shape of its characteristic on an impedance plane and the equation representing its input signals must be carefully examined.

A distance relay should be able to protect a transmission line efficiently in the event of a fault at any location within its protective zone. The relay should, therefore, be able to perform its intended tasks satisfactorily even if there is a collapse of the voltage to its input terminals. Distance relay designers, therefore, incorporate polarization and memory action in their designs. The polarization and memory action techniques have been outlined in Chapter 3. Details of the effects of polarization on the performance of relays have also been presented. The directional relay connections used in power systems have also been discussed.

The major factors that affect the accuracy of the results computed by a digital relay are the word size of the micro-processors, the A/D converters, the saturation of A/D converters and relay software. The details of these factors have been outlined in Chapter 4. Two important parts of a relay's

software are the relay algorithm and the relay logic. Several algorithms suggested in the past and techniques for implementing logic have been discussed in Chapters 4 and 5. The techniques used in implementing the relay logic are (1) amplitude comparison, (2) phase comparison, (3) impedance estimation and (4) memory mapped targeting.

The software, presented in this thesis, provides an interactive approach for studying the performance of digital distance and directional relays. The specifications of the software, its structure and its special features have been described in Chapter 6. The software includes programs for

1. evaluating the algorithms for estimating the peak values and phase angles of the power system voltages and currents.
2. calculating line impedances and implementing the models of digital distance relays.
3. implementing the models of digital directional relays.
4. generating the instantaneous values of voltages and currents.

The software facilitates the execution of the programs in two modes of operation. In the first mode, the computations are performed using the floating point format of numbers. In the second mode, the effects of A/D converters, truncations or roundings and bit shift multiplications are incorporated. The computations are performed using the integer format of the numbers. The former mode provides information concerning the errors due to the inadequacies in the designs of algorithms. The latter mode simulates the performance of the algorithms and relay logic if implemented on a digital processor.

The studies that were conducted to determine the capabilities of the software have been described in Chapter 7. The tests were conducted by considering transmission line shunt faults at different locations on a line. The movement of the trajectory of the calculated impedances from the pre-

fault to post-fault states shows the speed with which a mho relay detects faults that are in its operating zone. During the tests all the relays whose models have been implemented behaved as expected.

The developed software includes most of relay algorithms developed in the past. This package is a useful tool for designing digital relays. The present version of the software can be used for selecting an appropriate relay algorithm for use in an application. The software is also useful as an educational aid for learning and studying the characteristics of relaying algorithms. The use of the software in a class room environment provides the students a better understanding of the performance of algorithms in a variety of situations that might be encountered in a power system.

The relays which have been considered are for transmission and distribution lines protection. The software, however, can be extended to include relays which protect other equipment, such as, transformers, generators and station buses.

REFERENCES

1. M.S. Sachdev, Coordinator, *Computer Relaying Tutorial Text*, IEEE Publication No. 79 EH 0148-7-PWR, New York, 1979.

2. M.S. Sachdev, Coordinator, *Microprocessor Relays and Protection Systems*, IEEE Tutorial Course. Course Text 88EH0269-1-PWR Piscataway, NJ 08854-1331, 1988.

3. F.H. Last, and A. Stalewsky, "Protective Gear as a Part of Automatic Power System Control", *Symposium on Automatic Control in Electricity Supply, IEE Conference Publication NO. 16 Part 1, Manchester*, March 1966.

4. G.D. Rockefeller, "Fault Protection with a Digital Computer", *IEEE Transactions on Power Apparatus and Systems, Vol. PAS-88*, April 1969, pp. 438-464.

5. B. Ravindranath and M. Chander, *Power System Protection and Switchgear*, Wiley Eastern Limited, New Delhi, 1976.

6. A.T. Johns, "Generalized-Phase-Comparator Techniques for Distance Protection. Theory and Operation of Multi-Input Devices", *Proceedings of IEE, Vol. 119*, 1972, pp. 1595-1603.

7. W.D. Humpage and S.P. Sabberwal, "Developments in Phase Comparator Techniques for Distance Protection", *Proceedings of IEE, Vol. 112*, 1965, pp. 1383-1394.

8. V. Cook, *Analysis of Distance Protection*, Research Studies Press, Letchworth and John Wiley and Sons Inc., New York, 1985.

9. L.M. Wedepohl, "Polarized Mho Distance Relay. New Approach to the Analysis of Practical Characteristics", *Proceedings of IEE Vol. 112, No. 3*, March 1965, pp. 525-535.

10. V. Cook, "Generalized Method of Assessing Polarizing Signals for the Polarized-Mho Relay", *Proceedings of IEE, Vol. 112, No. 5*, May 1975, pp. 497-500.

11. V. Cook, "Improved Signals to the Polarized-Mho Distance Relay", *Proceedings of IEE, Vol. 130, No. 4*, July 1983, pp. 206-216.

12. C. Russell Mason, *The Art and Science of Protective Relaying,* B. Bhattacharya for Wiley Eastern Limited, New Delhi, 1979.

13. W.K. Sonnemann, "A Study of Directional Element Connections for Phase Relays", *AIEE Transactions, Vol. 69*, 1950, pp. 1438-1451.

14. B.J. Mann and I.F. Morrison, "Digital Calculation of Impedance for Transmission Line Protection", *IEEE Transactions on Power Apparatus and Systems, Vol. PAS-90*, January/February 1971.

15. G.B. Gilcrest, G.D. Rockefeller and E.A. Udren, "High Speed Distance Relaying Using a Digital Computer. Part-I-System Description", *IEEE Transactions on Power Apparatus and Systems, Vol. PAS-91, No. 3*, May/June 1972, pp. 1235-1243.

16. G.D. Rockefeller and E.A. Udren, "High Speed Distance Relaying Using a Digital Computer. Part II", *IEEE Transactions on Power Apparatus and Systems, Vol. PAS-91, No. 3*, 1972, pp. 1244-1256.

17. J. Makino and Y. Miki, "Study of Operating Principles and Digital Filters for Protective Relays with Digital Computer", *IEEE Publication No. 75 CH0990-2 PWR, Paper No. C75 197 9, IEEE PES Winter Power Meeting, New York,*, January 1975, pp. 1-8.

18. R.G. Luckett, P.J. Munday and B.E. Murray, "A Substation Based Computer for Control and Protection", *IEE Conference Publication No. 125, London*, March 1975, pp. 252-260.

19. A.E. Brooks, "Distance Relaying Using Least Squares Estimates of Voltage, Current and Impedance", *Proceedings of 10th Power Industry Computer Application Conference*, May 1977, pp. 394-402.

20. M.S. Sachdev and M.A. Baribeau, "A New Algorithm for Digital Impedance Relays", *IEEE Transactions on Power Apparatus and Systems, Vol. PAS-98, No.*, November/December 1979.

21. M. Ramamooty, "A Note on Impedance Measurement Using Digital Computer", *IEE-IRE Proceeding (India), Vol. 9, No. 6*, November/December 1974.

22. M. Nagpal, " Interactive Software for Evaluating Relay Algorithms", Master's thesis, University of Saskatchewan, Saskatoon, October 1986.

23. A.G Padke, T. Hlibka and M. Ibrahim, "A Digital Computer System for EHV Substation: Analysis and Field Tests", *IEEE Transactions on Power Apparatus and Systems, Vol. PAS-95, No. 1*, January/February 1976, pp. 291-301.

24. G.S. Hope and V.S. Umamaheswaran, "Sampling for Computer Protection of Transmission Lines", *IEEE Transactions on Power Apparatus and Systems, Vol. PAS-93, No. 5*, September/October 1974.

25. E.O. Schweitzer, R.R. Larson and A.J. Flechsig Jr., "The Design and Test of a Digital Relay for Transformer Protection", *IEEE Transactions on Power Apparatus and Systems, T-PAS*, May/June 1979, pp. 795-805.

26. G.S. Hope, O.P. Malik and P.K. Dash, "A New Algorithm for Impedance Protection of Transmission Lines", *Summer Meeting of IEEE Power Engineering Society, Vancouver, B.C*, July 1979.

27. A.D. McInnes and I.F. Morrison, "Real Time Calculation of Resistance for Transmission Line Protection by Digital Computer", *EE Transactions, Institution of Engineers, Australia, Vol. EE-7, No. 1*, 1970, pp. 16-23.

28. W.D. Breigan, M.M. Chen and T.F. Gallan, "Laboratory Investigation of a Digital System for the Protection of Transmission Lines", *IEEE Transactions on Power Apparatus and Systems, Vol. PAS-98, No. 2*, March/April 1979, pp. 350-357.

29. A.G. Phadke et al, "A Microcomputer Based Symmetrical Component Distance Relay", *Proceedings of Power Industry Computer Application Conference, IEEE Publication No. 79 CHI 301-3-PWR*, 1979, pp. 47-55.

30. J. Carr and R.V. Jackson, "Frequency Domain Analysis Applied to Digital Transmission Lines", *IEEE Transactions on Power Apparatus and Systems, Vol. PAS-94*, July/August 1975.

31. B.C. Kuo, *Digital Control Systems*, Holt, Rinehart and Winston, Inc., New York., 1980.

32. M.S. Sachdev and D.G. Hunchuk, "Digital Converters used in Computer Relaying", *IEEE Publication 76CH1075-1 PWR, Paper No. A76 154-5, IEEE PES Winter Meeting, New York, N.Y.*, January 1976, pp. 1-7.

33. B. Liu, "Effect of Finite Word Length on the Accuracy of Digital Filters", *Transactions of IEEE on Circuit Theory*, November 1971, pp. 670-677.

34. P.W. Davall and G. Yeung Au, "A Software Design for a Computer Based Impedance Relay for Transmission Line Protection", *IEEE Transactions on Power Apparatus and Systems, Vol. PAS-99, No. 1*, January/February 1980, pp. 235-244.

35. M.S. Sachdev and C. Cline, "Documentation on Files PEAKVA.APL, ZVALUE.APL, INDATG.APL", Tech. report, University of Saskatchewan, 1983/84.

36. J. Paulman, *Fundamentals of APL Programming*, Wm.C. Brown Company Publishers, Dubuque, Iowa, 1976.

37. *VAX-11 APL Reference Manual,* Digital Equipment Corporation, Maynad, Massachusetts, 1983.

A. ANALOG TO DIGITAL CONVERTER MODELLING

A.1. Introduction

An analog to digital converter (A/D) converts an electrical analog quantity to its corresponding digital representation. A/D converter simulation uses the following parameters,

- the word size of the A/D converter,
- the range of the input signal that the converter can handle and
- the quantization type.

A.2. Modelling

A simulation model can be used to study the effect of A/D converters in digital relaying. Equation A.1 is the mathematical expression for an A/D converter of b+1 bits.

$$FSR = V_{ref(+)} - V_{ref(-)} \tag{A.1}$$

where:

FSR is the full scale range of the A/D converter,

$V_{ref(+)}$ is the positive voltage saturation level of the A/D converter and

$V_{ref(-)}$ is the negative voltage saturation level of the A/D converter.

If the input is x *volts*, then the output of the converter is an integer number and can be obtained using Equation A.2.

$$(Z)_{10} = TRN \text{ or } RND \frac{x + FSR/2}{FSR} 2^{b+1} - 2^{b} \qquad (A.2)$$

where:

Z_{10} is an integer value with base 10,

TRN represents truncation and

RND represents rounding.

Errors resulting from truncation when using Equation A.2 are negative for both positive and negative numbers. The equation represents an A/D converter with b+1 bits and employing two's complement representation for negative numbers.

To study the saturation effects of an A/D converter, the positive input voltage should be selected to exceed $V_{eff(+)}$ and the negative input voltage should be less than $V_{eff(-)}$. The limits $V_{eff(+)}$ and $V_{eff(-)}$ define the effective range of an A/D converter. For an A/D converter employing the two's complement representation for negative numbers and b+1 bits, the equations for the limits are as follows:

$$V_{eff(+)} = V_{ref(+)} \left(1 - \frac{1}{2^{b}}\right) \qquad (A.3)$$

$$V_{eff(-)} = V_{ref(-)} \qquad (A.4)$$

B. BIT SHIFT APPROACH OF MULTIPLICATION

B.1. Introduction

The bit shift approach of multiplication is the procedure that the software which has been developed in this project uses to determine the product of an integer number and a decimal number. This multiplication approach helps the user of the software package to demonstrate the accuracy of an algorithm as would be implemented by a micro-processor. The following sections describe this approach of multiplication.

B.2. Mathematical Background

A decimal number b can be expressed in terms of inverse powers of two. This is demonstrated by Equation B.1.

$$b = \frac{m_1}{2^1} + \frac{m_2}{2^2} + \frac{m_3}{2^3} + \frac{m_4}{2^4} + \ \ldots \qquad (B.1)$$

where:

$m_1, m_2, m_3, m_4, \ \ldots$ are integers of values either as 1 or 0.

In a digital computer, when each of the above non-zero fractions multiplies an integer number, the procedure is equivalent to carrying out right bit shift operations on the integer number. The number of shift operations in this case is equal to the power of two in the denominator of the fraction. Employing Equation B.1, it could be shown that,

$$Jb = J\left(\frac{m_1}{2^1} + \frac{m_2}{2^2} + \frac{m_3}{2^3} + \frac{m_4}{2^4} + \ \ldots\right) \qquad (B.2)$$

or

$$Jb = J - J\ (1- (\frac{m_1}{2^1} + \frac{m_2}{2^2} + \frac{m_3}{2^3} + \frac{m_4}{2^4} + \ \ldots\ )) \qquad (B.3)$$

where:

J is an integer value.

B.3. Algorithm

The procedure below describes bit shift multiplication using APL programming language.

1. ⟨ exec ⟩ Multiply the decimal argument by 2^{b+1}, where $b+1$ is the number of bits to be used.

2. ⟨ exec ⟩ Find the binary equivalent of the integer portion of the value obtained in step 1.

3. ⟨ if ⟩ The number of ones are more than the number of zeros in the binary representation,

   a. ⟨ then ⟩ complement the binary representation.

   b. ⟨ else ⟩ Continue

4. ⟨ exec ⟩ For each one in the binary representation, multiply its inverse value by the integer argument and then truncate or round the results.

5. ⟨ exec ⟩ Add all the results obtained in step 4.

6. ⟨ if ⟩ The binary representation used in step 4 was the one obtained by complementing in step 3,

   a. ⟨ then ⟩ Subtract the sum obtained in step 5 from the integer argument to get the final product, BJ.

   b. ⟨ else ⟩ The sum obtained in step 5 is the final product.

7. ⟨ return ⟩

Step 4 above represents right bit shift operations on the integer J. In this way errors may be introduced. The result is J/2 + ϵ, where ϵ is the

error. These errors accumulate for multiple shift operations. The multiplication described so far applies to the ordinary approach of bit shift. Errors due to truncation or rounding can further be reduced by implementing the extended form of bit shift multiplication. The extended bit shift is similar to the one described above except that the integer number is first multiplied with 2^{b+1}, which is the largest number that can be stored in the word of the micro-processor. The result is then multiplied with the decimal value using the ordinary bit shift approach. The number with which the integer is multiplied then divides this result. The process of multiplying the integer argument by 2^{b+1} is similar to making the integer argument two b+1 bit words long with the lower word filled with zeros. It therefore, eliminates both truncation and rounding errors. The error due to truncation or rounding arises only if the final product is divided by 2^{b+1}. This is equivalent to neglecting the lower bit word of the product.

C. AMPLITUDE ESTIMATOR

C.1. Introduction

In relaying applications, the computations of amplitudes for phasors from their real and imaginary components are most often desired. Computation times increase if the calculations use exact methods. These calculations, however, can be replaced by piecewise linear approximations. The approximations require only additions and multiplications of constants and are much more efficient than the conventional multiplication of two unknowns, although they introduce errors in the final results. The errors can be made as small as possible. The following section describes the method of estimating the amplitudes of phasors using the piecewise linear approximations.

C.2. Mathematical Background

If R and I are the real and imaginary components of a phasor having magnitude M, then Equations C.1 and C.2 define a and b as

$$a = MAX\ (|R|,|I|) \tag{C.1}$$

$$b = MIN\ (|R|,|I|) \tag{C.2}$$

The coordinates (a,b) describe a point in the first octant at a distance M from the origin. Coefficients x and y are such that Equation C.3 gives the magnitude of $R + jI$.

$$p = x \times a + y \times b \tag{C.3}$$

This is the case when only one approximation region is under consideration. The method provides higher accuracy for multiple regions of approximations.

The processing time however increases as the number of regions also increases. In general, for n regions there will be a set of values of x and y as (x_1,y_1), (x_2,y_2), . . . , (x_n,y_n). Each set of coefficients, x and y are valid for a particular range of a/b ratios. The values for each set of coefficients can be calculated by applying the least error squares fit of the data (of a particular region for which the method provides the x and y values) to a linear equation of the form of Equation C.3. If m is the number of data points which fit the data for the n^{th} region, then the matrix equation is as follows:

$$\underset{m\times 1}{[P]} = \underset{1\times 1}{[x_n]}\ \underset{m\times 1}{[a]} + \underset{1\times 1}{[y_n]}\ \underset{m\times 1}{[b]} \qquad (C.4)$$

The values for the unknowns x_n and y_n can be calculated using Equation C.5.

$$\begin{bmatrix} x_n \\ y_n \end{bmatrix} = \begin{bmatrix} [[a]^T[a]]^{-1}[a]^T[P] \\ [[b]^T[b]]^{-1}[b]^T[P] \end{bmatrix} \qquad (C.5)$$

In the software these coefficients have been calculated for one, two, three, four, five, six, eight, ten and sixteen regions of approximations. The user has the ability to select the desired approximation.

D. REPRESENTATION OF PHASE-PHASE AND PHASE-GROUND FAULTS

D.1. Introduction

The analysis to be done in this Appendix uses the sample power system of Figure 7-1. This is reproduced as Figure D.1. The computations are for phase-phase as well as single-phase to ground faults at location F_1 of Figure D.1. The procedure applies similarly to faults at other locations such as F_2 and F_3.

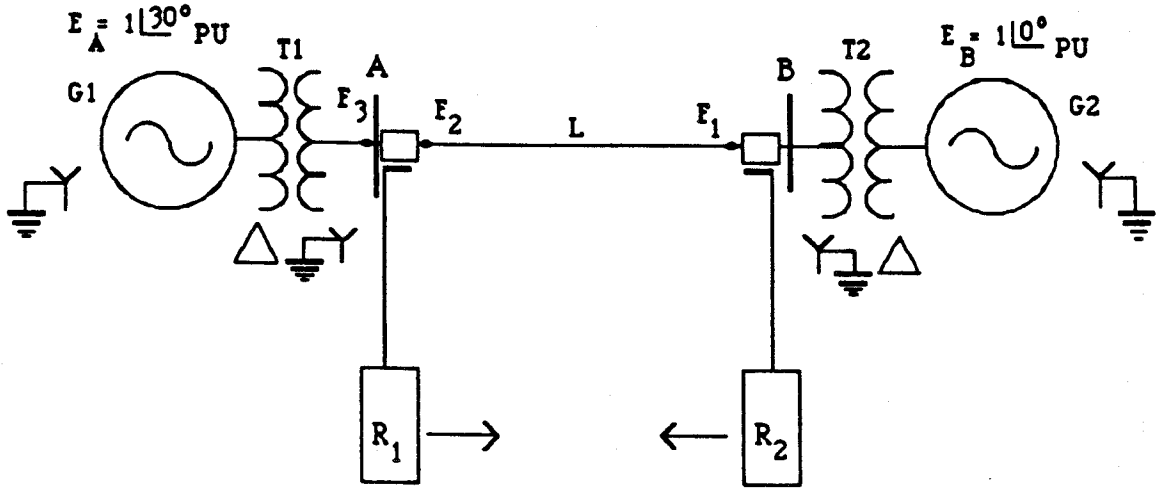

Figure D.1: A sample power system used for the studies.

D.2. Phase-Phase Faults

Consider that there is a phase-phase fault involving phases B and C and that there is no fault resistance effect. The system conditions at location F_1 during this fault can be expressed by Equations D.1 and D.2 as

$$I_{af} = 0 \ , \ I_{bf} + I_{cf} = 0 \qquad (D.1)$$

$$V_{bf} - V_{cf} = 0 \qquad (D.2)$$

where:

V_{bf} and V_{cf} are phases B and C fault voltages and

I_{af}, I_{bf} and I_{cf} are the fault currents flowing in the various phases.

Equations D.1 and D.2 give a parallel connection for the sequence network. This connection is illustrated by Figure D.2.

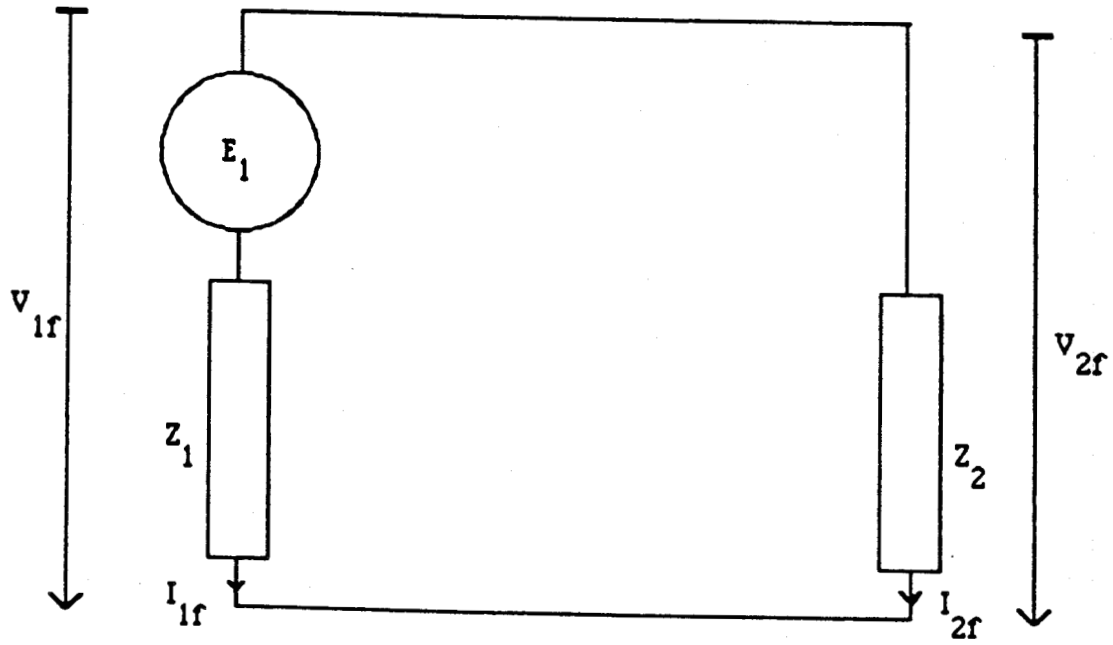

Figure D.2: The sequence network diagram for a phase B to phase C fault.

Using symmetrical components theory with phase A as the reference, the mathematical expressions for the sequence currents and voltages at the fault point are given by Equations D.3 to D.6.

$$I_{1f} = \frac{E_1}{Z_1 + Z_2} \qquad (D.3)$$

$$I_{2f} = - I_{1f} \qquad (D.4)$$

$$V_{1f} = E_1 - Z_1 I_{1f} \qquad (D.5)$$

$$V_{2f} = - Z_2 I_{2f} \qquad (D.6)$$

where:

I_{1f} and I_{2f} are the positive and negative sequence currents in the line during the fault,

V_{1f} and V_{2f} are the positive and negative sequence voltages at the fault point,

E_1 is the positive sequence source voltage and

Z_1 and Z_2 are the positive and negative sequence impedances of the line.

From Equations D.3 to D.6 the fault voltages and currents measured at the relaying point can be calculated. Table D.1 lists the single phase quantities at the relaying point calculated for a fault at location F_1. Tables D.2 and D.3 contain the quantities for the B-C faults at locations F_2 and F_3 respectively. The values given in these tables together with the pre-fault quantities were used to obtain the sampled values used for testing the software for phase-phase fault.

Table D.1: The calculated current and voltage phasors at the relaying point for a phase B to phase C fault at F_1.

$I_{ar} = 0.4904 \angle 36.4^\circ$	$V_{ar} = 0.7925 \angle 55.26^\circ$
$I_{br} = 1.3827 \angle 248.64^\circ$	$V_{br} = 0.5402 \angle 279.02^\circ$
$I_{cr} = 1.0008 \angle 83.36^\circ$	$V_{cr} = 0.5491 \angle 192.37^\circ$

Table D.2: The calculated current and voltage phasors at the relaying point for a phase B to phase C fault at F_2.

$I_{ar} = 0.4915 \angle 52.4^\circ$	$V_{ar} = 0.8583 \angle 48.05^\circ$
$I_{br} = 2.5773 \angle 238.44^\circ$	$V_{br} = 0.4292 \angle 228.09^\circ$
$I_{cr} = 2.0892 \angle 59.86^\circ$	$V_{cr} = 0.4292 \angle 228.01^\circ$

Table D.3: The calculated current and voltage phasors at the relaying point for a phase B to phase C fault at F_3.

$I_{ar} = 0.4908 \angle 52.37^\circ$	$V_{ar} = 0.8583 \angle 48.05^\circ$
$I_{br} = 1.1102 \angle 37.79^\circ$	$V_{br} = 0.4292 \angle 228.09^\circ$
$I_{cr} = 1.5901 \angle 222.24^\circ$	$V_{cr} = 0.4292 \angle 228.01^\circ$

D.3. Single-Phase to Ground Faults

Consider that there is a phase A to ground fault. The following equations express the system conditions at location F_1.

$$I_{bf} = I_{cf} = 0 \qquad (D.7)$$

$$V_{af} = 0 \qquad (D.8)$$

where:

I_{af} and I_{cf} are the fault currents in phases B and C and

V_{af} is the phase A fault voltage at the fault point.

Equations D.7 and D.8 give a series connection for the sequence network which is shown in Figure D.3.

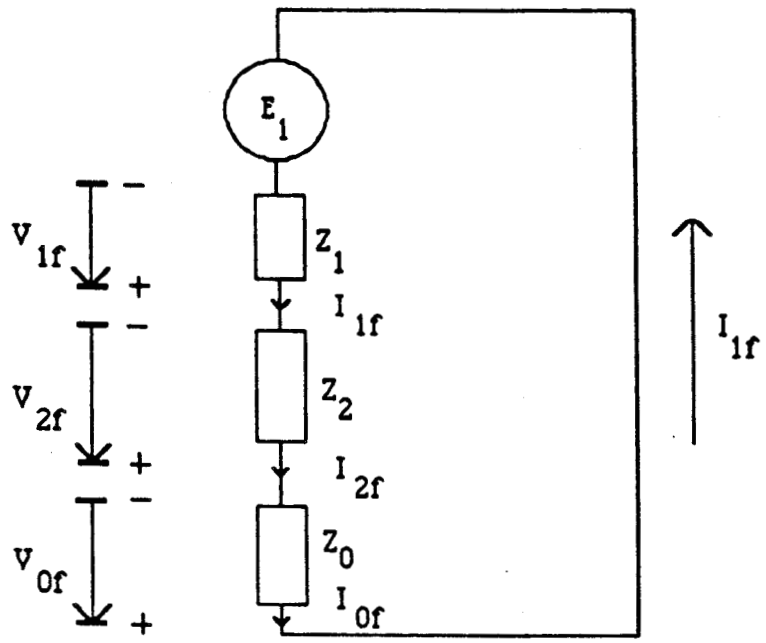

Figure D.3: The sequence network diagram for a phase A to ground fault.

The following equations represent the sequence quantities.

$$I_{1f} = \frac{E_1}{Z_1 + Z_2 + Z_3} \tag{D.9}$$

$$I_{1f} = I_{2f} = I_{of} \tag{D.10}$$

$$V_{1f} = E_1 - I_{1f}Z_1 \tag{D.11}$$

$$V_{2f} = -I_{2f}Z_2 \tag{D.12}$$

$$V_{0f} = - I_{0f}Z_0 \tag{D.13}$$

where:

I_{0f} is the zero sequence current and

Z_0, the zero sequence impedance of the line.

The phase quantities at the relaying point can be calculated using the results obtained from Equations D.9 to D.13. Table D.4 contain these quantities. Listed in Tables D.5 and D.6 are the quantities for faults at F_2 and F_3 respectively. These quantities were used to obtain the sampled values which were used to test the software for single-phase to ground faults.

Table D.4: The calculated current and voltage phasors at the relaying point for a phase A to ground fault at F_1.

$I_{ar} = 1.3269 \angle 344.84^\circ$	$V_{ar} = 0.4892 \angle 56.13.36^\circ$
$I_{br} = 0.3577 \angle 242.12^\circ$	$V_{br} = 0.7550 \angle 303.72^\circ$
$I_{cr} = 0.7714 \angle 153.08^\circ$	$V_{cr} = 0.7486 \angle 116.8^\circ$
$3I_{or} = 0.5289 \angle 323.61^\circ$	

Table D.5: The calculated current and voltage phasors at the relaying point for a phase A to ground fault at F_2.

$I_{ar} = 3.6927 \angle 326.78^\circ$	$V_{ar} = 0.00022 \angle 63.43^\circ$
$I_{br} = 0.8458 \angle 307.96^\circ$	$V_{br} = 0.8187 \angle 299.04^\circ$
$I_{cr} = 0.1949 \angle 223.79^\circ$	$V_{cr} = 0.7949 \angle 157.88^\circ$
$3I_{or} = 4.4739 \angle 320.84^\circ$	

Table D.6: The calculated current and voltage phasors at the relaying point for a phase A to ground fault at F_3.

$I_{ar} = 1.4901 \angle 128.69^\circ$	$V_{ar} = 0.00022 \angle 63.43^\circ$
$I_{br} = 0.8463 \angle 307.98^\circ$	$V_{br} = 0.8187 \angle 299.04^\circ$
$I_{cr} = 0.1950 \angle 223.98^\circ$	$V_{cr} = 0.7949 \angle 157.88^\circ$
$3I_{or} = 0.6669 \angle 147.26^\circ$	

E. DETERMINATION OF POLARIZATION COEFFICIENTS

E.1. Introduction

Distance relay polarization schemes require that the polarization coefficients K_1 and K_2 be determined. These coefficients are calculated using the anticipated fault voltages and currents measured at the relaying point. The performance of a polarized relay most often depends on these coefficients. The determination of these coefficients should be such that none of the relays operates falsely under either abnormal or normal system conditions.

E.2. Mathematical Background

The mathematical expression for the signal to the polarized mho relay is as follows:

$$S_2 = K_1 V_L + K_2 V_p \angle \theta \qquad (E.1)$$

where:

K_1 and K_2 are the polarization coefficients,

V_L is the faulted phase voltage,

V_p is the polarizing voltage and

θ is the phase angle shift of the polarizing voltage.

The determination of K_1 and K_2 are such that for a fault at the end of the protected line, V_L is equal to S_2. Using this condition the following equation is obtained.

$$V_L = K_1 V_L + K_2 V_p \angle\theta \qquad (E.2)$$

Rearranging, Equation E.2 becomes:

$$K_1 = (1 - K_2) \frac{V_p}{V_L} \angle\theta \qquad (E.3)$$

Reasonable values can be assigned to K_2, and from this K_1 can be calculated. For a phase-phase fault involving the B and C phases, the fault voltages and currents are as calculated in Appendix D. The voltages are reproduced here as

$$V_{BC} = V_L = 0.7475 \angle -33.81^\circ$$

and

$$V_{BA} = V_p = 1.2402 \angle -107.21^\circ .$$

Substituting V_{BC} and V_{BA} into Equation E.3 and rearranging Equation E.4 is obtained.

$$K_1 = 1 - (1.65928 \angle -13.4^\circ) \times K_2 \qquad (E.4)$$

For $K_2 = 0.2 \angle 13.4^\circ$, K_1 is calculated to be 0.6682.

In the case of a single-phase to ground fault involving phase A and ground, the fault voltages calculated are

$$V_A = V_L = 0.4892 \angle 56.13^\circ$$

and

$$V_C = V_p = 0.7486 \angle 116.8^\circ$$

$K_1 = 0.6940$ if K_2 is assigned a value of $0.2 \angle 59.33^\circ$ for polarization scheme 2. The same procedure can be used in calculating the coefficients for other polarization schemes.

F. SAMPLE RUN OF THE APL FUNCTION INTPAK

```
  APL
terminal..TTY
VAX APL V3.1-819
VTA3417 WEDNESDAY  1-MAR-1989 15:09:28.25 ADU [ADU]
CLEAR WS

      )LOAD INTPAK.APL
SAVED FRIDAY 27-JAN-1989 11:36:37.58 286 BLKS

      INTPAK
*****************************************************************
*                                                               *
*                          WELCOME TO                           *
*                                                               *
*       THE INTERACTIVE SOFTWARE FOR EVALUATING AND             *
*                                                               *
*           TEACHING DIGITAL RELAYING ALGORITHMS.               *
*                                                               *
*                             BY                                *
*                                                               *
*     M.S. SACHDEV     MUKESH NAGPAL      THOMPSON ADU         *
*                                                               *
*                POWER SYSTEM RESEARCH GROUP                    *
*             DEPARTMENT OF ELECTRICAL ENGINEERING              *
*                  UNIVERSITY OF SASKATCHEWAN                   *
*                  SASKATOON  CANADA S7N OWO.                   *
*                                                               *
*****************************************************************

**** ENTER  RETURN  TO  CONTINUE.
```

DURING THE LAST SEVERAL YEARS INTEREST IN DIGITAL PROCESSOR BASED POWER SYSTEM PROTECTIVE RELAYS AND INSTRUMENTS HAS RECIEVED TREMENDOUS ATTENTION. THE ACCURACY OF THESE RELAYS AND INSTRUMENTS IS ONE OF THE MAJOR AREAS OF CONCERN. IN DIGITAL PROCESSOR BASED RELAYS AND INSTRUMENTS THE ACCURACY OF THE ACQUIRED DATA AND COMPUTED RESULTS DEPENDS ON SEVERAL FACTORS, SUCH AS, CHARACTERISTICS OF THE ANALOG TO DIGITAL CONVERTES, DIGITAL PROCESSORS, RELAY SOFTWARE AND THE TYPE OF COMPARATOR USED. WITH THE POLARIZED IMPEDANCE RELAY THE DATA IS AFFECTED BY THE TYPE OF POLARIZED SIGNAL INCORPORATED. THIS INTERACTIVE PACKAGE HAS BEEN DEVELOPED FOR STUDYING THE INFLUENCE OF THESE FACTORS ON THE PERFORMANCE OF DIGITAL RELAYS AND INSTRUMENTS

PROGRAMS FOR EVALUATING THE PERFOMANCE OF DIGITAL IMPEDANCE AND DIRECTIONAL RELAYS HAVE BEEN DEVELOPED AND INCORPORATED.

**** ENTER RETURN TO CONTINUE.

THIS INTERACTIVE PACKAGE INCLUDES THE FOLLOWING FACILITIES:

1. AT ANY TIME THE USER CAN INSTRUCT THE PROGARM TO ABORT. ENTER * TO ABORT.

2. THE USER CAN INSTRUCT THE PROGRAM TO JUMP-BACK TO THE PREVIOUS QUESTION. A SERIES OF SUCH INSTRUCTIONS CAN TAKE THE USER TO ANY PREVIOUS STAGE OF THE PROGRAM. ENTER < TO JUMP BACK TO THE PREVIOUS QUESTION.

3. THE INTERACTIVE SOFTWARE CHECKS THE VALIDITY OF THE USER'S RESPONSES AND THE RETURNS CONTROL TO THE PRESENT QUESTION UNTIL A VALID ANSWER IS PROVIDED.

4. DATA FOR PERFORMANCE EVALUATION CAN EITHER BE ENTERED DIRECTLY FROM TERMINAL OR SPECIALLY FORMATTED FILES DURING THE EXECUTION OF THE PROGRAM.

5. THE USER CAN CHOOSE DIFFERENT TYPE OF ANALOG TO DIGITAL CONVERTER AND DIGITAL PROCESSOR.

6. THE RESULTS ARE IMMEDIATLY DISPLAYED AFTER THE EXECUTION OF CHOSEN ALGORITHM. THESE RESULTS CAN BE PLOTTED AND SAVED IN DATA FILES IF USER DESIRES SO.

**** ENTER RETURN TO CONTINUE.

TABLE OF THE LIST OF WORKSPACES,
THEIR PURPOSE AND EXECUTION CODE.

EXECUTION CODE	WORKSPACE NAME	PURPOSE
1	INDATG	GENERATES DATA AND WRITES THEM IN A DATA FILE TO BE READ BY OTHER PROGRAMS OF THE SOFTWARE.
2	DIRECT	SIMULATES DIRECTIONAL RELAY CHARACTERISTICS. ALSO COMPUTES THE PEAK VALUE AND PHASE ANGLE OF VOLATGE AND CURRENT SIGNALS.
3	DISTANCE	SIMULATES THE CHARACTERISTICS OF DIGITAL DISTANCE RELAYS AND COMPUTES THE IMPEDANCE OF A LINE AS SEEN BY THE RELAY.
4	FVALUE	COMPUTES THE FREQUENCY OF THREE PHASE AND SINGLE PHASE VOLTAGES.
5	FRQRES	COMPUTES THE FREQUENCY RESPONSE OF NON-RECURSIVE ALGORITHMS.

ENTER RETURN TO CONTINUE.

>>>> DO YOU WISH TO TEST RUN ANY OF THE ABOVE PROGRAMS?
ANSWER YES OR NO.

Y

>>>> WHICH OF THE PROGRAM DO YOU WISH TO TEST RUN?

ENTER THE EXECUTION CODE.

```
3
**************************************************************
*                                                            *
*    THIS PROGRAM MODELS THE CHARACTERISTICS OF THE DIF-     *
*      FERENT TYPES OF DIGITAL IMPEDANCE RELAY CHARAC-       *
*        TERISTICS. IT ALSO CALCULATES THE IMPEDANCE         *
*          OF THE TRANSMISSION LINE AS SEEN BY TH-           *
*            ESE DIGITAL PROCESSOR BASED RELAYS.             *
*                                                            *
**************************************************************

**** TO MODIFY THE PREVIOUSLY ENTERED INFORMATION
     ENTER < OR * TO ABORT THE PROGRAM.

>>>> WHAT IS THE  NOMINAL FREQUENCY  OF THE SYSTEM
     IN HZ?

**** THIS IS 60 HZ FOR THE NORTH AMERICAN SYSTEMS
     AND 50 HZ FOR THE EUROPEAN SYSTEMS.

*


>>>> DO YOU WISH  TO TEMPORARLY  ABORT  THE TERMINAL
     SESSION?  ANSWER YES OR NO.

N
  **** >>>> COMPUTATIONS ARE ABORTED <<<< ****

>>>> DO  YOU   WISH  TO  TEST   RUN  ANOTHER   PROGRAM?
     ANSWER  YES  OR  NO.

N


          ****************************************
          *                                      *
          *              GOOD-BYE!!!             *
          *                                      *
          ****************************************
```